Universidade de Aveiro Departamento de Biologia
2008

Sara Luisa de Castro Esteves

Caracterização de Proteínas de Cérebro Humano que Interagem com a Proteína Fosfatase 1α Através do Sistema Dois-Híbrido de Levedura

Characterization of Human Brain Protein Phosphatase 1α Interacting Proteins Using the Yeast Two-Hybrid System

Universidade de Aveiro Departamento de Biologia
2008

Sara Luisa de Castro Esteves

Caracterização de Proteínas de Cérebro Humano que Interagem com a Proteína Fosfatase 1α Através do Sistema Dois-Híbrido de Levedura

Characterization of Human Brain Protein Phosphatase 1α Interacting Proteins Using the Yeast Two-Hybrid System

Universidade de Aveiro Departamento de Biologia
2008

Sara Luisa de Castro Esteves

Caracterização de Proteínas de Cérebro Humano que Interagem com a Proteína Fosfatase 1α Através do Sistema Dois-Híbrido de Levedura

Characterization of Human Brain Protein Phosphatase 1 αInteracting Proteins Using the Yeast Two-Hybrid System

Dissertação apresentada à Universidade de Aveiro para cumprimento dos requisitos necessários à obtenção do grau de Mestre em Microbiologia Molecular, realizada sob a orientação científica do Doutor Edgar Figueiredo da Cruz e Silva, Professor Associado do Departamento de Biologia da Universidade de Aveiro

o júri

presidente

Prof. Doutor Edgar Figueiredo da Cruz e Silva
Professor Associado da Universidade de Aveiro

Prof. Doutora Ana Luísa Monteiro de Carvalho
Professora Auxiliar da Faculdade de Ciências e Tecnologia da Universidade de Coimbra

Prof. Doutora Margarida Sâncio da Cruz Fardilha
Professora Auxiliar Convidada da Universidade de Aveiro

agradecimentos

À FCT, ao projecto APOPIS (PL503330), ao Centro de Biologia Celular e à Universidade de Aveiro.

Ao Professor Edgar da Cruz e Silva a ciência, os ensinamentos, orientação, e ajuda que recebi desde o início.

À Margarida a orientação, o espírito crítico, ajuda, disponibilidade e paciência que sempre me dedicou.

A todos no laboratório, o companheirismo, a ajuda, presença nos momentos difíceis, o ambiente e tudo o que me ensinaram. Em especial à Sandra Vieira, à Sofia e ao Korrodi o carinho, assistência e ajuda preciosas que foram essenciais na recta final e nunca irei esquecer. E às verdadeiras amizades…

À Professora Odete da Cruz e Silva os conhecimentos, críticas e opiniões.

Aos amigos de sempre que me acompanharam, apoiaram e fizeram rir mesmo sem estarem presentes.

À minha família que sempre me apoiou e incentivou a seguir em frente e soube respeitar o meu espaço…obrigada pela paciência.

resumo

A Proteína Fosfatase Tipo1 (PP1) é uma proteína ubíqua, especifica para resíduos de serina/treonina, que interage de uma forma mutuamente exclusiva com uma variedade de proteínas reguladoras. Estas actuam como substratos, inibidores, chaperoninas, proteínas âncora ou indutoras de especificidade e são muitas vezes multifuncionais, mediando um vasto conjunto de eventos celulares. Uma maior complexidade é originada pela existência de três genes que codificam várias isoformas da PP1, organizadas tanto espacialmente como temporalmente e cuja localização intracelular pode ser alterar de forma dinâmica. A PP1 está envolvida em múltiplos processos de grande relevância fisiológica (por ex. aprendizagem, memória e neurotransmissão) e patológica (envelhecimento, doença de Alzeimer e outras doenças neurodegenerativas). No entanto, ainda não estão completamente esclarecidas todas as importantes interacções de relevância fisiológica, bem como a localização intracelular onde essas interacções ocorrem.

Esta tese teve como objectivo a identificação de proteínas expressas no cérebro humano que interagem com a isoforma α da PP1, usando o sistema Dois-Híbrido (YTH) de Levedura. Através desta técnica foram obtidos 298 clones positivos, permitindo a identificação de 74 proteínas que ligam a PP1α. Entre as quais algumas eram proteínas já conhecidas por interagirem com a PP1, outras nunca antes tinham sido associadas à PP1 e várias eram proteínas ainda não caracterizadas. Foi feito um estudo mais detalhado para o clone mais abundante neste rastreio, Chr9orf75, que corresponde a uma proteína não descrita até agora. A ligação da proteína Chr9orf75 à PP1 foi confirmada através de várias técnicas e a sua localização subcelular e co-localização com a PP1α foi estudada por imunocitoquímica. Os resultados aqui obtidos abrem novas perspectivas para o estudo da proteína Chr9orf75, a sua ligação à PP1 e localização subcelular. De modo geral, pode-se concluir que os resultados deste rastreio permitiram definir o interactoma do cérebro humano da PP1α, validando a técnica YTH como um meio de estudo para melhor compreender as funções da PP1 e a sua regulação em diferentes eventos celulares.

abstract

The ubiquitous serine/threonine-specific Protein Phosphatase 1 (PP1) interacts in a mutually exclusive manner with a variety of proteins that function as substrates, inhibitors, chaperones, anchoring proteins, or substrate-specifiers and are often multifunctional, mediating a wide range of cellular events. Further complexity is provided by the existence of three PP1 genes encoding various isoforms that are organized both spatially and temporally, and can change their intracellular localization dynamically. PP1 is involved in multiple processes of great physiological (e.g. learning, memory and neurotransmitter signaling) and pathological (aging, Alzheimer's disease and other neurodegenerative conditions) relevance. However, many physiologically important interactions remain to be established, as well as the exact intracellular locations where those interactions take place.

This thesis focused on the identification of human brain PP1α interacting proteins using the Yeast Two-Hybrid (YTH) system. With this technique 298 positive clones were recovered, allowing the identification of 74 proteins that bind PP1α. Among them are some already well known PP1 interacting proteins, other proteins never before associated with PP1 and several uncharacterized proteins. A more detailed study was performed for the most abundant clone in the screen, Chr9orf75, a novel and undescribed protein. Chr9orf75 binding to PP1 was confirmed by several techniques and its subcellular localization and co-localization with PP1α studied by immunocytochemistry. The results obtained provided new insights on Chr9orf75 protein binding to PP1 and subcellular localization. In general, it may be conclude that the results of this screen allowed an initial characterization of the human brain PP1α interactome, simultaneously validating the YTH system as a mean to study and understand PP1 functions and regulation in different cellular events.

ABBREVIATIONS

aa	Amino acid (s)
AD	Activation Domain
Ade	Adenine
Amp	Ampicillin
APP	Alzheimer's amyloid precursor protein
APS	Ammonium persulfate
DNA-BD	DNA-Binding domain
BLAST	Basic Local Alignment Search Tool
cDNA	Complementary deoxynucleic acid
CDS	Protein coding sequence
Chr	Chromosome
Cys	Cystein
dATP	2'-deoxyadenosine-5'-triphosphate
dCTP	2'-deoxycytidine-5'-triphosphate
dGTP	2'-deoxyguanosine-5'-triphosphate
DMSO	Dimethylsulfoxide
DNA	Deoxynucleic acid
dNTP	Deoxynucleotide triphosphate
dsDNA	Double strand deoxynucleic acid
dTTP	2'-deoxythymidine-5'-triphosphate
EDTA	Ethylenediaminotetraacetic acid
GAL4	Gal4 transcription factor
GAL4-AD	GAL4-Activation domain
GAL4-BD	GAL4-Binding domain
His	Histidine
LB medium	Luria-Bertani Medium (Miller)
LB	Loading Buffer
Leu	Leucine
LiAc	Lithium acetate
nt	Nucleotide

OD	Optical density
ORF	Open Reading Frame
PCR	Polymerase Chain Reaction
PEG	Polyethylene glycol
PMSF	Phenyl methylsulfoxide
PP1	Protein Phosphatase 1
PP1c	Protein Phosphatase 1 catalytic subunit
QDO	Quadruple dropout
RNA	Ribonucleic acid
RT	Room Temperature
SD	Supplement dropout medium
SDS	Sodium dodecyl sulfate
SDS-PAGE	Sodium dodecyl sulphate – polyacrylamide gel electrophoresis
Ser	Serine
TBS	Tris-buffered saline solution
TDO	Triple dropout
TEMED	N,N,N',N'-tetramethyletylendiamine
Thr	Threonine
Tris	Tris (hydroxymethyl)-aminoethane chloride
Trp	Tryptophan
Tyr	Tyrosine
UAS	Upstream activating sequence
UV	Ultraviolet
X-α-gal	5-bromo-4-chloro-3-indolyl-alpha-D-galactopyranoside
YPD	Yeast extract, Peptone and Dextrose medium for *S. cerevisiae*
YPDA	YPD with adenine
YTH	Yeast Two-hybrid

1 INTRODUCTION

1.1 PROTEIN PHOSPHORYLATION

The correct targeting and localization of proteins to specific subcellular compartments represent an important biological mechanism for regulating cellular function. Increasing evidence underlines the importance of macromolecular signalling complexes, where functionally related proteins are arranged in close proximity. Therefore, elucidating the molecular composition of these signalling complexes represents a fundamental step toward understanding the function of biological systems. Protein kinases and phosphatases are key players in the regulation of numerous cellular processes, and they exert their effects precisely through those signal transduction processes.

One of the most widespread mechanisms for the post-translational regulation of proteins involves either the addition of phosphate groups via the transfer of the terminal phosphate from ATP to an amino acid residue by protein kinases, or their removal by protein phosphatases (Figure 1).

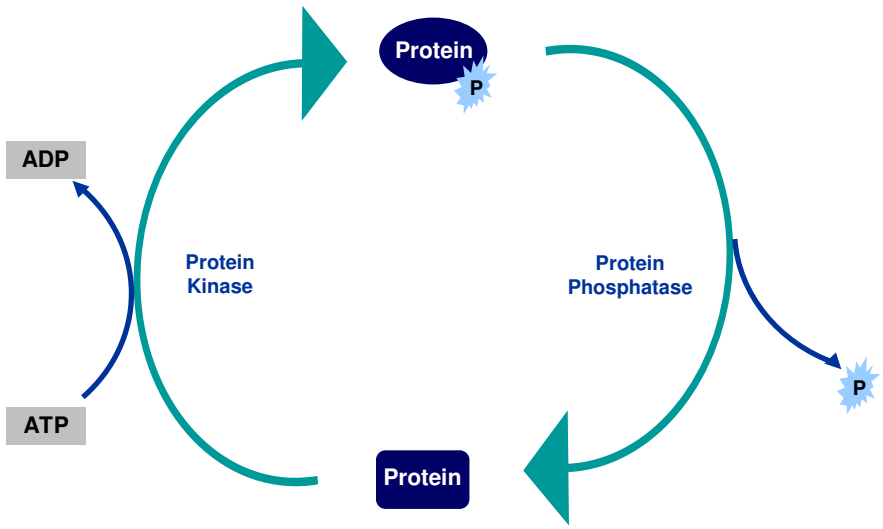

Figure 1- *Reversible protein phosphorylation, covalent modification via the transfer of the terminal phosphate from ATP to an amino acid residue of the target protein.*

The human genome encodes approximately 30000 proteins, one third of which is believed to be regulated by reversible protein phosphorylation (Johnson and Hunter 2005). Thus, the antagonistic actions of protein kinases and protein phosphatases are of equal importance in determining the degree of phosphorylation of each substrate protein.

The reversible phosphorylation of proteins is a post-translational modification and ubiquitous cellular regulatory mechanism that can regulate activity, subcellular localization and the binding affinity or association of the phosphorylated molecule, by inducing conformational changes. Protein kinases and protein phosphatases are often themselves phosphorylated in response to a myriad of extracellular and intracellular signals. An important feature of kinases and phosphatases is that a single molecule is able to activate many substrate molecules, thus allowing for amplification of the initial signal.

Virtually, all signal transduction pathways are regulated, at some level, by phosphorylation, making phosphorylation relevant to most, if not all, areas of cell signalling and neuroscience research. Different classes of protein kinases and phosphatases act specifically on serine/threonine residues or tyrosine residues. All protein kinases belong to a single gene superfamily but, in contrast, protein phosphatases are divided into distinct and unrelated protein/gene families.

Cellular health and vitality are dependent on the fine equilibrium of protein phosphorylation systems, since reversible protein phosphorylation is the major metabolic control mechanism of eukaryotic cells. Not surprisingly, many diseases and dysfunctional states are associated with the abnormal phosphorylation of key proteins. Indeed, cancer and other proliferative diseases, inflammatory diseases, metabolic disorders and neurological diseases are among those in which protein phosphorylation plays an important role. Thus, kinases and phosphatases are of interest to researchers involved in drug discovery, because of their broad relevance to health and disease.

In neurodegenerative diseases such, as Alzheimer's disease, there is evidence for abnormal regulation of protein phosphorylation. Altered activities and protein levels of several specific kinases suggest that abnormal phosphorylation contributes to the pathogenesis of these diseases. In Alzheimer's disease, neurofibrillary degeneration results from the aggregation of abnormally phosphorylated Tau protein into paired helical filaments. Protein kinase A and glycogen synthase kinase 3 β are likely to be key kinases involved (Delobel et al. 2002), and protein phosphatase 2A is thought to be the main Tau phosphatase (Planel et al. 2001). Furthermore, activation of protein kinase C, or inactivation of protein phosphatase 1, leads to a relative increase in the utilization of the non-amyloidogenic pathway for Alzheimer's amyloid precursor protein processing (Gandy and Greengard 1994; da Cruz e Silva et al. 1995a).

Other neurodegenerative diseases that may result from abnormal phosphorylation include Parkinson's disease and Huntington's disease. α-Synuclein has been implicated in the pathogenesis of Parkinson's disease, and is a major component of Lewy bodies (a major

anatomical hallmark of Parkinson's disease). α-Synuclein was demonstrated to be constitutively phosphorylated indicating that its function may be regulated by phosphorylation/dephosphorylation mechanisms (Okochi et al. 2000). Motor and cognitive deficits in Huntington's disease are likely caused by progressive neuronal dysfunction preceding neuronal cell death. Synapsin I is one of the major phosphoproteins regulating neurotransmitter release. In mice expressing the Huntington's disease mutation synapsin I is abnormally phosphorylated suggesting that an early impairment in its phosphorylation may alter synaptic vesicle trafficking and lead to defective neurotransmission in Huntington's disease (Lievens et al. 2002).

Altered phosphorylation has also been implicated in the etiology and/or symptoms of many other disorders such as heart failure (Neumann 2002) and diabetes (Sridhar et al. 2000). Therefore, protein phosphorylation systems represent attractive targets for diagnostics and therapeutics of several neurodegenerative and other diseases.

1.1.1 Protein phosphatases

The initial classification of protein phosphatases (PPs), according to their phospho-aminoacid substrates, the serine/threonine (Ser/Thr-specific) and the tyrosine (Tyr-specific) phosphatases led to the establishment of four classes of Ser/Thr-specific protein phosphatases, based on their enzymatic properties (Ingebritsen and Cohen 1983). Even though the four have overlapping substrate specificities *in vitro*, they can be distinguished by the use of inhibitor proteins and by their dependence on metal ions (Table 1). Although widely used, this initial classification does not reflect the actual phylogenetic relationship between the different Ser/Thr phosphatases.

The elucidation of complete cDNA and amino acid sequences allowed the separation of the Ser/Thr-specific protein phosphatases into two distinct gene families: the PhosphoProtein Phosphatases or PPP family (including PP1/PP2A/PP2B) and the PPM family (of metal dependent phosphatases) like PP2C (Table 1). The PPP family members (PP1, PP2A and PP2B) display high sequence similarities between their catalytic domains. The application of recombinant DNA techniques to the field also led to the identification of new protein phosphatases (PP4, PP5, PP6, PPZ, PPY,etc) and to the discovery of different isoforms (Berndt et al. 1987; da Cruz e Silva and Cohen 1987a; da Cruz e Silva et al. 1987; Cohen et al. 1988; da Cruz e Silva et al. 1988; da Cruz e Silva et al. 1995b; Fardilha et al. 2004).

Table 1 - *Gene families and corresponding functional classification of the serine/threonine-specific protein phosphatases.*

PPP	**PP1**	Dephosphorylates preferentially the beta subunit of phosphorylase kinase Inhibited by I-2, phospho-I-1 and phospho-DARPP-32
	PP2A	Dephosphorylates preferentially the alpha subunit of phosphorylase kinase Not inhibited by I-2, phospho-I-1 or phospho-DARPP-32 Activity not affected by divalent cations
	PP2B	Dephosphorylates preferentially the alpha subunit of phosphorylase kinase Not inhibited by I-2, phospho-I-1 or phospho-DARPP-32 Activity dependent on calcium ions and stimulated by calmodulin
PPM	**PP2C**	Dephosphorylates preferentially the alpha subunit of phosphorylase kinase Not inhibited by I-2, phospho-I-1 or phospho-DARPP-32. Activated by magnesium ions.

The remarkable degree of evolutionary conservation of these enzymes is undoubtedly related to their essential role in the regulation of fundamental cellular processes (Barford et al. 1998b; Barford and Neel 1998; Cohen 2002).

Among the Ser/Thr protein phosphatases, PP1 forms a major class and is highly conserved among all eukaryotes examined to date (Lin et al. 1999). Three genes are known to encode PP1 catalytic subunits, termed PP1α, PP1β and PP1γ, and PP1γ is known to undergo tissue-specific processing to yield an ubiquitously expressed PP1γ1 isoform and a testis enriched PP1γ2 isoform (da Cruz e Silva et al. 1995b) (Figure 2).

Two genes are known to encond PP2A catalytic subunits (da Cruz e Silva and Cohen 1987b), termed PP2Aα and PP2Aβ (da Cruz e Silva et al. 1987; da Cruz e Silva and Cohen 1987b), and three known PP2B genes (PP2Bα, PP2Bβ, PP2Bγ) are also subject to complex regulation to yield several alternatively spliced isoforms from each (Figure 2).

Other previously unknown phosphatase catalytic subunit isoenzymes were also discovered, from a variety of tissues and species, that were termed novel phosphatases (da Cruz e Silva et al. 1988), such as PP4, PP5 and PP6 (Cohen 1997) that are present in all mammalian tissues examined. In contrast, human PP7 is tissue specific and was found in the human retina (Huang and Honkanen 1998).

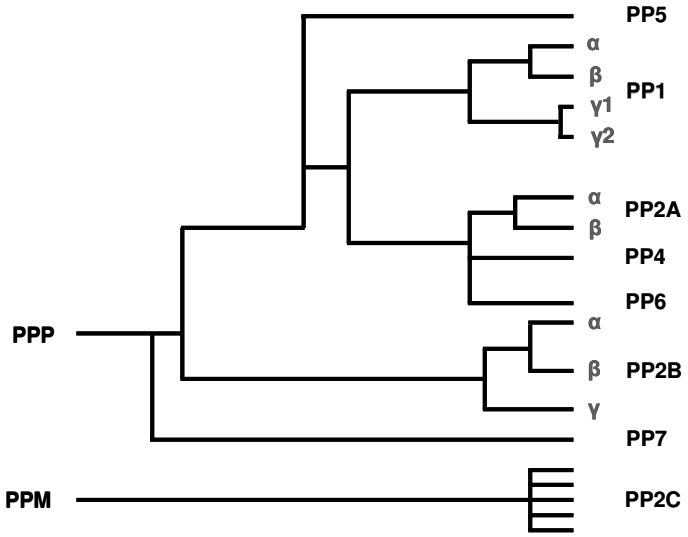

Figure 2 – *Phylogenic tree depicting the degree of similarity between the known phosphatases based on their primary amino acid sequence. PP1-PP7 belong to a single gene family (PPP) that is structurally distinct from the PPM family (PP2C) (Honkanen and Golden 2002).*

Diversification of protein Ser/Thr phosphatases during evolution can be largely attributed to an increase in the number of interacting proteins that determine when and where the phosphatases are active. On the other hand, protein Ser/Thr kinases appear to have used a different diversification strategy, largely based on a gradual increase in the number of catalytic subunits. Thus, in spite of the of the huge difference in the number of catalytic subunits of mammalian protein Ser/Thr kinases (ca. 1000) and phosphatases (ca. 100), the number of holoenzymes for these two classes of enzymes may be more or less balanced (Bollen 2001; Ceulemans and Bollen 2004).

There are approximately 25 genes encoding Ser/Thr protein phosphatases (Cohen 2004), and each phosphatase may have more than 300 physiological substrate proteins, which may increase considering each protein may have various phosphorylation sites as substrates.

1.1.2 Protein phosphatase 1 - PP1

PP1 is a ubiquitous eukaryotic enzyme that regulates a variety of cellular events through the dephosphorylation of multiple substrates. This multifunctionality of PP1 is due to its association with different regulators and/or targeting subunits. The levels of PP1 are thought not to change in response to most physiological stimuli. It was proposed that the general PP1 holoenzymes functions are centered on the rational use of energy, the recycling of protein factors and a reversal of the cell to a basal and/or energy-conserving state (Ceulemans and Bollen, 2004). When nutrients are abundant PP1 stimulates the synthesis of glycogen and also allows the recycling of transcription and splicing factors, the return to basal levels of protein synthesis and the relaxation of actomyosin fibers. PP1 also is important in recovering from stress but induces apoptosis in extreme situations. PP1 promotes the exit from mitosis and maintains cells in G1 or G2.

Post-translational regulation of mammalian PP1 can be accomplished in several ways:

- PP1 binds to other proteins that modulate PP1 activity and/or target PP1 to different substrates. Such heterodimers may be parte of larger multimeric protein complexes (Hubbard and Cohen 1993; Barford et al. 1998a; Bollen 2001; Cohen 2002; Ceulemans and Bollen 2004);
- Many regulatory subunits of PP1 are regulated by phosphorylation, thus also affecting PP1;
- PP1 catalytic subunits can undergo direct inhibitory phosphorylation by cyclin-dependent kinases (Cdks) (Dohadwala et al. 1994; Yamano et al. 1994; Kwon et al. 1997; Liu et al. 1999), Nek2 (Helps et al. 2000) and KPI-2 (Wang and Brautigan 2002).

The PP1 family, with three major 37 kDa catalytic subunit isoforms, exhibit 90% or greater identity in overall amino acid composition (Figure 3), is expressed in virtually all mammalian cells (Sasaki et al. 1990; Barker et al. 1994) and the different isoforms can all be expressed in the same cell (Puntoni and Villa-Moruzzi 1997).

The PP1 isoforms are highly conserved across their large catalytic domain, but are divergent at the N- and C-termini (Figure 3). Thus, regulatory proteins bind to the unique C-terminus of the PP1 isoforms to direct their isoform specific activities. To perform dephosphorylation reactions that are important in time and space, the diverse functions of PP1 must be independently regulated. For this reason, the regulatory subunits are believed to be much more specific for individual functions and are therefore better targets for examining specific pathways.

```
PP1gamma1       MADLDKLNIDSIIQRLLEVRGSKPGKNVQLQENEIRGLCLKSREIFLSQPILLELEAPLK 60
PP1gamma2       MADLDKLNIDSIIQRLLEVRGSKPGKNVQLQENEIRGLCLKSREIFLSQPILLELEAPLK 60
PP1alpha        MSDSEKLNLDSIIGRLLEVQGSRPGKNVQLTENEIRGLCLKSREIFLSQPILLELEAPLK 60
PP1beta         MADG-ELNVDSLITRLLEVRGCRPGKIVQMTEAEVRGLCIKSREIFLSQPILLELEAPLK 59
                *:*  :**:**:* *****:*.:*** **: * *:****:********************

PP1gamma1       ICGDIHGQYYDLLRLFEYGGFPPESNYLFLGDYVDRGKQSLETICLLLAYKIKYPENFFL 120
PP1gamma2       ICGDIHGQYYDLLRLFEYGGFPPESNYLFLGDYVDRGKQSLETICLLLAYKIKYPENFFL 120
PP1alpha        ICGDIHGQYYDLLRLFEYGGFPPESNYLFLGDYVDRGKQSLETICLLLAYKIKYPENFFL 120
PP1beta         ICGDIHGQYTDLLRLFEYGGFPPEANYLFLGDYVDRGKQSLETICLLLAYKIKYPENFFL 119
                ********* **************:**********************************

PP1gamma1       LRGNHECASINRIYGFYDECKRRYNIKLWKTFTDCFNCLPIAAIVDEKIFCCHGGLSPDL 180
PP1gamma2       LRGNHECASINRIYGFYDECKRRYNIKLWKTFTDCFNCLPIAAIVDEKIFCCHGGLSPDL 180
PP1alpha        LRGNHECASINRIYGFYDECKRRYNIKLWKTFTDCFNCLPIAAIVDEKIFCCHGGLSPDL 180
PP1beta         LRGNHECASINRIYGFYDECKRRFNIKLWKTFTDCFNCLPIAAIVDEKIFCCHGGLSPDL 179
                ************************:***********************************

PP1gamma1       QSMEQIRRIMRPTDVPDQGLLCDLLWSDPDKDVLGWGENDRGVSFTFGAEVVAKFLHKHD 240
PP1gamma2       QSMEQIRRIMRPTDVPDQGLLCDLLWSDPDKDVLGWGENDRGVSFTFGAEVVAKFLHKHD 240
PP1alpha        QSMEQIRRIMRPTDVPDQGLLCDLLWSDPDKDVQGWGENDRGVSFTFGAEVVAKFLHKHD 240
PP1beta         QSMEQIRRIMRPTDVPDTGLLCDLLWSDPDKDVQGWGENDRGVSFTFGADVVSKFLNRHD 239
                ***************** *************** ***************:**:***::**

PP1gamma1       LDLICRAHQVVEDGYEFFAKRQLVTLFSAPNYCGEFDNAGAMMSVDETLMCSFQILKPAE 300
PP1gamma2       LDLICRAHQVVEDGYEFFAKRQLVTLFSAPNYCGEFDNAGAMMSVDETLMCSFQILKPAE 300
PP1alpha        LDLICRAHQVVEDGYEFFAKRQLVTLFSAPNYCGEFDNAGAMMSVDETLMCSFQILKPAD 300
PP1beta         LDLICRAHQVVEDGYEFFAKRQLVTLFSAPNYCGEFDNAGGMMSVDETLMCSFQILKPSE 299
                ************************************.*****************::

PP1gamma1       KKK---------PNATRPVTPPRG------MITKQAKK-------- 323
PP1gamma2       KKK---------PNATRPVTPPRVGSGLNPSIQKASNYRNNTVLYE 337
PP1alpha        KNKGKYGQFSGLNPGGRPITPPRN-------SAKAKK--------- 330
PP1beta         KKAKYQYG---GLNSGRPVTPPRT--------ANPPKKR------- 327
                *:      .**:****     : :
```

Figure 3 – *Analysis of homology among of PP1 isoforms using a CLUSTAL W multiple sequence alignment.*

Over the last decade, PP1 has been implicated in many cellular processes, including, but not limited to, cell cycle control, apoptosis, transcription, adhesion, motility, metabolism, memory and HIV-1 viral transcription. However, very few PP1 physiological substrates have been established so far. Besides proteins engaged in glycogen metabolism, muscle contraction and protein synthesis, that were recognized as PP1 substrates early on, more recently, PP1 was found to dephosphorylate a number of proteins important for cell proliferation and survival. For example, the tumour suppressor pRb, lamin B, Bad, Aurora and focal adhesion kinase (Thompson et al. 1997; Ayllon et al. 2000; Helps et al. 2000; Hsu et al. 2000; Fresu et al. 2001; Katayama et al. 2001; Meraldi and Nigg 2001; Berndt 2003; Margolis et al. 2003; den Elzen and O'Connell 2004).

The three-dimensional structure of PP1c (Figure 4) was first resolved over a decade ago and highlighted key features of a bimetallic catalytic centre, but also an overall pattern of

protein folding conserved in other protein Ser/Thr phosphatases was revealed (Griffith et al. 1995; Das et al. 1996; Cohen 2002; Yang et al. 2005; Xu et al. 2006; Cho and Xu 2007).

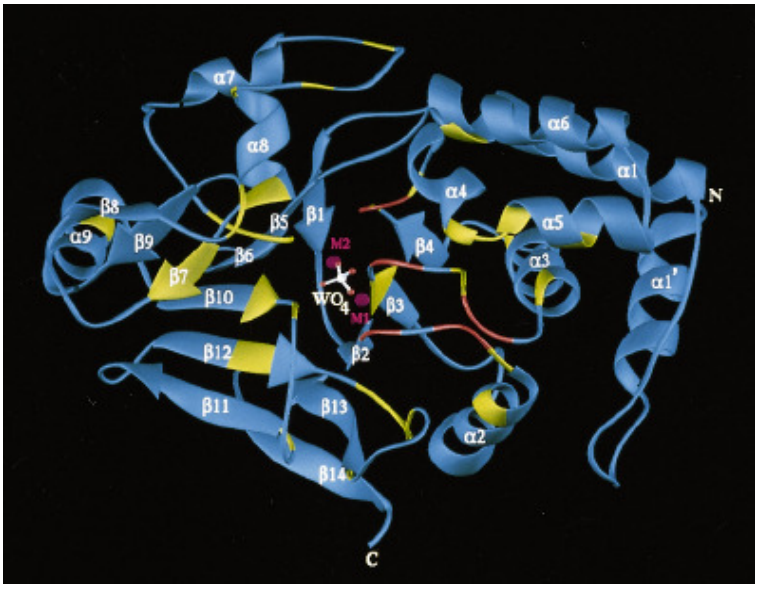

Figure 4 - *Secondary structure elements of PP1, the catalytic site and invariant residues. Metal ions M1 (Fe2+) and M2 (Mn2+) are shown as purple spheres and the tungstate ion is indicated. (Egloff et al. 1995)*

Subsequent studies co-crystallized PP1c with synthetic peptides or fragments derived from targeting or regulator subunits (Egloff et al. 1997; Terrak et al. 2004). These crystallization studies identified a site, some distance from the catalytic centre, where sequences homologous to RVxF, found in most PP1 regulators, interact and facilitated the identification of additional PP1 regulators. The structures also highlighted interactions along the C-terminus of PP1c that impart isoform specificity to some PP1 interacting proteins. Some mammalian PP1c proteins have a 25-27 amino acid C-terminal region that contains a Cdk phosphorylation motif (T P P / Q R) (Ishii et al. 1996), the threonine residue of which (T320 in human PP1α) has been show to be important for G_1 progression in cell cycle (Dohadwala et al. 1994; Berndt et al. 1997; Liu et al. 1999).

The large majority of PP1 interacting proteins contain a degenerate, so-called RVxF-motif that conforms to the consensus sequence [RK]-x_{0-1}-[VI]- [FW], where x denotes any residue and any residue except proline (Bollen 2001; Wakula et al. 2003). This motif binds with high affinity to a hydrophobic channel that is remote from the catalytic site of

PP1. The binding of the RVxF-motif has itself no major effects on the conformation or activity of PP1 (Egloff et al. 1997). However, RVxF-mediated anchoring of PP1 promotes the occupation of secondary, lower affinity binding sites and this often does affect the activity and/or substrate specificity of PP1 (Bollen 2001; Wakula et al. 2003). The RVxF-motif is present in about one third of all eukaryotic proteins but only a small fraction are PP1-binding proteins. It seems that RVxF-consensus sequences function as PP1 interaction sites only when they are present in a flexible and exposed loop that can be modelled into a β-strand. Additionally, other low affinity binding regions on the PP1 regulators further strengthen the binding.

Another PP1 binding motif has been described, F-X-X-R-X-R, that also appears to exist in several PP1 interactors (Ayllon et al. 2002). Recently, another generic PP1-binding motif was identified, the SILK-motif: [GS]-IL-[KR]. It was first described for I2, a specific PP1 inhibitor (Lin et al. 2005; Hurley et al. 2007). This motif is present in nearly 10% of proteins containing the RVxF-motif and is normally N-terminal to it. The SILK and RVxF-motifs are functionally interchangeable and can both be essential for PP1 anchoring.

The existence of common binding sites for the regulatory subunits explains why a relatively small protein such as PP1c can interact with numerous different regulatory proteins and why the binding of most regulatory subunits is mutually exclusive. The relative abundance of each isoform may be an important factor in determining the composition of numerous PP1 holoenzymes and the relative contribution of each PP1c isoform to different biological functions. A possibility is that holoenzymes containing the same binding subunit but different PP1c isoforms may have distinct functions (Rudenko et al. 2004).

The broad *in vitro* substrate specificity of PP1 leads to the idea that the enzymatic specificity is mainly dictated by the interacting subunits. Thus, a complete understanding of PP1 function requires the identification of the associated subunits that direct PP1c specific functions, as well as functional analysis of PP1 holoenzymes. A variety of approaches has identified close to 100 mammalian proteins known to interact with PP1. These PP1 interacting proteins function as inhibitors, substrate specifiers, and substrate targeting proteins, or a combination thereof. Sometimes PP1 interactors are themselves substrates for associated PP1 (Bollen 2001; Ceulemans and Bollen 2004). Given the number of protein phosphatases and phosphoprotein substrates encoded in the human genome, a large number of PP1 interacting proteins surely remain to be discovered.

1.1.3 Protein phosphatase 1α - PP1α

PP1α is one of the three mammalian catalytic subunits isoforms of PP1 and by binding to different partners has been shown to participate in a large variety of events, such as metabolism, cell division, apoptosis, protein synthesis, transcription and neuronal signalling. PP1α, like the other PP1 isoforms, can also be inhibited by natural occurring toxins such as tautomycin, cantharidin, calyculin A, okadaic acid, and microcystin-LR (da Cruz e Silva 1997).

PP1α activity can be modulated directly by post-translational modification of the catalytic subunit by phosphorylation. Some mammalian PP1 isoforms contain a TPPR sequence at the C-terminus that can be phosphorylated by Cdks, with concomitant inhibition of the catalytic activity. Indeed, PP1α catalytic subunit is phosphorylated at Thr-320, a Cdk consensus site, as cells approach and traverse S-phase (Dohadwala et al. 1994; Berndt et al. 1997; Liu et al. 1999). It has also been reported that the activities of the PP1α and PP2A are inhibited by tyrosine phosphorylation of the C-terminus Tyr-306 catalyzed by c-src, v-src, and v-abl (Johansen and Ingebritsen 1986; Chen et al. 1992; Villa-Moruzzi and Puntoni 1996). Ionizing radiation causes dephosphorylation of Thr-320 on PP1α resulting in its activation (Guo et al. 2002). This event was shown to be dependent on ATM (Ataxia Telangiectasia Mutated) kinase, the gene product that is deficient in the human autosomal recessive disease (ataxia telangiectasia).

PP1α is expressed ubiquitously. At the protein level PP1α was found to be more highly expressed in brain, testis and lung than in other peripheral tissues analysed as heart, liver, intestine, kidney, spleen, adrenal gland and skeletal muscle. PP1α was also shown to be extensively expressed in cortex, basal ganglia, hippocampus and thalamus (da Cruz e Silva et al. 1995b; Herzig and Neumann 2000; Luss et al. 2000).

Mammalian PP1α, PP1β and PP1γ1 localize to distinct subcellular locations in mammalian cells (Andreassen et al. 1998; Trinkle-Mulcahy et al. 2001; Lesage et al. 2005). In the brain the mRNAs for PP1α, PP1β and PP1γ1 were found to be particularly abundant in hippocampus and cerebellum (da Cruz e Silva et al. 1995b). At the protein level PP1α and PP1γ1 were found to be more highly expressed in brain than in peripheral tissues, with the highest levels being measured in the striatum, where they were shown to be relatively enriched in the medium-sized spiny neurons (da Cruz e Silva et al. 1995b). At the electron microscopic level, PP1 immunoreactivity was demonstrated in dendritic spine heads and spine necks, and possibly also in the postsynaptic density (Ouimet et al. 1995). PP1 immunoreactivity has also been reported in human hippocampal neuronal cytoplasm

(Pei et al. 1994). In addition, most neuronal nuclei were not immmunoreactive for PP1γ1 but were usually strongly immunoreactive for PP1α (Ouimet et al. 1995). It is thought that such specific localization and function is mediated by the regulators that bind the PP1c isozyme with different affinities.

One unresolved issue is the extent to which different PP1c isoforms interact with distinct regulatory proteins. Neurabin I and Neurabin II/Spinophilin were identified to bind PP1γ1 and PP1α, but not PP1β (MacMillan et al. 1999; Terry-Lorenzo et al. 2002), and several PP1α and PP1γ1 specific regulators have been identified in mouse fetal lung epithelial cells (Flores-Delgado et al. 2007). In human erythrocytes, the powerful oxidant $ONOO^-$ down regulates the activity of PP1α through tyrosine phosphorylation. Human erythrocytes express both PP1α and PP2A, but results indicate that only PP1α is a substrate of the peroxynitrite-activated fgr tyrosine kinase (Mallozzi et al. 2005).

Of all mammalian tissues, the brain expresses the highest levels of protein kinases and phosphatases, and PP1 is highly expressed both in neurons and glia (da Cruz e Silva et al. 1995b; Ouimet et al. 1995). It is increasingly evident that protein phosphorylation is a fundamental process associated with memory, learning and brain function, with prominent roles in the processing of neuronal signals and in short-term and long-term modulation of synaptic transmission. In neurodegenerative disorders, such as Alzheimer's disease, there is evidence for abnormal regulation of protein phosphorylation, which appears to contribute to the pathogenesis of such diseases (Wagey and Krieger 1998). An impaired balance of cellular phosphorylation, including abnormalities in both expression and activity levels of kinases and/or phosphatases, has been reported to occur in Alzheimer's disease (Gandy 1994; Gandy et al. 1994; da Cruz e Silva et al. 1995a; Tian and Wang 2002).

Even though PP1 is involved in the regulation of numerous cellular processes, relatively little is known about specific and nonredundant functions of the different PP1c isozymes. In mice, PP1γ, probably the testis-enriched splice variant PP1γ2, has a nonredundant function in spermatogenesis, as PP1γ knockout male mice are viable but sterile with defects in spermatogenesis, while knockout female mice are viable and fertile (Varmuza et al. 1999). Presumably, the somatic and female germ line functions of PP1γ are redundant with PP1α and/or PP1β. No knockout analysis exists for the other PP1c genes, although PP1α was shown to have a specific function in murine lung growth and morphogenesis (Hormi-Carver et al. 2004).

It is important, when considering the involvement of protein phosphatases in neurodegenerative diseases and other disorders, to notice that phosphatases play important roles in numerous physiological and cellular events and exist in macromolecular

signalling complexes in association with specific regulatory subunits. So, it is clear the usefulness of considering their regulatory subunits as possible targets for therapeutic and diagnostic approaches.

1.2 YEAST TWO-HYBRID SYSTEM

The Yeast Two-Hybrid (YTH) assay was developed by Fields and colleagues (Fields and Song 1989) in the late 80´s and has since become one of the most popular tools used in molecular biology. The original description of the YTH assay introduced the idea of splitting into two domains a specific transcription factor, whose activity could be reconstituted via the interaction of heterologous proteins fused to those two domains. The results of the test assay led to the suggestion that this approach might be applicable to the identification of new interactions, via screening of libraries of activation domain-tagged proteins, which was shown to be feasible (Chien et al. 1991).
The Two–Hybrid concept also proved to be remarkably malleable, with adaptations that detected protein-DNA, protein-RNA, or protein-small molecule interactions that are dependent on post-translational modifications that occur in cell compartments other than the nucleus, or that yield signals other than transcription of a reporter gene (Vidal and Legrain 1999).

1.2.1 Principle of the Yeast Two-Hybrid system

The monosaccharide galactose is imported into the cell and converted to galactose-6-phosphate by six enzymes (GAL1, GAL2, PGM2, GAL7, GAL10, MEL1), which are transcriptionally regulated by the proteins Gal80, Gal3 and Gal4, the latter of which plays the central role of DNA-binding transactivator. Gal80 binds Gal4 and inhibits its transcriptional ability. Gal3, in the presence of galactose, binds and causes a conformational change in Gal80, which then allows Gal4 to function as a transcriptional activator. Gal4 like other transcriptional activators is a modular protein that needs both DNA-binding (BD) and activation (AD) domains.
In a Gal4-based Two-Hybrid assay a bait gene is expressed as a fusion with the GAL4 DNA-BD (bait), while another gene or cDNA is expressed as a fusion with the GAL4 DNA-AD (prey) (Fields and Song 1989; Chien et al. 1991). The Two-Hybrid technique exploits the fact that Gal4 cannot function as a transcription activator unless physically bound to an activation domain, through an interaction that does not need to be covalent. A Two-Hybrid assay is performed by expressing the two fusion proteins in yeast. The prey and bait constructs are introduced, by co-transformation or mating, into yeast strains

containing the appropriate "Upstream Activating Sequence" (UAS) proximal to a reporter gene. The reporter gene is expressed if a binding interaction occurs between the DNA-BD fused protein and the DNA-AD fused protein. Each Gal4 responsive gene contains a UAS target site, when Gal4 binds the UAS transcription is activated from a downstream promoter. By linking the Gal4 UAS with other metabolic genes (e.g. ADE2, HIS3, MEL1 and lacZ) and by eliminating the wild type GAL4 gene, researchers have developed yeast strains that change phenotype when Gal4 is activated. Although the Gal4 DNA-BD can bind the UAS, it cannot activate transcription by itself. Transcription is activated only when the other half of the protein, Gal4 DNA-AD, joins the DNA-BD at the UAS (Figure 5).

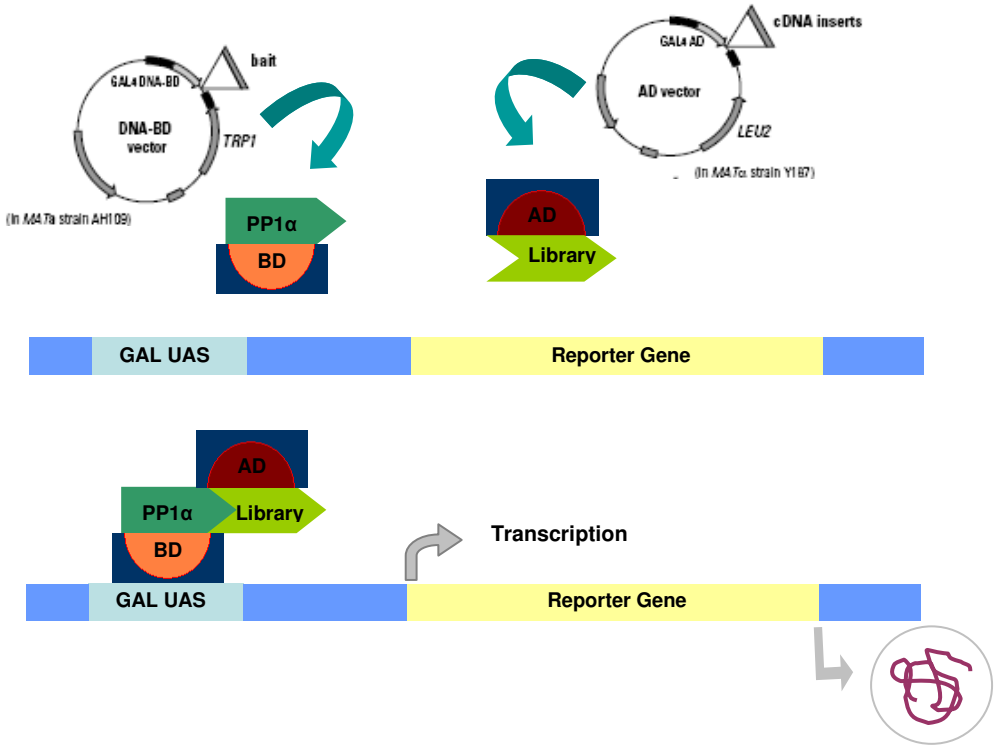

Figure 5 - *The Yeast Two-Hybrid system. Two fusion proteins are expressed in yeast: GAL4 DNA-binding domain (BD) fused to a bait protein, PP1α in the present work, and GAL4 activation domain (AD) fused to a prey protein, a human brain library in this case. The BD-bait hybrid protein can bind to upstream activation sites (UAS) but cannot activate transcription. The AD-prey protein cannot recognize the UAS, thus, alone is not capable of initiating transcription. When the bait and the prey interact, the BD and AD are brought together and can activate reporter gene transcription.*

When using a large scale screen, a plasmid library, expressing cDNA-encoded AD-fusion proteins, can be screened by introduction into a yeast strain. These larger scale Two-

Hybrid approaches typically rely on interaction by yeast mating (Finley and Brent 1994; Serebriiskii et al. 2001b).

When the two transformant cultures, from compatible yeast strains, are matted to each other, diploid cells containing four reporter genes (HIS3, ADE2, MEL1 and lacZ) are originated. If the protein interaction occurs, transcription of the reporter genes is activated allowing growth on nutritional selection media and expression of α-galactosidase (MEL1 product) and β-galactosidase (lacZ product). Hence, high-stringency selection uses medium lacking tryptophan, leucine, histidine and adenine, and also the presence of X-α-Gal. The selection of positive clones with the five reporter genes TRP1, LEU2, HIS3, ADE2 and MEL1 was designed to reduce the number of false positives, since the various reporter genes are under the control of distinct UAS and TATA boxes. An additional benefit of using yeast mating is that diploid cells are more tolerant to expression of toxic proteins and yield less false positives, since the diploids have reporter genes less sensitive to transcription (Kolonin 2000).

1.2.2 Advantages and Limitations of the Yeast Two-Hybrid System

Disadvantages

- An obvious problem would arise if the protein of interest was capable of activating transcription on its own (auto-activation). It is, therefore, imperative to test the transcriptional activity of the protein of interest, in preliminary experiments.
- The use of fusion proteins may change the conformation of the prey or bait, which may consequently alter activity or binding. Nevertheless, few problems have been reported with tagged proteins, perhaps due to their modular nature, where domains can fold independently, often allowing the introduction of artificial modules.
- A major concern of testing protein-protein interactions using a heterologous system such as yeast, is the fact that some interactions may depend on specific post-transcriptional modifications, such as disulfide bridge formation, glycosylation, or phosphorylation, which may not occur properly or at all in the yeast system (Fields and Sternglanz 1994).
- Since the fusion proteins in the Two-Hybrid system must be targeted to the nucleus, extracellular proteins or proteins with stronger targeting signals may be at a disadvantage.

- It has been shown that certain protein domains may interact better than the full length protein, perhaps due to the lack of certain folding restraints. Since library screening selects for optimized reactions, one may obtain a false representation. This problem can be minimized by using libraries enriched for full-length cDNAs in the correct reading frame.
- Given that the Two-Hybrid assay relies on reporter activity, it cannot be excluded that a third protein may be bridging the prey and the bait. Although unlikely, this possibility should not be excluded.
- Certain proteins, when expressed in the yeast system or targeted to the nucleus, may become toxic. Other proteins may degrade essential yeast proteins or proteins whose presence is required for the assay. Such genes may be counter-selected for during growth and may distort the results obtained.
- The identification of false binding partners presents itself as the main disadvantage of the Two-Hybrid assay. Even though two proteins can interact, it is not certain that they will interact in physiological conditions. Therefore, the biological relevance of the proteins identified must always be confirmed using alternative methodology.

Advantages

- The yeast Two-Hybrid system has a clear advantage over classical biochemical or genetic methods, in that it is an *in vivo* technique.
- The use of the yeast host, as it bears a greater resemblance to higher eukaryotic systems, is an advantage over systems based on bacterial hosts.
- The Two-Hybrid system has minimal requirements to initiate screening, since only the cDNA of the gene of interest is needed.
- In signalling cascades, weak and transient interactions are often very important. The YTH system provides a sensitive method for detecting those interactions because such interactions are significantly amplified due to transcriptional, translational and enzymatic events. Such interactions may not be biochemically detectable, but even so be critical for proper cell functions (Guarente 1993; Estojak et al. 1995).
- The Two-Hybrid assay is also useful for the analysis of known interactions. It can be used to pinpoint specific residues critical for protein interaction and to evaluate protein variants for the relative strength of their interactions (Yang et al. 1995).

- Interactions can be measured semi-quantitatively using the YTH system, allowing discrimination between high, intermediate, and low-affinity binding, the power of which correlates with that of *in vitro* approaches .
- Although the Two-Hybrid assay was predicted to be limited to the study of cellular proteins, given that extracellular proteins often undergo modifications such as glycosylation or disulfide cross-links that are not expected to occur in the yeast nucleus, there have been various reported successes with extracellular receptor/ligand complexes.
- Two-Hybrid screens are sometimes termed "functional screens", since if at least one of the proteins screened has a known function in a well-defined pathway, it might provide a functional hint in the current interaction.
- Although there are certain disadvantages involving the Two-Hybrid assay, the most convincing argument for its use is the speed and ease by which the molecular mechanisms of many signalling cascades have been defined using this technique.

1.3 AIMS OF THIS THESIS

Taking into account all the roles that have been attributed to PP1 based on its binding subunits, it is extremely important to identify novel PP1α binding proteins which may play critical regulatory and targeting roles for. Moreover, relatively little is known about isoform specific PP1 regulators. The Yeast Two-Hybrid (YTH) systems provide a sensitive method for detecting relatively weak and transient protein interactions.
The main goal of this thesis was to identify the proteins expressed in human brain that interact with PP1α, since it is known to be highly and specifically enriched in dendritic spines. Ultimately, the identification of hitherto uncharacterised PP1α interacting proteins may address novel functions of PP1α in brain and PP1 associated diseases. It was hoped that this work could lead to the potential identification of new therapeutic targets for neurodegenerative disorders and aging. Thus, the specific aims of this thesis were:

- To identify proteins expressed in human brain that interact with the PP1α isoform using the Yeast Two-Hybrid system – the human brain PP1α interactome.

- To select proteins of interest by careful analysis of the identified proteins by bioinformatic methods.

- To confirm the interaction of such proteins with PP1α and other PP1 isoforms.

In order to identify potential PP1 interacting and regulating proteins, and to characterize the PP1α human brain interactome a large scale screen for PP1α binding proteins was performed, using the Yeast Two-Hybrid (YTH) system (Fardilha et al. 2004). A total of 76 proteins were identified from the 298 positive clones obtained, that are expressed in human brain and bind PP1α.

2 YEAST-TWO HYBRID SCREENING BY YEAST MATING

2.1 INTRODUCTION

In order to find new interactions between PP1α and other proteins a screen using the MATCHMAKER GAL4 Two-Hybrid System was carried out using a human brain cDNA library (Clontech). The transformants were assayed for HIS3, ADE2 and MEL1 reporter gene activation after first clearing bait protein expression by immunoblotting, following preparation of yeast protein extracts.

The YTH screen was performed by yeast mating, instead of the more common cotransformation protocol. By using the yeast mating protocol more unique positive clones are obtained due primarily to the "jump-start" that the new diploids receive before being plated on selective medium. Diploid yeast cells are also more resistant than haploid cells and can tolerate better the expression of toxic proteins. Additionally, in diploids, the reporters are less sensitive to transcription activation than in haploids, thus reducing the incidence of false positives from transactivating baits.

The Gal4 System identifies the interaction between two proteins by reconstituting active Gal4 protein. The two proteins involved are expressed as fusion proteins with the Gal4 BD and AD. The two plasmids containing these constructs were introduced into yeast strains AH109 and Y187, containing the upstream activation sequences from the GAL1-GAL10 regions, which promote transcription of the MEL1 gene. When interaction occurs between the DNA-BD and DNA-AD fusion proteins, MEL1 is transcribed, resulting in the development of blue colour for the strain when plated in medium containing X-gal (a chromogenic substrate). The yeast host lacks functional GAL4 and GAL8 genes.

The vector used to insert the bait cDNA encoding PP1α, was Clontech's GAL4 binding domain expression vector pAS2-1 (see Appendix III). pAS2-1 has several characteristics that make it suitable for YTH usage. It has the GAL4-BD, two independent yeast and bacteria replication origins, confers ampicillin and cycloheximide resistance and allows the yeast to grow without tryptophan in the culture media. It also has a multiple cloning site useful for inserting the bait cDNA.

2.2 MATERIAL AND METHODS

All solutions compositions are described in Appendix I.

2.2.1 Construction of the bait plasmid

The pAS2-1 vector was digested with the restriction enzymes *BamHI* and *EcoRI*. The PP1α coding insert was generated by PCR, with the *EcoRI* and *BamHI* restriction sites incorporated into the primers used. The PCR product was sequentially digested with *BamHI* and *EcoRI* and then ligated to the previously prepared vector. Plasmid DNA was analysed with a convenient restriction endonuclease, namely *HindIII*. The resulting plasmid, named pAS-PP1α, was fully sequenced to check the orientation of the PP1α sequence, to validate the reading frame of the fusion protein, did to ensure it did not contain any mutations introduced by the PCR process. This part of the work was partly carried out in collaboration with Ana Paula Vintém and Carla Lopes.

2.2.2 Expression of the bait protein in yeast

In order to verify the ability of the recombinant construct to drive PP1α expression, it was transformed into yeast strain AH109. The transformed cells were grown on appropriate media (see below) and PP1α expression was confirmed by immunobloting of the corresponding protein extracts.

2.2.2.1 Yeast transformation with plasmid DNA

Preparation of competent yeast cells

One yeast colony was inoculated into 1 mL of YPD medium in a 1.5 mL microtube and vortexed vigorously to disperse cell clumps. The culture was transferred into a 250 mL flask containing 50 mL of YPD and incubated at 30º C with shaking at 230 rpm overnight, until it reached stationary phase with $OD_{600nm} > 1.5$. Enough of this culture (20-40 mL) was transferred into 300 mL YPD in a 2 L flask to yield an OD_{600nm}= 0.2-0.3. The culture was incubated at 30º C with shaking at 230 rpm, until OD_{600nm} = 0.4-0.6, and then centrifuged

at 2,200 rpm for 5 min, at RT, and the supernatant was discarded and the cells resuspended in 25 mL H_2O. The cells were recentrifuged and the pellet was resuspended in 1.5 mL of freshly prepared, sterile 1X TE/LiAc.

Yeast transformation- Lithium acetate (LiAc)-mediated method

In a microtube 200 ng of plasmid DNA were added to 100 µg of salmon testes carrier DNA. Then, 100 µL of freshly prepared competent cells were added to the microtube, followed by 600 µL of sterile PEG/LiAc (40% PEG 4000/ 1X TE/ 1X LiAc). The solution was incubated at 30º C for 30 min with shaking (200 rpm). After adding 70 µL of DMSO the solution was mixed gently and then heat-shocked for 15 min in a 42º C water bath. The cells were chilled on ice and pelleted by centrifugation for 5 sec at 14,000 rpm and resuspended in 0.5 mL of 1X TE buffer. The cells (100 µL) were then plated in the appropriate SD selection medium (e.g. SD/-Trp for the plasmid pAS2-1), and incubated at 30º C for 2-4 days, until colonies appear.

2.2.2.2 Expression of proteins in yeast

Preparation of yeast cultures for protein extraction

A colony of the previously transformed yeast was inoculated into 5 mL of the appropriate SD selection medium and incubated at 30º C with shaking at 230 rpm overnight. As a negative control an untransformed yeast colony was inoculated in YPD. The overnight cultures were vortexed and separately added to 50 mL aliquots of YPD. These cultures were incubated at 30º C with shaking (220 rpm) until OD_{600nm} = 0.4-0.6. At this point the cultures were quickly chilled by pouring them into a prechilled 50 mL centrifuge microtube halfway filled with ice. The tubes were immediately centrifuged at 1,000 g for 5 min at 4º C. The supernatant was discarded and the cell pellet was washed in 50 mL of ice-cold water. The pellet was recovered by centrifugation at 1,000 g for 5 min at 4º C and immediately frozen by placing tubes in liquid nitrogen.

Preparation of protein extracts

The cell pellet, prepared as previously described, was quickly thawed by resuspending each one in 100 µL of prewarmed cracking buffer (60º C) per 7.5 OD_{600} units of cells (OD_{600} of a 1 mL sample multiplied by the culture volume). The samples were briefly thawed in a 60º C water bath. After 15 min an additional aliquot (1 µL of 100X PMSF per 100 µL of cracking buffer) of the 100X PMSF stock solution was added to the samples

and every 7 min thereafter during the procedure. Each cell suspension was transferred into a 1.5 mL microtube containing 80 µL of glass beads per 7.5 OD_{600} units of cells. The samples were heated at 70º C for 10 min to release the membrane-associated proteins. Then, the microtubes were vortexed vigorously for 1 min and centrifuged at 14,000 rpm for 5 min at 4º C. The supernatants were transferred to fresh microtubes and placed on ice. The pellets were boiled for 5 min, vortexed for 1min and centrifuged again, with the resulting supernatants being combined with the previous. The samples were boiled and loaded immediately on a gel.

SDS-PAGE

In order to visualize the fusion protein GAL4-BD/PP1α, with a calculated molecular weight around 58 kDa, a 12% acrylamide gel was used (Table 2).

Table 2 - *Composition of the running and stacking gels for SDS-PAGE.*

Components	Running gel (12%)	Stacking gel (3.5%)
Water	10.35 mL	6.60 mL
30%Acryl./8%Bisacryl.	12.00 mL	1.20 mL
4X LGB	7.50 mL	-
5X UGB	-	2.00 mL
SDS 10%	-	100.0 µL
10% APS	150.0 µL	100.0 µL
TEMED	15.0 µL	10.0 µL

The 12% running gel was prepared by sequentially adding the components indicated on Table 2 (APS and TEMED were added last, as they initiate the polymerising process). The solution was then carefully pipetted down the spacer into the gel sandwich, leaving some space for the stacking gel. Then, water was carefully added to cover the top of the gel and the gel was allowed to polymerise for 1 hr. The stacking gel was prepared according to Table 2. The water was poured out and the stacking gel was added to the sandwich; a comb was inserted and the gel was allowed to polymerise for 30 min. Then, the samples were prepared by the addition of ¼ volume of loading gel (LB) buffer. The microtube was boiled and centrifuged, the combs removed and the wells filled with running buffer. The samples were carefully applied into the wells that were filled with running buffer, and the

samples were run at 45 mA until the bromophenol blue from the LB reached the bottom of the gel.

2.2.2.3 Immunoblotting

For immunoblotting the tank transfer system was used as follows: 3MM blotter paper was cut to fit the transfer cassette and a nitrocellulose membrane of the gel size was also cut. The gel was removed from the electrophoresis device and the stacking gel removed and discarded. The transfer sandwich was assembled under transfer buffer to avoid trapping air bubbles. The cassette was placed in the transfer device filled with transfer buffer. Transfer was allowed to proceed overnight at 200 mA. Afterwards, the transfer cassettes were disassembled; the membrane carefully removed and allowed to air dry prior to further manipulations.

Immunodetection by enhanced chemiluminescence (ECL)

ECL™ is a light emitting non-radioactive method for the detection of immobilised antigens, conjugated directly or indirectly with horseradish peroxidase-labelled antibodies. In order to visualize the fusion protein GAL4 DNA-BD/PP1α the blots was probed with a polyclonal antibody (CBC2C), which recognizes human PP1α (da Cruz e Silva et al. 1995b).

The membrane was soaked in 1X TBS for 10 min. Non-specific binding sites were blocked by immersing the membrane in 5% low fat milk in TBST for 1 hr. After washing with 1X TBST, the membrane was incubated with a solution of the primary (anti-PP1α) antibody diluted in 3% low fat milk in TBST for 1 hr with shaking. After three washes of 10 min each in 1X TBST the membrane was incubated with a solution of the anti-rabbit secondary antibody diluted (1:5000) in 3% low fat milk in TBST for 1 hr with shaking. The membrane was then washed 3 times for 10 min.

Subsequently the membrane was incubated for 1 min at RT with the ECL detection solution (a mixture of equal volumes of solution 1 and solution 2 from the ECL kit (Amersham), approximately 0.125 mL/cm^2 membrane). Inside the dark room, the membrane was gently wrapped with cling-film, eliminating all air bubbles and placed in a film cassette and an autoradiography film (XAR-5 film, KODAK) was placed on the top. The cassette was closed and the blot exposed for short periods of time. The film was then removed and developed in a developing solution, washed in water and fixed in fixing solution. If needed, a second film was exposed more or less time according to the first result.

2.2.3 Library screening by yeast mating

A human brain cDNA library was screened to identify neuronal interacting partners for PP1α. By using a pretransformed library the most costly and time-consuming steps of library screening are optimized. These include, constructing the library, amplifying the library in *E. coli*, isolating the library DNA, performing the library-scale transformation of yeast strain Y187, plating the transformation mixture and harvesting the transformants at high viability and density in freezing medium.

A concentrated overnight culture of the bait strain (AH109 + pAS-PP1α) was prepared by inoculating a colony of the bait strain into 50 mL of SD/-Trp medium and incubating it at 30º C overnight with shaking at 250 rpm. The next day, when OD_{600}>0.8, the culture was centrifuged at 1,000 g for 5 min, the supernatant was decanted and the pellet was resuspended in the residual liquid (5 mL) by vortexing. Just prior to use, a frozen aliquot (1 mL) of the library culture (Pretransformed Human Brain MATCHMAKER cDNA Library, Clontech) was thawed in a room temperature water bath. The library was gently mixed and 10 µL were set aside for later tittering (see below). The entire bait strain culture was combined with the 1 mL library aliquot in a 2 L sterile flask, 45 mL of 2X YPDA were added and gently swirled. This culture was incubated at 30º C for 20-24 hr, with shaking at 40 rpm. After 20 hr of mating a drop of the mating culture was checked under a phase-contrast microscope to check for the presence of zygotes, thereafter allowing the mating to proceed for more 4 hr. The mating mixture was transferred to a sterile 50 mL tube and the cells spun at 1,000 g for 10 min. The mating flask was rinsed twice with 2X YPDA (50 mL) and the rinses were combined and used to resuspend the first pellet. The cells were centrifuged again at 1,000 g for 10 min, the pellet resuspended in 10 mL of 0.5X YPDA and the total volume (cells + medium) was measured. Half of the library mating mixture was plated on SD/QDO (SD without Leu, Trp, Ade and His), and the other half on SD/TDO (SD without Leu, Trp and His), at 200 µL per 150 mm plate. For mating efficiency controls, 100 µL of 1:10,000, 1:1,000; 1:100 and 1:10 dilutions of the mating mixture were plated in 100 mm SD/-Leu, SD/-Trp and SD/-Leu/-Trp plates. All plates were incubated at 30º C until colonies appeared, generally 3-8 days on TDO and 8-21 days on QDO medium. Then, growth of the control plates was scored and the mating efficiency and number of clones screened were calculated. All positive clones were replated twice in SD/QDO medium containing X-α-Gal and incubated at 30º C for 3-8 days. True positives form blue colonies. The master plates were sealed with parafilm and stored at 4º C. Glycerol stocks were prepared for all the positive clones.

2.2.3.1 Library tittering

A library aliquot (10 µL) was transferred to 1 mL of YPDA in a 1.5 mL microtube – *dilution A* (dilution factor 10^{-2}). 10 µL from *dilution A* were added to 1 mL of YPDA in another microtube and mixed gently – *dilution B* (dilution factor 10^{-4}). From *dilution B*, 100 µL were spread onto three SD/-Leu plates. All the plates were incubated at 30º C for 3 days after which the number of colonies was counted. The titter of the library was calculated using the following expression: [#colonies]/[plating volume (mL)x dil factor] = cfu/mL.

2.3 RESULTS

The plasmid pAS-PP1α was fully sequenced to check the orientation of the PP1α sequence, in order to validate the reading frame of the fusion protein (Figure 6)

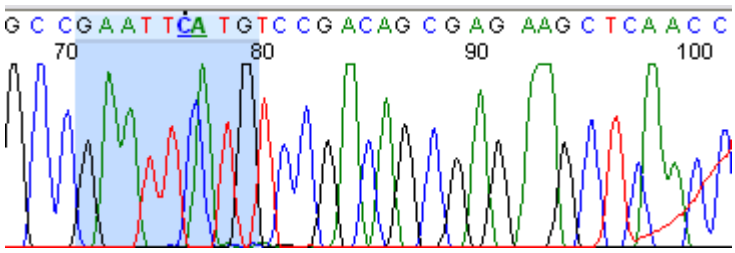

Figure 6 – *pAS-PP1α construct sequence analysis, EcoRI restriction sequence used for insertion with the starting codon ATG in frame is highlighted in blue colour.*

The fusion protein GAL4-BD-PP1α from the protein extracts was detected with an anti-PP1α antibody (da Cruz e Silva et al. 1995b) and an anti-rabbit secondary antibody conjugated to peroxidase. A protein extract from rat brain was used as a positive control and as a negative control the protein extract from the untransformed yeast strain (Figure 7).

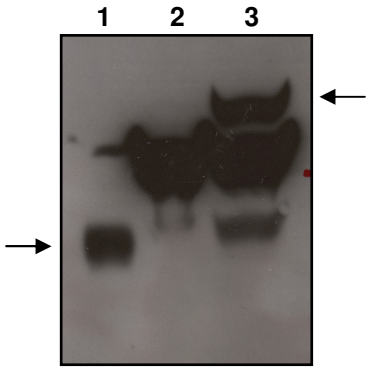

Figure 7 – *Immunoblot analysis of AH109 yeast protein extracts, probed with anti-PP1α antibody. Lane 1: protein extract from rat cortex; lane 2: untransformed yeast control; lane 3: yeast transformed with pAS-PP1α. The arrows indicate PP1α in lane 1, at 37 kDa and BD-PP1α fusion protein in lane 3, at 58 kDa.*

When probed with the anti-PP1α antibody, PP1α was detected in rat cortex (Figure 6, lane 1). Unspecific bands were also detected in the protein extract from untransformed yeast cells (Figure 6, lane 2). A band of the expected molecular mass (58 KDa) was only detected in the protein extract from yeast cells containing the pAS-PP1α plasmid (Figure 6, lane 3), demonstrating that this strain expresses the fusion protein.

The BD-PP1α protein was also tested for transcriptional activation of the reporter genes. The bait construct did not activate transcription from the UAS (the DNA sequence that is recognized by GAL4-BD), as detected by lack of growth of yeast cells containing the bait plasmid pAS-PP1α on selective media SD/-Trp-His, SD/-Trp-His-Ade and SD/-Trp-His-Ade/X-α-Gal (data not shown).

Once yeast cell expression of the fusion protein GAL4-BD-PP1α was confirmed as well as its inability to initiate transcription of the reporter genes by it self, the Yeast Two-Hybrid screen was performed. After transforming the bait plasmids into the appropriate yeast strain, AH109 (mat *a*), the next step was to obtain the desired library pretransformed in a yeast strain of the opposite mating type. A pretransformed pACT-2 library in the yeast strain Y187 (mat *α*) containing human brain cDNA sequences fused to the GAL4 transactivation domain was used.

The mating culture was checked under a phase-contrast microscope to check for the occurrence of zygotes (Figure 8), indicative that mating was occurring as expected.

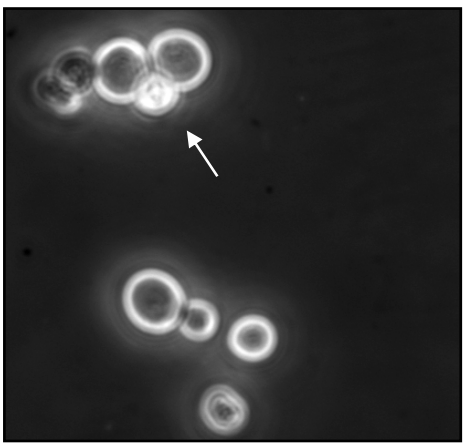

Figure 8 – *Zygote formation in the mating mixture with its typical three-lobed shape. The small lobe in the middle is the budding diploid cell (arrow), the other two lobes are the two haploid (parental) cells. This picture was taken using an inverted microscope in phase contrast mode, during the mating event (40X magnification).*

To calculate de number of clones screened the following equation was used [# cfu/mL of diploids X resuspension volume]. To calculate the mating efficiency the following equation was used [# cfu (in SD –Leu/-Trp) X 1000µL/mL/ volume plated (µL) x dilution factor] / [#

cfu (in SD -Trp) X 1000µL/mL/ volume plated (µL) X dilution factor] X 100. A summary of the results obtained is presented below in Table 3.

Table 3 - *Results from the Yeast Two-Hybrid screen.*

Positive clones	Mating efficiency (% diploids)	Clones screened
298	30.25	$1{,}72\times10^{7}$

In the YTH screen 495 clones were initially obtained, 446 from SD/TDO and 49 from SD/QDO media. All the colonies were re-streaked in SD/QDO plates in order to test for the expression of the nutritional reporter genes HIS3 and ADE2. These clones were further tested for MEL1 expression, another reporter gene, by growing these putative primary positive clones in SD/QDO medium with X-α-Gal. True positive clones produce a blue colour (Figure 9), resulting in a total of 298 true positive clones, thus identified in this screen. Of these, 258 were originated from SD/TDO and 40 from SD/QDO media. The positive clones were named *1-298 T* or *Q* as they were obtained from TDO or QDO media, respectively.

Figure 9 – *Positive clones identified in the YTH screen, recovered from the original SD/TDO or SD/QDO plates. MEL-1 expression of the positive clones obtained in the YTH screen is detected by the formation of blue colonies in the presence of X-α-GAL. White colonies represent false positives that grew on SD/QDO medium but could not turn blue in the presence of X-α-GAL.*

2.4 DISCUSSION

As with all detection methods, the YTH system is known to result in the detection of some false positives. This was a relatively serious problem in the early days of the YTH method but the elimination of such false positive results has been greatly improved in recent times. False positive signals result from cells in which the reporter genes are active even though the bait and prey do not interact. There are several classes of false positives. For example, false positives may arise from a prey that interacts with DNA upstream of the reporter genes or with proteins that interact with promoter sequences. These two classes of false positives can be eliminated by the use of more than one reporter gene under the control of different promoters, as was the case with the present work. Another inherent problem with the system is that not all proteins will be efficiently folded and/or post-translationaly modified in the yeast nucleus, which may result in the protein not interacting with the true partner. In the same way, the protein may adopt a different tertiary structure when expressed as fusions with the transcription factor domains. Also, some proteins may be toxic when expressed as fusions in yeast, inhibiting growth when expressed at high levels. This can be avoided to some extent by the use of inducible expression plasmids. Other false positive results include interactions that occur in the YTH screen but not in a physiological context, because the partners are not expressed in the same cellular or subcellular environment at the same time.

The credibility of interactions identified in an YTH screen should be evaluated through supplementary data from other sources. By this means, the verification of a putative interaction can be achieved in a variety of ways. One approach is to mix the recombinant proteins and verify binding *in vitro* through a variety of biochemical assays. Another approach is to express both proteins in mammalian cells by transfection and analyse interactions by immunoprecipitation studies. However, even if co-immunoprecipitation is successful, there is still the possibility that the proteins only interact under the conditions used. So, a crucial validation of the Two-Hybrid results is to prove that the two proteins exist in the same subcellular environment, by doing immunoprecipitation in the tissue of interest.

In the present work, the PP1α bait vector was successfully constructed, shown to drive PP1α expression in yeast and to be unable to drive reporter gene expression by it self. It was then used successfully to screen a human brain cDNA library, thus defining the human brain PP1α interactome. By screening $1{,}72\times10^{7}$ clones from a human brain cDNA

library with PP1α as bait 298 positive clones were obtained as accessed by their ability to grow on SD/QDO selective media and to turn blue in the presence of X-α-Gal.

The following chapter will deal with the analysis and the characterization of the positives obtained. Although it was expected most of the 298 positives to encode true PPα interacting proteins, some may prove to be false positives. Further work will be required to define the relevant physiological interactors.

3 CHARACTERIZATION OF THE POSITIVE CLONES

3.1 INTRODUCTION

The majority of the PP1 binding proteins that have been identified to date were discovered using the YTH method. Frequently, when performing a YTH screen, only few clones are selected and further characterized. Using such an approach many of the rarer positive clones are never analyzed, and some important potential interacting proteins may be missed.

In this screen, 298 positive clones were obtained and we decided to analyse all in order to identify not only the most abundant interactions but also the more interesting ones, even though they may have been detected only once or twice in the screen. This does not mean they are not important but may simply reflect the low abundance of the mRNA in the library used or its low abundance in the tissue from which the library was made.

All positive clones were partially sequenced, their identity was verified by comparison to the Genbank database and preliminary analysis was performed on all the positives identified. Some of the identified PP1α interacting proteins were chosen for further study.

3.2 MATERIALS AND METHODS

All solutions compositions are described in Appendix I.

3.2.1 Plasmid isolation from yeast

3.2.1.1 Yeast plasmid extraction by the "Boiling" method

A single yeast colony was grown in SD/QDO medium and 3 mL of yeast cells were pelleted for 3 min at 14000 rpm and resuspended in 100 µL of STET solution. About 300 µL of 0.5 mm acid-washed glass beads (Sigma) were added and vortexed on high for 6-8 min. After adding 100 µL of STET solution the tubes were boiled for 3 min. After chill on ice, the tubes were centrifuged for 10 min at 14000 rpm at 4º C. The supernatant was transferred into a new microtube, 500 µL of ammonium acetate 7.5 M was added and mixed briefly and the tubes were incubated for 1-2 hrs at -20º C. The tubes were, then, centrifuged for 20 min at 14000 rpm and 4º C and the supernatant transferred to new tubes containing 200 µL of ice cold ethanol. After spinning down for 10 min at 14000 rpm and 4º C, the supernatant was removed and the tubes rinsed with 200 µL of 70% ethanol. Another 5 min centrifugation was performed and the pellet was dried in a vacuum device. The pellet was resuspended in 15 µL of sterile 20 µg/mL RNase solution.

3.2.2 Bacteria transformation

3.2.2.1 Preparation of *E. coli* competent cells

A single colony of *E. coli* XL1-Blue was incubated in 10 mL of SOB medium at 37º C overnight. Then, 1 mL of this culture was used to inoculate 50 mL of SOB and the culture was incubated at 37º C with shaking at 220 rpm for 1-2 hr, until OD_{550nm}=0.3. The culture was cooled on ice for 15 min and centrifuged at 4,000 rpm at 4º C for 5 min. The supernatant was discarded and the pellet resuspended in 15 mL of Solution I. After standing on ice for 15 min, the cells were centrifuged at 4,000 rpm for 5 min at 4º C and

3 mL of Solution II were added to resuspend the cell pellet. The cells were immediately divided in 100 µL aliquots and stored at -80º C.

3.2.2.2 Bacteria transformation with plasmid DNA

Competent cells (100 µL) were thawed on ice and 1-50 ng of DNA were added to the cells and gently swirled. The microtube was incubated on ice for 20 min and heat shocked at 42º C for 90 sec. The microtubes were then incubated on ice for 30 min before adding 0.9 mL of SOC medium. The tubes were subsequently incubated at 37º C for 30 min with shaking at 220 rpm. The culture was centrifuged at 14,000 rpm and the supernatant discarded. The cells were then resuspended in 100 µL of the selective medium and spread on the appropriate agar medium. The plates were incubated at 37º C for 16 hr until colonies appeared. Control transformations were also performed in parallel. These always included a negative control transformation without DNA and a positive control transformation with 1 ng of a control plasmid, such as pAS2-1.

3.2.3 Analysis of the positive plasmids by restriction digestion and sequencing

In order to screen for the recombinant plasmid in the transformants, the plasmid DNA was extracted from several isolated bacterial colonies and digested with the restriction endonuclease *HindIII*, and the fragments produced were separated by agarose gel electrophoresis.

The vector used (pACT-2) produces a characteristic pattern of fragments that allows its differentiation from colonies resulting from transformation by the bait vector. Plasmids generating DNA fragments characteristic of the pACT-2+library insert digested with *HindIII* were further analysed by sequencing with the GAL4-AD primer (Clontech; see Appendix IV).

A search for similar sequences in the Genbank database was performed using the BLAST algorithm [Basic Local Alignment Search Tool, (Altschul et al. 1990)].

3.2.3.1 Isolation of plasmids from transformants

Method 1 – Alkaline lysis "mini-prep"

A single bacterial colony was transferred into 3 mL of LB medium containing ampicillin (100 µg/mL) and incubated overnight at 37º C with vigorous shaking (220-250 rpm). 1.5 mL of this culture were transferred into a microtube and centrifuged at 14,000 rpm for 1 min at 4º C and the supernatant was discarded. The cell pellet was resuspended in 100 µL of ice-cold solution I by vigorous vortexing. Then, 200 µL of freshly prepared solution II were added to the microtube that was mixed by inverting several times. Keeping the microtube on ice, 150 µL of ice-cold solution III were added and again the microtube inverted several times. The microtube was then allowed to stand on ice for 5 min, centrifuged at 14,000 rpm for 10 min at 4º C and the supernatant transferred to a clean microtube. The DNA was precipitated by adding 2 volumes of ice-cold ethanol. The mixture was vortexed and placed at -20º C for 30 min. After centrifugation at 14,000 rpm for 10 min at 4º C, the supernatant was completely removed and the pellet washed with 70% ethanol. Following centrifugation, the pellet was allowed to air-dry for 10 min. The DNA was dissolved in DNAase-free H_2O containing RNAase (20 µg/mL) and stored at -20º C.

Method 2 – QIAGEN "miniprep"

The bacterial pellet was obtained as described above. The pellet was then resuspended in 250 µL of buffer P1, 250 µL of buffer P2 were added and the microtube was mixed by gently inverting until the solution became viscous and slightly clear. Afterwards, 350 µL of buffer N3 were added and the microtube was repeatedly inverted until the solution became cloudy. The microtube was centrifuged for 10 min and the resulting supernatant was applied to a QIAprep spin column placed in a microtube. After a 1 min centrifugation the flow-through was discarded. The column was washed by adding 0.75 mL of buffer PE and centrifuged for 1 min to discard the flow-through, and then a subsequent 1 min centrifugation to remove residual wash buffer. Finally, the column was placed in a clean microtube and 50 µL of H_2O were added to elute the DNA by centrifuging for 1 min having let it stand for 1 min. This method gives a cleaner DNA preparation than Method 1 and with better yields. This method was used when the DNA was subsequently to be processed for DNA sequencing. For enzymatic restriction the first method was more commonly employed.

3.2.3.2 Restriction fragment analysis of DNA

Plasmid DNAs were analysed through the digestion with a convenient restriction endonuclease, namely *HindIII* (New England Biolabs). For plasmid DNA digestion the manufacturer's instructions were followed. In a microtube the following components were added:

100 µg/mL DNA
1X reaction buffer (specific for each restriction enzyme)
1 U/µg DNA of restriction enzyme

The mixture was incubated at the appropriate temperature (37º C for *HindIII*) for a few hrs.

3.2.3.3 Electrophoretic analysis of DNA

The electrophoresis apparatus was prepared and the electrophoresis tank was filled with enough 1X TAE to cover the agarose gel. The appropriate amount of agarose was transferred to an Erlenmeyer with 50 mL 1X TAE. The slurry was heated until the agarose was dissolved and allowed to cool to 60º C before adding ethidium bromide to a final concentration of 0.5 µg/mL. The agarose solution was poured into the mold and the comb was positioned. After the gel became solid the comb was carefully removed and the gel mounted in the tank. The DNA samples were mixed with the 6X loading buffer (LB) and the mixture was loaded into the wells of the submerged gel using a micropipette. Marker DNA (1kb ladder or λ-HindIII fragments) of known size was also loaded onto the gel. The lid of the gel tank was closed and the electrical cables were attached so that the DNA migrated towards the anode. The gel was run until the bromophenol blue had migrated the appropriate distance through the gel. At the end, the gel was examined under UV light and photographed or otherwise analysed on a Molecular Imager (Biorad).

3.2.3.4 DNA sequencing

All the DNA samples to be sequenced followed the same protocol. If the DNA had been obtained by the "alkaline lysis miniprep" method and had not been purified by QIAGEN miniprep spin column, then it was purified in a QIAquick spin column (QIAGEN DNA Purification Kit) as described bellow, before being processed for sequencing.

QIAGEN DNA Purification

Briefly, 5 volumes of buffer PB were added to 1 volume of the solution to be purified and mixed. The QIAquick spin column was placed in a collection microtube and the sample was applied to the column and centrifuged for 1 min at 14000 rpm to bind the DNA. The flow-through was discarded and the column was washed with 0,75 mL of buffer PE, centrifuged for 1 min at 14000 rpm and the flow-through discarded. The column was placed back in the same microtube and centrifuged again to remove traces of washing buffer. Then, the column was placed in a clean microtube, 50 mL of H2O were added and allowed to stand for 1 min. To elute the DNA the column was centrifuged for 1 min at 14000 rpm. The DNA was stored at -20º C.

Sequencing PCR reaction

In a 0,2 mL microtube the following components were mixed:

500 ng dsDNA
4 µL Ready Reaction Mix*
10 pmol primer
H_2O to a final volume of 20 µL

* Ready Reaction Mix is composed of dye terminators, deoxynucleoside triphosphates, AmpliTaq DNA polymerase, FS, rTth pyrophosphatase, magnesium chloride and buffer (Applied Biosystems).

This reaction mixture was vortexed and spun down for a few seconds. The PCR was then performed using the following conditions:

96º C 1 min
96º C 30 sec
42º C 15 sec
60º C 4 min — 25 cycles

Afterwards, the samples were purified by ethanol precipitation. Briefly, 2.0 µL of 3 M sodium acetate (pH 4.6) and 50 µL of 100% ethanol were added to the reaction microtube. The microtube was vortexed and incubated at RT for 20 min to precipitate the

extension products. The microtube was then centrifuged at 14,000 rpm for 20 min at RT. After discarding the supernatant 250 µL of 70% ethanol were added, the microtube was briefly vortexed and recentrifuged for 5 min at 14000 rpm at RT. The supernatant was discarded and the pellet dried. After this procedure the DNA was sent to the sequencing facility where there is an Automated DNA Sequencer (ABIPRISM 310, Applied Biosystems).

3.2.4 Yeast colony hybridization

In order to reduce the number of clones that needed to be sequenced, all positives resulting from the screen were subjected to colony hybridization using appropriate oligonucleotides.

3.2.4.1 Filter preparation

The nitrocellulose filter was placed on an agar plate containing the nutritional selective media QDO. Using autoclaved toothpicks isolated colonies were patched onto the filter, including positive and negative controls, already confirmed by sequencing. The filter was incubated overnight at 30º C. Pieces of 3MM Whatman paper were cut, with the same size of the filters, placed in Petri dishes and then soaked with 6 mL of freshly made SCE/DTT/Lyticase solution. The filters were lifted from the growth media and placed (cell side up) on the satured paper avoiding the formation of air bubbles. The Petri dish was covered and placed into a plastic bag and incubated overnight at 30º C. Filter sized pieces of 3MM paper were cut, placed in Petri dishes and soaked, avoiding the formation of bubbles, with 6 mL of each one of the different treatment solutions. Then the filters were placed on the following solutions, for the given times: Lysis solution, 5 min; Denaturing solution, 10 min; Neutralizing solution, 5 min and Washing solution, 3 times 5 min. The filters were placed on a sheet of 3MM paper to dry for an hr and then were UV cross linked (2 times autocross link for 30 sds) or baked for 1 hr in a 80º C vacuum oven, between pieces of 3MM paper. The filters were stored between pieces of 3MM paper and kept in the dark.

3.2.4.2 Probe preparation and labelling

The probe DNA was separated in a 1% low melting agarose gel at 4º C and 50 V. Part of the gel was stained with etidium bromide (0.2 µg/mL) and aligned with the non stained part of the gel in order to cut the appropriate band. The cutted band was placed in a pre-weighted tube. Water was added in a ratio of 3 mL/g of gel slice and placed in a boiling water bath for 7 min and stored at -20º C. Just before use the sample was re-boiled for 3 min and stored at 37º C (for 10-30 min) until the labelling reaction.
For DNA probe labelling the High Prime DNA Labeling Kit (Roche) was used to label 25 ng of template DNA adding sterile water to a final volume of 8 µL. A control reaction was performed side by side with control DNA. The reaction mixture was obtained by mixing the 8 µL of DNA , on ice, with 4 µL of high prime reaction mixture, 3 µL of dATP, dGTP, dTTP mixture and 5 µL of 50 µCi [α^{33}P]dCTP, 3000Ci/mmol, aqueous solution. After 2 hrs of incubation, at 37º C, the reaction was stopped by adding 2 µL of 0.2M EDTA (pH 8.0) solution and by heating to 65º C for 10 min. The probe was, then, purified using a push column beta shield device and Nuctrap probe purification columns (Stratagene).

3.2.4.3 Filter Hybridization

The filters were floated in destilled water and once completely wet were submerged for a few min. Afterwards the filters were transferred to 3xSSC/0.1%SDS/1mMEDTA solution at 45º C for 15 min. After rubbing the filters to remove cell debris, they were left in the same solution for another 15 min with shaking. Then the filters were incubated in hybridization solution (0.1 mL/cm2) at the hybridization temperature (65º C) in a glass hybridization bottle for 1 hr, making sure that there were no air bubbles and the solution was evenly distributed all over the filter.
The radioactively labelled DNA probe was denatured at 100º C for 5 min and then quickly chilled on ice. The labelled probe was added to the hybridization solution in the proportion of 1-2x10^6 cpm/mL and the hybridization was performed overnight at 65º C. The filter was rinsed with wash solution 1 (2xSSC/0.05%SDS) pre-warmed to 60º C, two times for 15 min. Then the filters were rinsed again with solution 1, at 65º C for 5 min, and with wash solution 2 (0.1xSSC/0.1%SDS) for another 5 min at 65º C. Then filters were removed from the hybridization bottles, the excess solution was removed without letting the filters dry, and were immediately covered with plastic wrap and exposed using a phosphor imaging

screen, or alternatively were exposed to X-ray films at -70º C with two intensifying screens.

3.2.4.4 Probe Striping

The filters were placed in pre-heated sterile 0.5% SDS solution to 100º C, making sure that the air exposal was minimal, for filters not to dry, and were incubated for 10 min with frequent shaking. Then the solution was left to cool down for about 10 min, the filters were removed and left to air dry and were finally stored at -20º C. The filters thus processed may be re-hybridized several times with different probes.

3.2.5 Verifying protein interactions by yeast co-transformation

To verify protein interactions, a small-scale LiAc yeast transformation procedure was performed, as previously described, combining the bait plasmid pAS-PP1α with specific positive clones isolated from the AD/library. The AD/library and pAS-PP1α plasmids to be tested were co-transformed into AH109 and selected on SD/-Leu-Trp. In parallel, co-transformation with the vectors pAS2-1 and pACT-2 was performed as a negative control. The association of murine p53 (encoded by plasmid pVA3) and SV40 large T antigen (plasmid pTD1) served as a positive control. To confirm protein-protein interactions, the fresh diploid colonies were assayed for growth on SD/QDO plates and for X-α-Gal activity.

3.2.6 Preparation of the pC9orf75-GFP construct

For a translational fusion of the clone Chr9orf75 cDNA with a reporter gene encoding GFP (pEGFP vector, Appendix III), the cDNA of Chr9orf75 was amplified by PCR using specific primers (Appendix IV). To that end, cDNA of clone 100T was used, since it contains the complete coding sequence of the corresponding protein. As the EGFP-tag is C-terminal, the stop codon of the protein was eliminated with the primers used.

3.2.6.1 PCR reaction

PCR reactions were performed using Pfu DNA Polymerase (Promega), a high fidelity polymerase that ensures that few or no mutations are introduced as a result of the PCR. In a 0.2 mL microtube the following components were added:

0,5 µL (50 ng) DNA template
1 µL (10 pmol) Primer Chr9orf75-F4
1 µL (10 pmol) Primer Chr9orf75-R5
2 µL (10 mM) dNTPs mixture
5 µL (10X) Pfu Buffer
0,5 µL Pfu
H_2O to a final volume of 50 µL

The PCR amplification condition used are described below:

94º C 5 min		
94º C 1 min 50º C 2 min 72º C 2 min	|	10 cycles
94º C 1 min 72º C 4 min	|	15 cycles
72º C 2 min		

Amplification was confirmed by running a 5 µL PCR reaction aliquot in a 1% agarose electrophoresis gel. The PCR products were ethanol precipitated, as previously described.

3.2.6.2 DNA restriction digestions

For subcloning of Chr9orf75 in the pEGFP mammalian expression vector, the PCR product and pEGFP vector were digested with *EcoRI* and *SalI* (New England Biolabs), at 37º C. For the DNA digestion the manufacturer's instructions were followed.

The digestions were performed sequentially, although in the same buffer, for several hrs. The first enzyme used (*EcoRI*) was heat inactivated, then BSA was added and also the second enzyme (*Sal I*). In a microtube the following components were added:

100 µg/mL DNA
1X reaction buffer (appropriate for both restriction enzymes)
1X BSA (Bovine Serum Albumin)
1 U/µg DNA of restriction enzyme
Water for a final volume of 150 µL

Afterwards, the digested DNAs were precipitated, as described before, resuspended in water and quantified by analysis in a 1% agarose electrophoresis gel.

3.2.6.3 DNA ligation of cohesive termini

Ligation of *EcoRI SalI* digested pEGFP vector and Chr9orf75 was carried out overnight at 16º C using bacteriophage T4 DNA ligase (Promega), in a final volume of 20 µL. Additional control reactions were also set up (Table 4).

Table 4 - *pEGFP vector and Chr9orf75 ligation reactions*

Tube	Vector (ng)	Chr9orf75 (ng)	Ligase (µL)	Buffer (µL)
Negative Control	-	-	-	2
Positive Control	20 (non cutted)	-	-	2
Vector (unligated)	20	-	-	2
Vector (ligated)	20	-	1	2
Ligation 1:3 ratio	20	16,6	1	2
Ligation 1:5 ratio	20	27,6	1	2
Ligation 1:10 ratio	20	55,3	1	2

Bacteria transformation for each ligation product was performed as described before, and cells were plated on agar medium plates, with the appropriate antibiotic (Kanamycin 30 µg/mL), and incubated at 37º C for 16-18 hrs, until colonies appeared. Control transformations were also carried out in parallel, as described in Table 4, including a negative control transformation without DNA and a positive control transformation with 1,0 ng of the control plasmid.

Bacterial plates were screened for transformant colonies, a single colony was transferred to a tube containing 5 mL of liquid LB/Kanamycin medium and incubated overnight at 37º C and 220 rpm. Subsequently, isolation of plasmids from transformants was performed using the "Miniprep" method, already described. In order to confirm the insertion of Chr9orf75 in the pEGFP vector restriction digestion reactions were performed using *BamHI, EcoRI and SalI* restriction enzymes. The pEGFP vector was also digested as a control. After digestion electrophoretic analysis of the DNA was carried out to identify those that yielded the expected bands. The next step was to confirm the correctness of the open reading frame of the fusion protein, by DNA sequencing.

3.2.6.4 Sequencing of the pC9orf75-GFP vector

All DNA samples to be sequenced were processed using the same protocol, as described before. In this case, two additional primers, one forward and one reverse (see Appendix V), were also used for sequencing procedures.

Thus the pC9orf75-GFP DNA fusion was confirmed in the correct reading frame as well as the entire coding sequence.

3.2.6.5 pC9orf75-GFP DNA amplification and purification

The Promega Pure Yield™ Plasmid Midiprep System was used for pC9orf75-GFP construct DNA purification. A single-transformant cell 200 mL culture was pelleted by centrifugation at 4000 g for 10 min at RT. The cells pellet was resuspended in 6 mL of cell resuspension solution by manually disrupting the pellet with a pipette. Next, 6 mL of cell lysis solution were added to the cells; mixed by gently inverting the tube and left to incubate for 3 min at RT. Then, 10 mL of Neutralization Solution were added and immediately mixed by gentle tube inversion; the lysate was allowed to sit for 3 min. After this initial procedure DNA Purification by Centrifugation was the chosen protocol. A blue PureYield™Clearing Column was placed on top of a 50 mL plastic tube, the lysate was transferred to the column and allowed to incubate for 2 min. The column assembled to the

tube was then centrifuged at 1500 g for 5 min, at RT. A white PureYield™ Binding Column was assembled in a new 50 mL tube and the filtered lysate was transferred to this column and centrifuged at 1500 g for 3 min, at RT. The column was washed by adding 5 mL of Endotoxin Removal Wash solution and centrifugating at 1500 g for 3 min, at RT. After that, 20 mL of Column Wash solution were added and the column centrifuged was performed at 1500 g for 5 min, at RT. The flowthrough was discarded and an additional 10 min, 1500 g centrifugation was performed, at RT. Excess ethanol was removed by tapping the column on a paper towel. Afterwards, the column was placed in a new 50 mL disposable plastic tube and 800 µl of Nuclease-Free Water were added to the centre of the column. After 1 min standing, the DNA was eluted by centrifugation at 1500 g for 5 min. Two 400 µl DNA aliquots were purified by ethanol precipitation and its concentration and 260/280 nm purity ratio calculated by densitometry measurements.

3.2.7 Cell culture and transfection

A cervical cancer cell line (HeLa cells) was the model system used in this study. HeLa cells were grown in Minimal Essential Medium with Earle's salts and GlutaMAX (MEM, Gibco) supplemented with 10% fetal bovine serum (FBS; Gibco), 1% MEM Non-Essential aminoacids (Gibco, Invitrogen) and 100 U/mL penicillin and 100 mg/mL streptomycin (Gibco). Cultures were maintained at 37º C and 5% CO_2. Cells were subcultured whenever ≈ 95% confluence was reached.

3.2.7.1 Transfection with Lipofectamine 2000

Lipofectamine 2000 (Invitrogen) is a cationic liposome formulation that functions by complexing with nucleic acid molecules, allowing them to overcome the electrostatic repulsion of the cell membrane and to be taken by the cell. This method of DNA delivery in culture cell lines is well described (Dalby et al. 2004).

Cells were grown in complete MEM until 85 - 95% confluence and on the transfection day the culture medium was replaced with complete medium (antibiotic/antimycotic-free). The appropriate amount of DNA for each plate/well was diluted in Opti-MEM (serum- and antibiotic/antymicotic-free) (Table 5). The Lipofectamine 2000 reagent was diluted appropriately in the same medium, and the tubes were left to rest for 5 min. The DNA solution was added to the Lipofectamine solution drop by drop, and the solution was

mixed by gentle bubbling with the pipette. In order to form the DNA-lipid complexes, the tube was allowed to rest for 25 - 30 min at RT. Then what the complexes solution was directly added into the cell medium, drop by drop and with gentle rocking of the plate. The cells were further incubated at 37º C/5% CO_2 for the indicated transfection time, prior to cell collection or fixation.

Table 5 – *HeLa cells transfection reagents*.

Culture Plates	Medium w/o serum (plate)	DNA (µg)	Lipofectamine 2000 (µL)	Medium w/o serum (tube)
100 mm plate	15 mL	8	50	1500 µL
35 mm 6-wells	2.0 mL	2	10	250 µL

3.2.8 Immunoprecipitation procedure

After 24 hrs transfection, HeLa cells were washed once with PBS 1X and then collected with 1.2 mL of lysis buffer containing a protease inhibitor cocktail. Using a cell scrapper, cells were detached from the plate and collected in a microtube already on ice. The samples were sonicated for 10 seconds three times intercalating the samples in order not to over-heat them. After BCA protein quantification described previously, mass normalized lysates were precleared with 25 µl Protein A Sepharose beads (Pharmacia) for 1 hr at 4º C with agitation. After centrifuging for 5 min at 10000 g at 4º C, the supernatant was transferred to a new microtube with 50 µl of Sepharose beads and the primary antibody (anti-PP1α or anti-PP1γ) was added and incubated overnight with shaking at 4º C.
The mixture was then centrifuged for 1 min at 4º C at 10000 g and the pellet washed four times with 500 µl of washing solution, for 15 min with agitation at 4º C and then centrifugations were performed. After the last wash, the tubes were centrifuged for 10 min at 18000 g and 4º C, and the supernatant was fully discarded. The beads were then resuspended in 60 µl of fresh Loading Buffer/1% SDS; boiled for 10 min and frozen at -20º C.

Lysates were collected and the appropriate volume of 10% SDS was added in order to obtain a final concentration of 1% SDS. Afterwards, they were boiled for 10 min and frozen.

Immunoprecipitates and lysates were electrophoreted through in a 10% SDS-PAGE gel and transferred to a nitrocellulose membrane that was incubated with anti-GFP antibody, or anti-PP1α, or anti PP1γ1 antibodies and developed by ECL, as previously described. Between the use of the different antibodies (anti-GFP in 1:1000 dilution, anti-PP1α in 1:2500 dilution and anti-PP1γ1 in 1:5000 dilution) membrane stripping was performed. Briefly, the membrane was incubated for 30 min with stripping solution at 50º C and 75 rpm, washed three times with TBST, for 15 min with agitation, and two times with water and left to air dry.

3.2.9 Overlay blot assay

The pC9orf75-GFP construct, was used for transfect HeLa cells and the corresponding lysates containing the fusion protein was separated on a SDS-PAGE gel and transferred to a nitrocellulose membrane. For this procedure 25, 50 and 100 µg of total protein extracts were loaded on a 10% polyacrilamide gel. The membrane was blocked with TBST/5% non-fat milk solution for 1 hr and then overlaid with purified PP1γ1 protein (1 µg/mL) (Watanabe et al. 2003) in TBST/3% non-fat milk for 1hr. After washing three times with TBST, to remove excess protein, the bound PP1γ1 was detected by incubating the membrane with anti-PP1γ antibody (1:5000 dilution, in TBST/3% non-fat milk) for 1 hr. Immunoreactive bands appeared after incubating with horseradish peroxidase conjugated secondary antibody (1:5000 dilution, in 3% non-fat milk in TBST), for 1 hr, and developing with ECL.

3.2.10 Protein assay

Total protein measurements were carried out using Pierce's BCA protein assay kit, following the manufacturer's instructions. The method combines the reduction of Cu^{2+} to Cu^{+} by protein in an alkaline medium (the biuret reaction), with a sensitive colorimetric detection of the Cu^{+} cation using a reagent containing bicinchoninic acid (BCA). The purple-coloured reaction product of this assay is formed by the chelation of two molecules

of BCA with one Cu^+ ion. This water-soluble complex exhibits a strong absorbance at 562 nm that is linear with increasing protein concentration over a working range of 20 μg/mL to 2000 μg/mL. At least duplicate microtubes per sample were prepared to be assayed with 25 μL of each sample plus 25 μL of 1% SDS, or water in the case of immunoprecipitation procedures. Microtubes with standard protein concentrations were prepared as described below (Table 6).

Table 6 – *Standard curve used in the BCA protein assay method.*

Standard	BSA (μL)	10% SDS (μL)	H_2O (μL)	Protein mass (μg)	W.R. (mL)
P_0	-	5	45	0	1
P_1	1	5	44	2	1
P_2	2	5	43	4	1
P_3	5	5	40	10	1
P_4	10	5	35	20	1
P_5	20	5	25	40	1
P_6	40	5	5	80	1

The BSA stock solution used had a concentration of 2 mg/mL. The Working Reagent (WR) was prepared by mixing BCA reagent A with BCA reagent B in the proportion of 50:1. Then, 1 mL of WR was rapidly added to each microtube (standards and samples) and the microtubes were incubated at 37 º C for exactly 30 min. Once the tubes cooled to RT the absorbance was measured at 562 nm. A standard curve was obtained by plotting BSA standard absorbance *vs* BSA concentration, and used to determine the total protein concentration of each sample.

3.2.11 Immunocytochemistry procedure

HeLa cells were grown in 1 M HCl pre-treated glass coverslips pre-coated with 100 μg/mL poly-L-ornithine. HeLa cells were cultured until 80-90% confluence was reached and

transfected as described above. Each well was washed three times with 1mL serum-free MEM medium and then 1 mL of 1:1 MEM/4% paraformaldehyde fixative solution was gently added and left to stand for 5 min. Subsequently, 1 mL of fixative solution was gently added and left for 30 min. Finally, cells were washed three times with 1mL 1X PBS for 10 min, with gentle agitation. For permeabilized cells, 1 mL of methanol was added for 2 min and, afterwards, 5 washes with 1 mL 1X PBS for 10 min were performed. Blocking was carried out for 1 hr with PBS/3%BSA, and then 100 μL of primary antibody diluted 1:500 in PBS/3% BSA was added drop by drop onto the cover slip and incubated at RT for 2 hrs. After three washes with 1X PBS, the secondary antibody (1:300 dilution) was added using the same methodology and incubated for 2 hrs. Finally, three washes were performed and coverslips were mounted on microscope glass slides with 1 drop of anti-fading reagent containing DAPI for nucleic acid staining (Vectashield, Vector Laboratories). Epifluorescence microphotographies were acquired with an Olympus IX-81 inverted epifluorescence microscope, equipped with EGFP (Chroma 41020) and Texas Red (Chroma 41004) filter cubes for fluorophore microscopy visualization.

3.3 RESULTS

3.3.1 Preliminary analysis of the positive clones

In order to identify the library insert present in a given positive clone, the plasmid DNA was first isolated from yeast. Thus, a mixture of different plasmid DNAs can be isolated from a single yeast clone, namely the bait plasmid and one or more library plasmids, being that each yeast cell can incorporate more than one library plasmid. Hence, in order to obtain single plasmids and pure DNA for sequence analysis, the plasmid DNA isolated from yeast cells was used to transform E. coli XL1-Blue. The plasmid DNA obtained from the resulting transformants was further analysed by restriction digestion with the endonuclease *HindIII*. The restriction fragments were then separated by agarose gel electrophoresis. Figure 10 exemplifies a typical result obtained with this procedure:

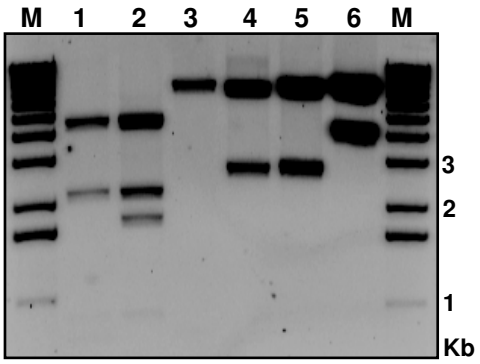

Figure 10 – *HindIII restriction analysis of YTH plasmids. Lane M, 1Kb ladder DNA marker; Lane 1, pAS2-1 vector (4.6+2.2+0.9Kb); Lane 2, pASPP1α bait plasmid (4.6+2.2+1.7+0.9 Kb); Lane 3, pACT-2 vector (7.4+0.7Kb); Lanes 4,5 and 6, pACT-2+library inserts [(7.4+(0.7+ insert)Kb].*

The same strategy was adopted for each of the 298 positive clones. After identifying transformants carrying the cDNA library plasmids, their respective inserts were sequenced with the GAL4-AD primer (Appendix IV).

The nucleotide sequence of each clone (Figure 11) was then converted to FASTA format (Figure 12). In this format, the signal ">"in the first line precedes the name or additional information on the sequence and the sequence itself starts on the second line.

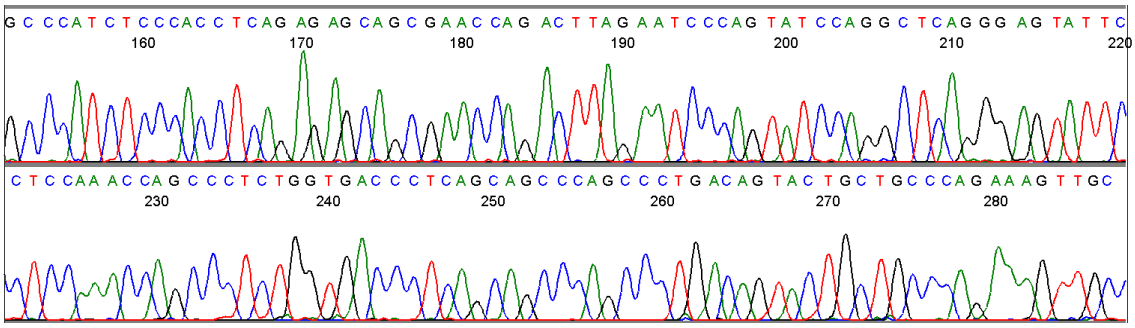

Figure 11 – *Partial nucleotide sequence obtained for positive clone 282Q.*

```
>Clone 282
CTGGATGGCCACAGCCCATCTCCCACCTCAGAGAGCAGCGAACCAGACTTAGAATCCCAGTATCC
AGGCTCAGGGAGTATTCCTCCAAACCAGCCCTCTGGTGACCCTCAGCAGCCCAGCCCTGACAGTA
CTGCTGCCCAGAAAGTTGCCACAAGTCCCAAGAGTGCCCTCAAGTCTCCATCTTCCAAGCGTAGG
ACATCTCAGAACTTAAAACTGAGAGTTACCTTTGAGGAGCCTGTGGGCAGATGGAGCAGCCTAGC
CTTGAACTGAATGGAGAAAAGACAAGATAAGGGCAGGACTCTCCAGCGGGACCTCCACAAGTAAC
GAATCGGGGGGATCAACTGAAAAGGCCTTTTGGAGCCTTTCGATCTATCATGGAA
```

Figure 12 – *Partial sequence of clone 282Q converted to FASTA format.*

The sequence in FASTA format was then copied to the BLAST window (www.ncbi.nlm.nih.gov/BLAST/) (Figure 13) to be compared with the GenBank Database of human nucleotide sequences.

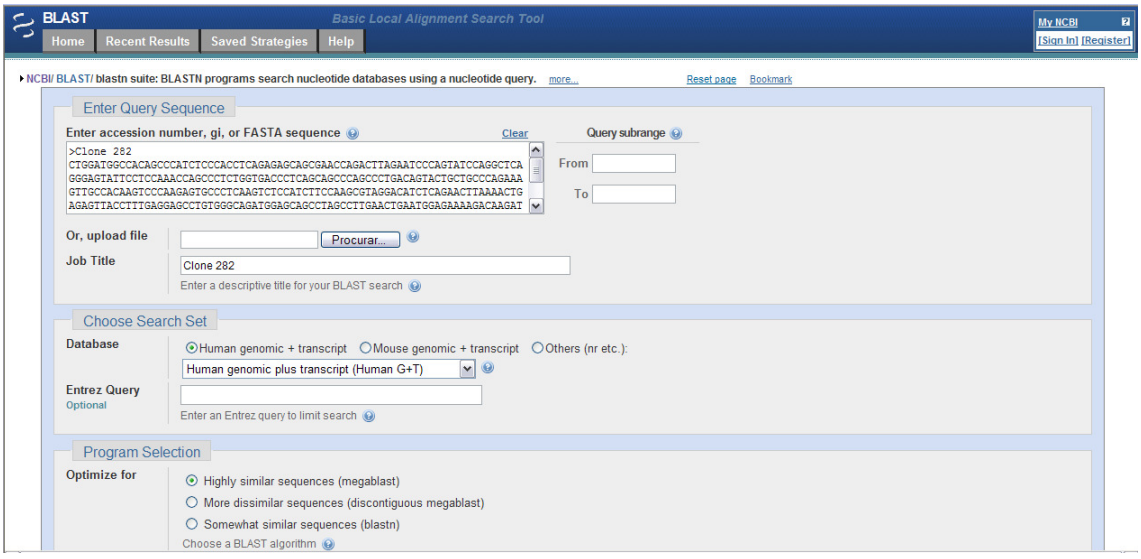

Figure 13 – *Blast window where the query sequence for each positive was introduced.*

The identity of the positive clones isolated was thus obtained. Figure 14 shows a representative example of the results obtained for clone 282Q.

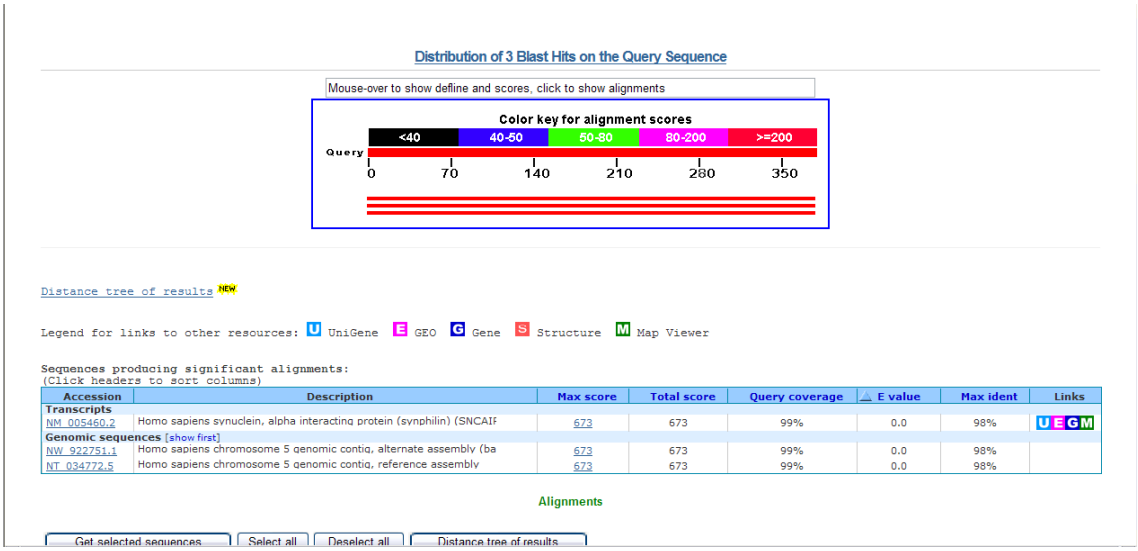

Figure 14 – *Blast results for clone 282Q. Alignment with protein synphilin-1A.*

3.3.2 Yeast colony hybridization

Yeast colony hybridization is an efficient mean to screen a large collection of library transformants for the presence of an abundant cDNA insert. Transformants carrying the same or overlapping library plasmid can be easily identified. For example, to identify putative positive spinophilin clones among the large number of transformants obtained, the insert of clone *268Q* was release by *EcoRI* digestion and radiolabeled with ^{32}P-ATP and hybridised to the full collection of yeast positive colonies arrayed onto nitrocellulose membranes. Figure 14 is an example of the results obtained with one of the filters hybridized.

This approach allowed the rapid identification of some of the most abundant positives in a short period of time. This method was used not only for spinophilin but also for other abundant positives (e.g. Chr1orf 71 and Torsin A interacting protein).

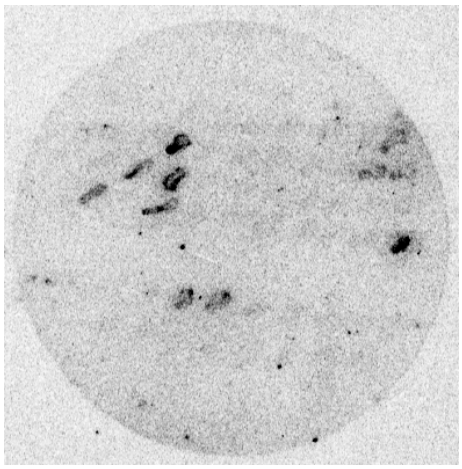

Figure 14 – *Identification of putative Spinophilin positives by colony hybridization.*

This technique can be very helpful and fast but the results obtained in this work were not always as accurate as expected. In practice, more careful in the arraying of the positives on the filters and avoiding excessive colony growth that leads to colony overlap signal loss, should improve significantly the results obtained in this powerful technique.

3.3.3 Identification of the positive clones

Of the 298 positives obtained all were recovered and definitively identified by partial DNA sequence analysis (Table 7).

Table 7 – *Complete list of positive clones – The human brain PP1α interactome.*

Clone ID	No Clones	PP1BM	Chr	Data Base ID	YTH clone ID
Chr1orf71	25	RVRF	1	NM_152609	4T,5T,14T,35T,37T,56T, 71T,109T,110aT,118T,126T, 128T,132T,146T,201T,202T,205T, 215T,263Q,269Q,270Q, 274Q,278Q,284aQ,285Q
Chr9orf75	45	KISF / RAIRW	9	NM_173691	13T,40T,41T,43T,53T,65T,74T, 84T,91T,100T,104T,105T,110bT, 117bT,129T,139T,142T,148T,149T, 150T,151T,154T,155aT,164T,169T,170T, 172T,180T,181T,186T,190T,199T,209T, 221T,223T,228T,232T,235T,237aT, 239T,265Q,267Q,272Q,292Q,298bQ
NEK2A	2	KVHF	1	NM_002497	80T,155bT
PPP1R2	1	-	3	NM_006241	99T

PPP1R3C	5	KRVVF / KNVSF / RITF / KIEF	10	NM_005398	2T, 8T,101T, 183T,200T
PPP1R3D	2	RVQF	6	XM_371796	275Q,290Q
PPP1R3E	1	RVRF	14	XM_927029	130T
PP1R9B / Spinophilin / NeurabinII	15	RKIHF	17	NM_032595	9T,63T,87T,94T, 254T,255T,259Q,266Q, 268Q,276Q,277Q,279Q, 280Q,286Q,289Q
PP1R13A / ASPP2 / TP53BP2	17	RVKF	1	NM_005426	3T,7T,23T,67T,113T, 127T140T,156T,173T, 226T,231T,240T,242T, 251T,252T,256T,287Q
PPP1R13B / ASPP1	5	RVRF	14	NM_015316	68T,106T,119T, 123T,296Q
PP1R13L	2	-	19	NM_006663	1T,47T
PPP1R15B	3	KVTF	1	NM_032833	136T,229T,258T
PPP1R16A	1	KQVLF	8	NM_032902	187T
KIAA1949	4	KISF	6	BC_066644	6T,81T,124T,233T
PHACTR3	2	RNIF	20	NM_080672	66T,70T
RIF1	9	KIAF/ RVSF	2	NM_018151	25T,11T,116T,117aT, 167T,175T,203T,204T,206T
STAU	16	KVTF	20	NM_017453	29T,34T,38T,44T,51T,120T, 125T,145T,158T,159T,160T, 174T,176T,197T,243T,245T
WBP11	1	RKVGF	12	NM_016312	168T
ZAP3	8	KEVEF / RGRW / RAIGF	14	NM_019589	10T,19T,20T,58T, 78T,157T,166T,216T
ZFYVE9 / SARA	3	RVWF / KVIRW	1	NM_004799	152T,247T,253T
AATK	1	KAVSF	17	NM_001080395	297Q
ANKRD15	2	-	9	NM_015158	189T,194T
AXIN1	4	RVAF / RVEF	3	NM_033027	115T,198T,295Q,298aQ
BTBD10	1	RHVDF	11	NM_032320	153T
C1QA	16	-	1	NM_015991	21T,22T,30T,60T,114T,121T, 134T,135T,191T,193T,208T, 213T,214T,218T,227T,241T
CEP170	1	RILF	1	NM_014812	28T
CLTC	1	-	17	NM_004859	217T
CNTN1	2	-	12	NM_001843	85T,92T
CLCN2	1	-	3	NM_004366	49T
CKB	1	-	14	NM_001823	103T
CNP1	1	KIFF	17	NM_033133	179T
CRKII	1	-	17	NM_005206	250T, 270T
CXXC1	1	-	18	NM_014593	46T
CYCS	1	KGIIW	7	NM_018947	246T
DEAF1	1	-	11	NM_021008	77T
DCTN1	2	KIKF / KVTF	2	NM_004082 NM_023019	138T,171T
FRMPD4	1	KVRF / KVSF	X	NM_014728	26T
GLTSCR2	1	-	19	NM_015710	95T
IBTK	1	KVSF	6	NM_015525	42T
IIP45	1	RVTF	1	NM_021933	89T

JPH3	1	-	16	NM_020655	55T
KCTD20	3	RHVDF	6	NM_173562	143T,230T,238T
LPIN2	1	-	18	NM_014646	108T
MAP4K4	2	-	2	NM_004834	39T,210T
NDP	2	-	X	NM_000266	15T,33T
PHC1	2	-	12	NM_004426	131T,225T
PRR16	2	RVRF	5	NM_016644	107T,211T
PIAS1	1	-	15	NM_016166	73T
PIAS3	1	-	1	NM_006099	122T
PREX1	1	KVCF / KVIF	20	NM_020820	64T
RANBP9	20	RMIHF	6	NM_005493	11T,69T,79T,82T, 86T,133T,162T,162T, 163T,165T,178T,182T, 207T,212T,224T,236T, 237bT,244T,248T,249T
SH3RF2	4	KTVRF	5	NM_152550	141T,144T,177T,264Q
SLC45A1	1	RNVTF	1	NM_001080397	219T
SPRED1	1	RHVSF	15	NM_152594	24T
SNCAIP-1A	6	RVTF	5	DQ_227317	27T,90T,222T, 281Q,282Q,288Q
MAL2	1	-	8	NM_052886	112T
TOR1AIP1	14	REVRF/ KVNF/ KVKF	1	NM_015602	12T,31T,36T,45T,50T, 61T,76T,96T,184T,192T, 261Q,262Q,271Q,273Q
UBE2Z	1	-	17	NM_023079	17T
ULK1	1	-	12	NM_003565	220T
MAFG	1	-	17	NM_002359	137T
ZBTB11	1	-	3	NM_014415	52T
Chr11orf32	1	-	11	BC_040643	185T
FLJ35856	1	-	12	AK_093175	257T
KIAA0460	1	RVGW	1	NM_015203	93T
KIAA1377	9	KLRW	11	NM_020802	59T,75T,97T,102T,260Q, 188T,195T,196T,284bQ
LOC648791	1	-	6	XR_018474	291Q
ZNF827	1	-	4	NM_178835	32T
C-2190G12	1	-	14	AL_139194	16T
C2genomic	1	-	2	NW_001838769	54T
C2genomic	1	-	2	NW_001838818	62T
C2genomic	1	-	2	NW_001838863	283Q
C3genomic	1	-	3	NW_001838877	18T
C4genomic	1	-	4	NW_001838915	48T
C17genomic	3	-	17	NW_001838448	72T,293Q,294Q
16S ribosomal RNA	1	-	Mit	AM_263191.1	88T
IDH2	1	-	15	NM_002168	57T

The occurrence of a consensus PP1 binding motif (PP1 BM) is indicated by the corresponding sequence. Letters a and b corresponde to two different prey plasmids extracted from the same positive clone.

The identified positive clones, corresponding to a total of 76 proteins, were divided in five groups: proteins already known to interact with PP1 (blue); proteins known in other contexts (green); proteins of unknown function present in the database (purple); clones present in the database only at the genomic level (yellow) and mitochondrial proteins (orange). Inasmuch as several positives corresponded to independent hits on the same protein, the human brain PP1α interactome thus defined comprised 74 different proteins, two were considered potential false positives.

All clones were subject to the same analysis: they were partially sequenced, the full length sequence present in the database was searched for special features of the amino acid sequence using motif search databases and specially for a consensus PP1 binding motif ([RK]-x0-1-[VI]-{P}[FW]). The number of clones for each identified binding protein varied considerably, from 1 clone to 45 clones, and every group type includes positives recovered from high and low stringency selection media.

3.3.3.1 Proteins matching known PP1 interactors

In this YTH screen, of the 298 clones identified, 167 (56%) could be assigned to previously known PP1 interactors (Table 7, blue), among these there are some well established PP1 regulators, such as NEK2A, Spinophilin and ASPP1 (PPP1R13B). This group of positives includes also various proteins identified as PP1 interactors, but the means by which they regulate PP1 are not yet completely or even at all described. That is the case of Chr9orf75, Chr1orf71 and SARA (ZFYVE9). Chr9orf75 and SARA will be further discussed below.

Interestingly, the two most abundant interactors detected in this screen were Chr9orf75, with a total of 45 and Chr1orf71, with 25 positives; proteins identified only as mRNAs in the GenBank database.

3.3.3.2 Proteins matching other known proteins

With this screen, 41 proteins never before related to PP1 were identified as potential PP1α regulators encoded by 108 of the positive clones. This corresponds to 36% of the total positives. RAN binding protein 9 (RANBP9) was the most abundant positive with a total of 20 clones identified, Complement component 1, q subcomponent, A chain (C1QA) and torsin A interacting protein 1 (TOR1AIP1) were other two abundant positives, with 16

and 14 clones, respectively. Two interesting proteins were analysed more toughly and are discussed below, they are dynactin-1 (DCTN1) and synphilin-1A (SNCAIP).

3.3.3.3 Unknown proteins

In various cases database searching yielded homologies with sequences annotated in the Genbank database as ORFs encoding proteins of unknown function (Table 7, purple). This was the case for 14 positives (approximately 5%) encoding 6 proteins. The most abundant with in this group was KIAA1377 that was encoded by 9 of the isolated positives.

3.3.3.4 Genomic clones

Table 7 (yellow) also lists several positives that only allowed significant homology to human genomic clones. While it can not be excluded that these may represent hitherto unknown genes encoding novel proteins, further work would be necessary to confirm this. In this category fit 9 (approximately 3%) of the independent positives isolated, corresponding to homologies to human chromosomes 2, 3, 4, 14 and 17.

3.3.3.5 Mitochondrial clones

Two clones, *88T* and *57T*, were identified using the GenBank database as 16S ribosomal RNA and mitochondrial isocitrate dehydrogenase 2 (IDH2). Isocitrate dehydrogenases catalyze the oxidative decarboxylation of isocitrate to 2-oxoglutarate, is found in the mitochondria and plays a role in intermediary metabolism and energy production. This protein may tightly associate or interact with the pyruvate dehydrogenase complex. Although IDH2 is a nuclear-encoded mitochondrial protein, the interaction with PP1α is unlikely to occur in a physiologically relevant context, because the partners are not expressed in the same subcellular environment. Mitochondrial clones, including 16S rRNA, have previously been described as common false positives in YTH screens (Serebriiskii et al. 2001a; Serebriiskii et al. 2001b). The emergence of only two false positives can be considered a very good outcome of this screen, in what concerns the reliability of the results and considering the high number of clones screened and identified.

3.3.4 Functional analysis of the human brain PP1α interactome

In the present work, 74 different human brain proteins were identified by the YTH technique that bind and regulate PP1α. The functional distribution of the identified proteins is shown in Figure 15. The potential false positive clones (Table 3, in orange) were left out of this analysis. The unidentified proteins encoded by the genomic clones (7; Table 7, in yellow) plus 6 proteins (Table 3, in purple) have unknown function. Clones matching proteins of unknown function correspond to 25% of the total proteins identified. For the remainder 75%, the most abundant group corresponds to proteins involved in cell signalling processes (18%) followed by proteins involved in splicing and transcription (11%), and proteins involved in apoptosis (8%). Known PP1 regulators make up 8% of the proteins identified. Other protein functions include components of the cytoskeleton, cellular transport, metabolism and energy and cell cycle.

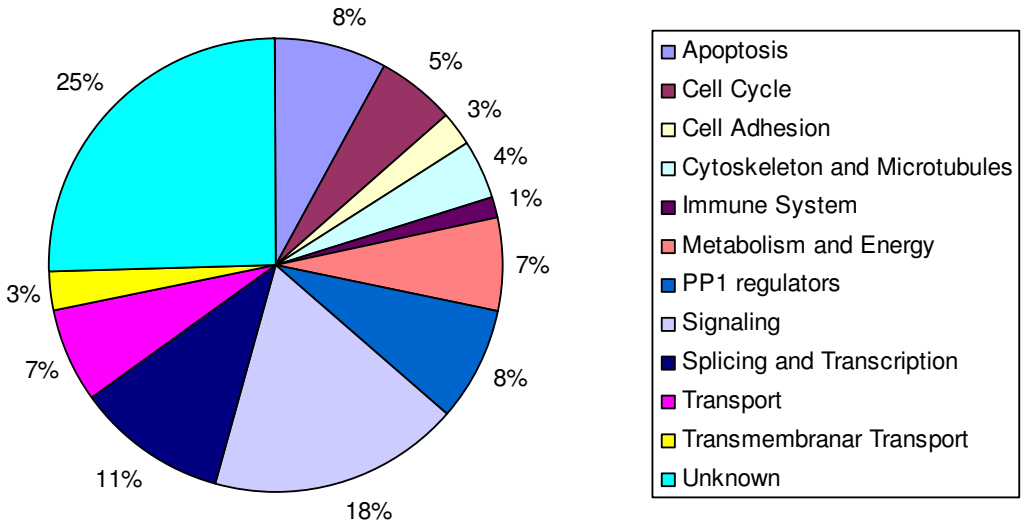

Figure 15 – *Functional distribution of the human brain PP1α binding proteins identified by the Yeast Two-Hybrid method.*

3.3.5 Proteins selected for further study

Four interacting proteins were selected for further confirmation of their interaction with PPα. This selection had in consideration several factors, including that all four proteins

have at least one canonical PP1 binding motif and two were already reported to be PP1 interactors.

The four proteins selected were Chr9orf75, Synphilin-1A, SARA and dynactin-1. Chr9orf75 was the most abundant positive in the YTH screen and was reported as a PP1 interactor, while this work was in progress, although no further information exists regarding protein function. Synphilin-1A (Synuclein alpha interacting protein – 1A), an alternative splice variant of synphilin-1, interacts with α-synuclein in neuronal tissue and is an aggregation-prone protein that causes neuronal toxicity and is involved in neurodegenerative disorders. SARA (Smad Anchor for Receptor Activation), is an anchoring protein, which recruits Smad2 and Smad3 to the vicinity of the TGF-β receptor, being an essential component of Smad-dependent signalling through TGF-β. SARA was previously described as a PP1 interacting protein, nevertheless the means by which that interaction occurs is not yet known. Finally, dynactin-1 is a dynein activator that binds to both dynein and microtubules. The dynein/dynactin complex is essential for a diversity of cellular trafficking events and was related to human neurodegenerative diseases.

In order to verify the interactions between the four proteins described above (Chr9orf75, synphilin-1A, SARA and dynactin) and PP1α, but also to test if they could interact with PP1 isoforms γ1 and γ2, a yeast co-transformation assay was performed. Clones corresponding to the mentioned proteins (as prey; in the pACT-1 vector) and the three PP1 isoforms (as bait; in the pAS2-1 vector) were co-transformed in yeast strain AH109 and tested in SD/QDO/X-α-gal medium. Additionally, the same clones were co-transformed with the vector pAS2-1 alone to see if they alone would be capable of initiating transcription, in the absence of PP1α. That was not the case for any of them, as none was able to grow in SD/QDO and turn blue in the presence of X-α-gal (data not shown).

3.3.5.1 Synphilin-1A (Synuclein alpha interacting protein – 1A – SNCAIP-1A)

In this YTH screen six positive clones were identified as synphilin-1, by partial sequencing (Table 8). Further sequencing of the C-terminus, using the reverse primer 3`-Amplimer (Appendix IV), revealed that they correspond to the novel isoform synphilin-1A (DQ227317) (Figure 16).

Table 8 - *Independent synphilin-1A clones isolated in the YTH screen.*

First Nucleotide (DQ_227317)	**Positive clones**
946 (in frame)	90T
1381 (in frame)	27T, 222T, 281T, 282T, 288Q

The first gene linked to Parkinson's disease encodes α-synuclein, a presynaptic protein (Maroteaux et al. 1988), so far with unknown physiological functions. Three missense mutations in α-synuclein and gene locus triplication have been found to cause autosomal dominant Parkinson's disease (Polymeropoulos et al. 1997; Kruger et al. 1998; Singleton et al. 2003; Zarranz et al. 2004). α-Synuclein was also identified as a major constituent of Lewy bodies in sporadic Parkinson's disease patients (Spillantini et al. 1997) and also in inclusions characteristic of other neurodegenerative disorders, such as Diffuse Lewy Body disease (Takeda et al. 1998).

Synphilin contains several protein-protein interaction domains, including ankyrin-like repeats, a coiled-coil domain, an ATP/GTP-binding motif, and interacts with α-synuclein in neuronal tissue and may play a role in the formation of cytoplasmic inclusions and neurodegeneration. Mutations in this gene have been associated with Parkinson's disease. Synphilin-1A is an alternative splice variant of synphilin-1 that lacks exons 3 and 4 and contains a previously unidentified exon 9A of the SNCAIP gene (Figure 17A). However, the transcripts of synphilin-1A and synphilin-1 differ not only by their exon content but also by their start codon and initial reading frame. Synphilin-1A lacks exons 3 and 4 found in synphilin-1, and displays an extra exon between exons 9 and 10. Interestingly, the translation of synphilin-1A occurs in a different initial reading frame than that of synphilin-1. Nevertheless, the merge of exon 2 with 5 results in a frame shift leading to an identical reading frame for both synphilin-1A and synphilin-1 after exon 2. As a result, synphilin-1A amino acid sequence differs from synphilin-1 at the N-terminus but is the same between exons 5 and 9. Moreover, synphilin-1A has an additional 51 amino acid stretch at the C-terminus because of exon 9A insertion (Figure 17B).

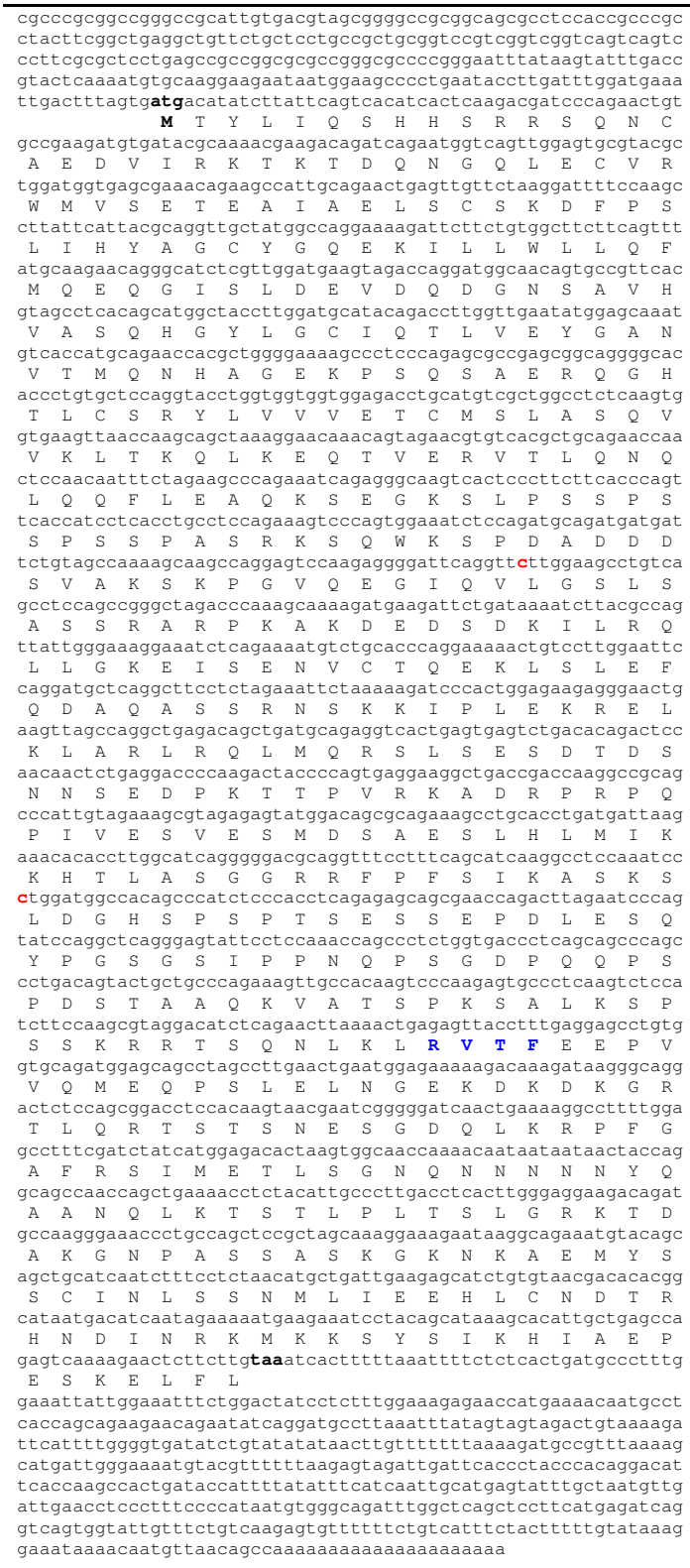

Figure 16 – *Nucleotide and corresponding amino acid sequence of synphilin-1A (DQ_227317). PP1 binding motifs are highlighted in blue color (positions 449-452 in a.a. sequence). The first nucleotides of the positive clones are highlighted in red color.*

Synphilin-1A, a novel synphilin isoform, is an aggregation-prone protein that causes neuronal toxicity. The presence of synphilin-1A was demonstrated in Lewy bodies and in the insoluble fraction of protein samples obtained from the brains of Diffuse Lewy Body

Disease patients (Eyal et al. 2006). Synphilin-1A also binds to α-synuclein, but displays a much higher tendency to aggregate compared to synphilin-1. It spontaneously aggregates in human dopaminergic cells, recruiting a-synuclein into intracellular inclusions (Eyal and Engelender 2006).The findings suggest an important role for synphilin-1A in inclusion-body formation and its possible involvement in the pathogenesis of Parkinson's disease.

A

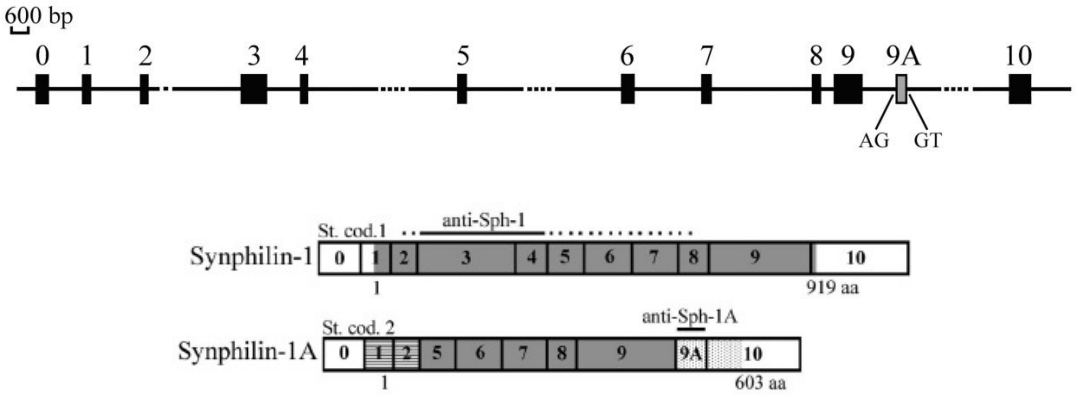

B

Figure 17 – *Synphilin-1 and synphilin-1A differ in their exon organization and are translated from different start codons. (**A**) Exon organization of the SNCAIP gene, demonstrating the position of the previously unidentified exon 9A. (**B**) Exon organization of synphilin-1A and synphilin-1, with the different start codons used for translation. The synphilin-1 transcript via start codon 1 results in the generation of a 919-aa protein (gray shading). The synphilin-1A transcript via start codon 2 results in a different initial amino acid sequence (horizontal stripes), which, distal to the exons 2 and 5 splice junction, is identical to that of synphilin-1 (gray shading). The 51 amino acids present in the C-terminus of synphilin-1A are encoded by exons 9A and 10 (dots), (adapted from Eyal et al. 2006).*

Synphilin-1, whose function is currently unknown, was initially identified as an α-synuclein-interacting protein. In normal or physiological conditions, synphilin-1 is predominantly expressed in neurons, located in the cytoplasm and presynaptic nerve terminals, and associated with synaptic vesicles (Engelender et al. 1999; Ribeiro et al. 2002). However, in several neurodegenerative disorders called α-synucleinopathies, such as Parkinson's disease, dementia with Lewy bodies, and multiple system atrophy, synphilin-1 is mainly localized in neuronal and glial cytoplasmic inclusions (Wakabayashi et al. 2000; Wakabayashi et al. 2002), in which α-synuclein (Spillantini et al. 1997; Wakabayashi et al. 1997), ubiquitin (Takahashi and Wakabayashi 2001), and the proteasome (Iwatsubo et al. 1996; Ito et al. 2003) are also present.

It was recently found that synphilin-1 is ubiquitylated by the E3 ubiquitin ligase SIAH (Liani et al. 2004), which is also present in Lewy bodies of Parkinson's disease patients. When synphilin-1 and SIAH-1 ubiquitin ligase are coexpressed in cells and proteasomal function is inhibited, ubiquitylated synphilin-1 inclusions are found in the vast majority of cells (Liani et al. 2004) and this process is modulated by GSK3β phosphorylation of synphilin-1 (Avraham et al. 2005). Two findings further highlight the importance of synphilin-1 in the study of Parkinson's disease. First, synphilin-1 is present in Lewy bodies of Parkinson's disease patients, as well as in inclusion bodies characteristic of other α-synucleinopathies (Wakabayashi et al. 2003). Second, two sporadic Parkinson's disease patients were found to carry a missense mutation, R621C, in the gene encoding synphilin-1 (Marx et al. 2003). Furthermore, synphilin-1 is a substrate of parkin (Chung et al. 2001) and it is thought to link the ubiquitin proteasome system with synaptic function. Synphilin-1 seems to play an important role in the formation of Lewy Bodies since coexpression of α-synuclein, synphilin-1 and parkin results in the formation of cytoplasmic inclusions which resemble Lewy Bodies (Engelender et al. 1999; Chung et al. 2001).

The identity of the individual molecules that may affect α-synuclein aggregation, the molecular etiology of Lewy Body formation, and the resulting impact on neuronal survival are still obscure. However, the evidence that the co-expression of α-synuclein and synphilin-1 leads to Lewy Body-like inclusion body formation in cultured cells may suggest that the functional interaction between these factors is crucial for this process (Engelender et al. 1999). Therefore, it is reasonable to predict that the identification of factors that regulate the physical and functional interactions between α-synuclein and synphilin-1 will help to uncover the molecular etiology of Lewy Body formation and Parkinson's Disease pathogenesis. Casein kinase II (CKII) has been recently reported as a potent kinase that phosphorylates both α-synuclein and synphilin-1 and regulates the binding between these two proteins (Okochi et al. 2000; Lee et al. 2004). Significantly, the CKII inhibitor, 5,6-dichrolo-1-β-D-ribofuranosylbenzimidazole, abolishes this interaction and reduces inclusion body formation in cell cultures (Figure18).

Synphilin-1 and synphilin-1A, provide a new model regarding the role of ubiquitylation and inclusion body formation in Parkinson`s disease (Figure 18). Synphilin-1A has similar phosphorylation sites as synphilin-1 and it is possible that synphilin-1A aggregation is also controlled by phosphorylation (Eyal and Engelender 2006; Eyal et al. 2006). Marked neurotoxicity was observed with synphilin-1A but not with synphilin-1, indicating that synphilin-1A is directly involved in cell death. The attenuation of synphilin-1A toxicity by the formation of intracellular inclusions should shed some light on the controversial role of

inclusion bodies in neurodegenerative disorders. To date, it is still debatable whether inclusion bodies promote or inhibit neuronal toxicity. These findings could suggest a cytoprotective role for inclusion bodies (Eyal and Engelender 2006; Eyal et al. 2006).

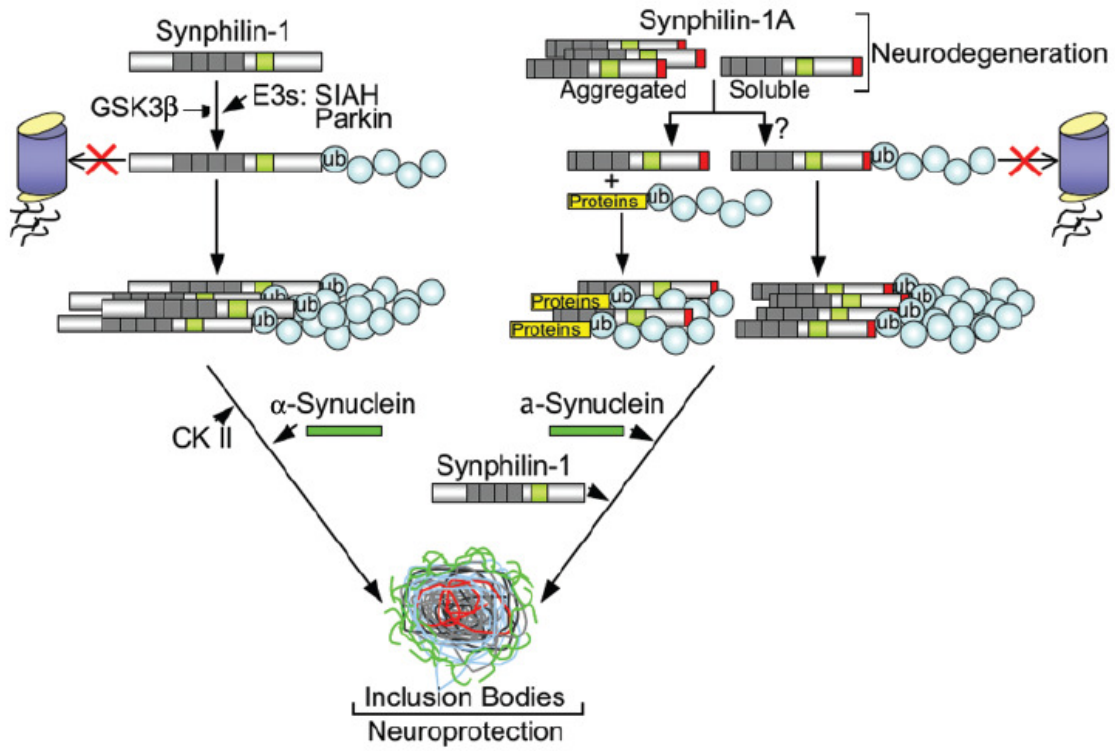

Figure 18 –*Schematic representation of synphilin inclusion body formation and the contribution of the ubiquitin proteasome system. Ubiquitylation of synphilin-1 by SIAH is essential for its accumulation into inclusions upon proteasome inhibition. Parkin also mediates synphilin-1 ubiquitylation, but it is less efficient than SIAH (Lim et al. 2005). Synphilin-1 inclusions further resemble Lewy bodies since they are able to recruit a-synuclein and parkin. Phosphorylation of synphilin-1 by GSK3β and CK II was shown to modulate the formation of synphilin inclusions, suggesting that phosphorylation of critical proteins, in concert with ubiquitylation, might play a role in Lewy body formation. The new synphilin-1 isoform, synphilin-1A, promotes striking neuronal toxicity and death, and spontaneously aggregates in dopaminergic cells and neurons. Upon addition of proteasome inhibitors, synphilin-1A accumulates into more organized inclusions within neurons leading to a marked decrease of its toxicity, and recruiting synphilin-1 and α-synuclein. It is still unknown whether synphilin-1A requires ubiquitylation for inclusion formation or if it is also a target for Siah-1 and parkin. Since proteasomal dysfunction has been implicated in the pathogenesis of Parkinson`s disease, accumulation of synphilin proteins into inclusions might work as core for Lewy body formation.* (Eyal and Engelender 2006)

The interaction of all clones with PP1α was corroborated and all interacted also with the others two PP1 isoforms (Figure 19). Light blue colonies also represent positive interactions, but took longer to turn blue in the presence of X-α-GAL. Synphilin-1A has a PP1 BM (RVTF) predicted by bioinformatic analysis of its sequence that is present in all the synphilin-1A positives isolated.

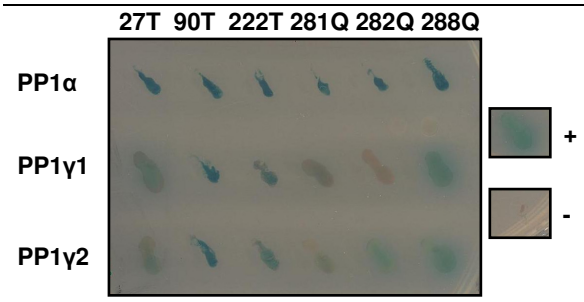

Figure 19 – *Analysis of the interaction of the different positive clones encoding synphilin-1A with various PP1 isoforms: α, γ1 and γ2. The interaction was tested in SD/QDO/x-α-gal medium. Plus and minus represent the positive and negative controls, respectively.*

3.3.5.2 Smad Anchor for Receptor Activation (SARA / ZFYVE9)

Three alternatively spliced transcripts encoding distinct isoforms have been found for this gene (ZFYVE9, zinc finger, FYVE domain containing 9) and the three positive clones found in this screen (Table 9) encode isoform 3 of SARA (Figure 20), the longest isoform (NM_004799).

Table 9 – *Independent SARA clones isolated in the YTH screen.*

First Nucleotide (NM_004799)	**Positive clones**
867 (out of frame)	152T
998 (out of frame)	253T
2408 (in frame)	247T

This gene encodes a double zinc finger (FYVE domain) protein (Figure 20) that interacts directly with Smad2 and Smad3, which may be involved in Alzheimer's disease (Lee et al. 2006; Ueberham et al. 2006). Smad proteins transmit signals from transmembrane Ser/Thr kinase receptors to the nucleus. The FYVE domains have been identified in a number of unrelated signalling molecules and are zinc-containing modules of 60–80 amino acid residues (Burd and Emr 1998; Patki et al. 1998; Lawe et al. 2000; Gillooly et al. 2001; Stenmark et al. 2002).

Transforming growth factor (TGF)-β is a ubiquitously expressed cytokine that has different roles, affecting cellular processes including proliferation, differentiation, apoptosis, fibrosis and tumorigenesis (Roberts 1990). TGF-β signalling is initiated when ligand-bound TGF-β type II receptor, with a constitutively active kinase, binds to and phosphorylates TGF-β type I receptor (Piek et al. 1999; Attisano and Wrana 2000; Wrana 2000; Shi and Massague 2003). This phosphorylation, in the type I receptor cytoplasmic GS region, leads to its activation and its ability to activate the receptor-regulated Smads (R-Smads), Smad2 and Smad3, by C-terminal serine phosphorylation, which then translocate to the nucleus and regulates gene expression (Massague 1998; Massague and Chen 2000; Massague and Wotton 2000; Wrana 2000; Attisano and Wrana 2002). Once phosphorylated, R-Smads associate with Smad4 (Lagna et al. 1996; Zhang et al. 1997), and mediate nuclear translocation of the heteromeric complex. In the nucleus, Smad complexes then activate specific genes through cooperative interactions with DNA and other DNA-binding proteins such as FAST1, FAST2, and Fos/Jun (Chen et al. 1996; Liu et al. 1997; Labbe et al. 1998; Zhang et al. 1998; Zhou et al. 1998).

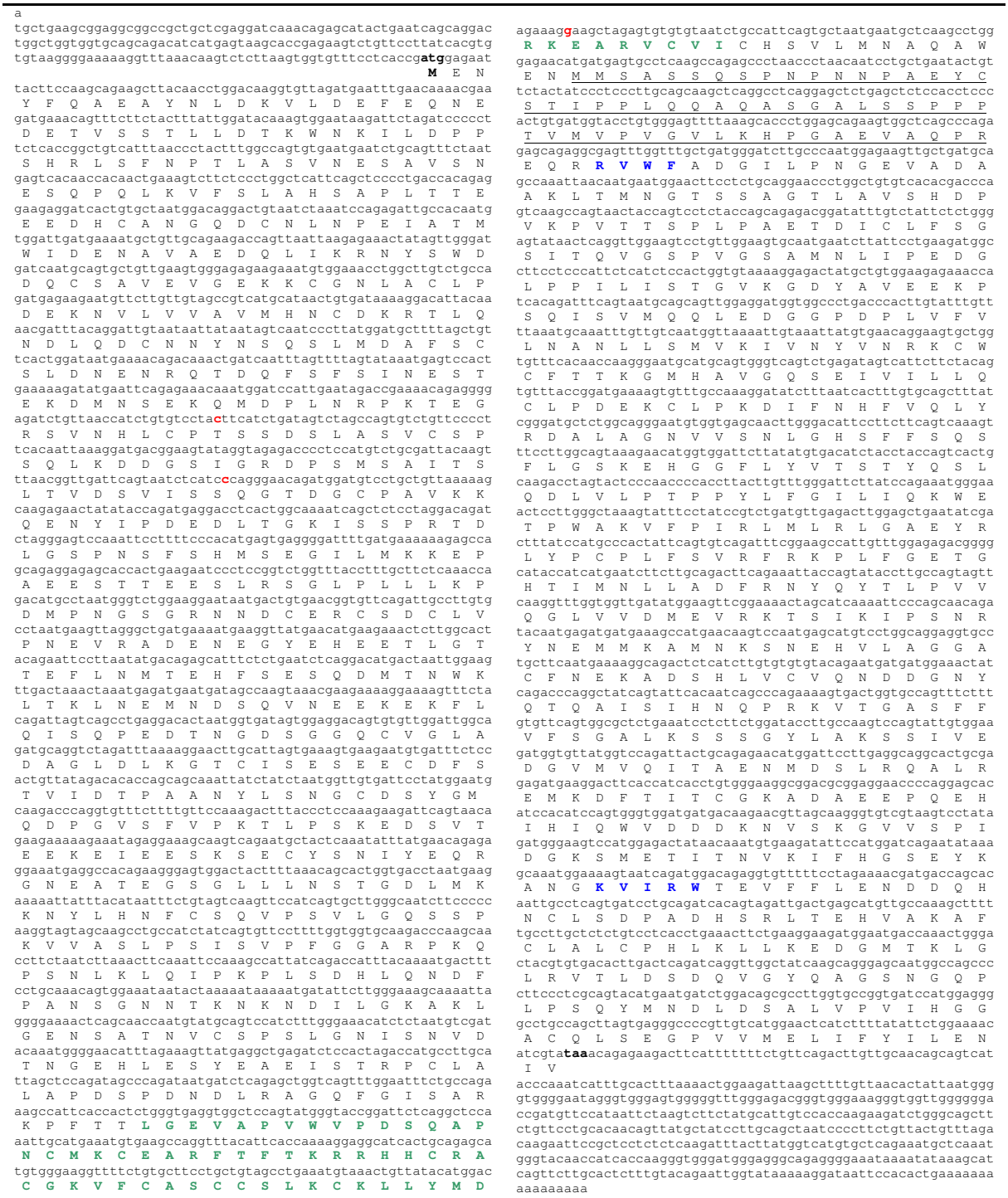

Figure 20 – *Nucleotide and corresponding amino acid sequence of isoform 3 of SARA. PP1 binding motifs are highlighted in blue colour (positions 827-830 and 1307-1311 in a.a. sequence). The first nucleotides of the positive clones isolated are highlighted in red colour. The FYVE domain, which is thought to bind phosphatidylinositol 3-phosphatase and so to localize SARA to the membrane (Tsukazaki et al. 1998), is in green and the minimal Smad-binding domain (Wu et al. 2000) is underlined.*

Although several protein kinases in the TGF-β pathway are known, including the receptors themselves, the relevant phosphatases are not yet identified. Serine/threonine protein phosphatases are likely involved in the dephosphorylation of these phosphorylated signalling components. Also little is known of how Smad interaction with receptors is controlled.

SARA was first described as a novel Smad2 and Smad3 interacting protein, that functions as an anchoring protein to recruit Smad2 to the TGF-β receptor complex (Tsukazaki et al. 1998). The FYVE domain is required to maintain the normal localization of this protein but is not involved in mediating interaction with Smads. The C-terminal domain of this protein interacts with the TGF-β receptor. As a component of the TGF-β pathway, SARA controls the subcellular localization of Smad and brings the Smad substrate to the receptor, increasing the efficiency of its phosphorylation (Tsukazaki et al. 1998).

SARA also contains a phosphatidylinositol 3-phosphate (PI3P)-binding FYVE domain (Stenmark et al. 1996), which localizes it predominantly to the early endocytic compartment (Stenmark and Aasland 1999). Activated receptors internalized into the early endocytic compartment might encounter the SARA-Smad complex there, initiating signals from this compartment (Hayes et al. 2002; Panopoulou et al. 2002). Alternatively, small amounts of SARA are known to localize to the plasma membrane by binding to the receptor; the SARA-Smad complex might encounter activated receptors there, initiating signals at this location. Following internalization into the early endosome, signalling could then continue in a SARA-enriched environment (Di Guglielmo et al. 2003).

The isolation of a *Drosophila melanogaster* homolog of SARA (Sara) in a screen for proteins that bind PP1c was already reported (Bennett and Alphey 2002; Colland et al. 2004). The disruption of the identified PP1c-binding motif in Sara reduced its ability to bind PP1c. The expression of this non-PP1c-binding mutant resulted in hyperphosphorylation of the type I receptor and stimulated expression of a target of TGF-β signalling (Bennett and Alphey 2002). These data demonstrate that the relevant substrate of PP1c is the type I receptor or some intracellular element upstream of the type I receptor. The only known upstream element, however, is the type II receptor kinase. This phosphorylates the type I receptor, but its own kinase activity is constitutive (Wrana et al. 1992; Wrana et al. 1994; Massague 1998). Thus, type I receptor is implicated as the relevant substrate of PP1c. Smad is thought to dissociate from the complex after phosphorylation, so it is an unlikely target for a receptor-bound protein phosphatase.

The additive effect of loss of PP1 and induction by TGF-β suggests that the key role of PP1 bound to Sara is to minimize the uninduced signal. The type II receptor is a

constitutively active kinase (Lin et al. 1992), which will occasionally encounter and phosphorylate the type I receptor even in the absence of the extracellular ligand (Ventura et al. 1994; Chen et al. 1995). It is critical that this background signal be minimized, as the system must be able to respond accurately to a very small number of ligand molecules relative to the number of receptors. Therefore, it is suggested that the role of PP1c in the receptor complex is to antagonize the type II receptor, ensuring that the presence of the ligand is required for continued signal transduction (Figure 21).

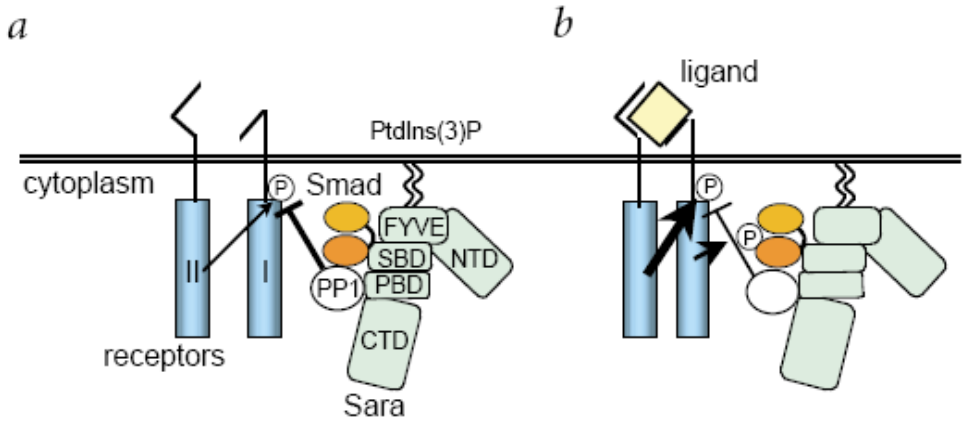

Figure 21 – *A model of PP1c in the TGFβ receptor complex. The two known activating phosphorylations by the receptor kinases are shown. PP1c has an inhibitory role, suggesting that it may antagonize one or both of these kinases.* ***a****, In the absence of the ligand, occasional phosphorylation and activation of the type I receptor is rapidly reversed by PP1c, leading to very low signalling through phospho-Smad.* ***b****, In the presence of the ligand, the type II receptor forms a stable complex with the type I receptor, which favours phosphorylation of the type I receptor over dephosphorylation. PP1c bound to Sara therefore acts as a check for the presence of the ligand. This may seem energetically inefficient, but allows tight regulation of signalling. Similar instances of complexes containing PP1, its substrate and an antagonistic kinase, and a scaffold protein that brings them together, have been described (Printen et al. 1997; Westphal et al. 1999). SBD, Smad-binding domain; PBD, phosphatase-binding domain; CTD, carboxy-terminal domain; NTD, amino-terminal domain, (adapted from Bennett and Alphey, 2002).*

By functioning to recruit Smad2 to the TGF-β receptor, SARA is located in an important regulatory position in the pathway. Thus, control of SARA localization, protein levels, or interactions with Smad2 could potentially modulate TGF-β signalling.

Recently, it was reported that the TGF-β-induced Smad7 can interact with the growth arrest and DNA damage protein 34 (GADD34) (Hollander et al. 1997), which is a regulatory subunit of PP1. The Smad7- GADD34 complex was shown to recruit PP1c to

TGF-β type 1 receptor, and thereby dephosphorylate and inactivate it (Shi et al. 2004). PP1c is recruited to ALK5 via a Smad7-GADD34 complex and then dephosphorylates activated ALK5. SARA enhances the recruitment of PP1c to the Smad7-GADD34 complex by enhancing the availability of PP1c to the Smad7-GADD34 complex. Which regulatory subunit of PP1α holoenzyme cooperates with Smad7 to interact with ALK1 remains to be investigated. It was also suggested that Smad7, induced by ALK1 activation, recruits PP1α to ALK1 and thereby inhibits TGF-β/ALK1-induced Smad1/5 phosphorylation in endothelial cells (Valdimarsdottir et al. 2006).

The interaction of the isolated positive clones encoding SARA with PP1α was tested in SD/QDO/x-α-gal medium and was reconfirmed for all. They also interacted with the other PP1 isoforms: PP1γ1 and PP1γ2 (Figure 22). Two PP1 BMs were predicted by bioinformatic analysis of the SARA sequence (RVWF / KVIRW) and all three clones have both, although the three miss part of the N-terminus and only 247T is in the correct reading frame.

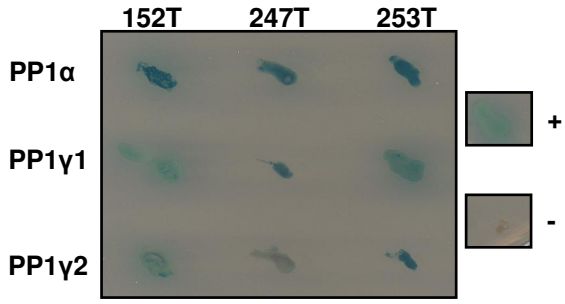

Figure 22 – *Analysis of interaction of the isolated positives for the protein SARA with various PP1 isoforms: α, γ1 and γ2. The interaction was tested in SD/QDO/x-α-gal medium. Plus and minus represent the positive and negative controls, respectively.*

3.3.5.3 Dynactin 1 (DCTN1) / p150^{Glued}

The gene DCTN1 encodes the largest subunit of dynactin, a macromolecular complex consisting of 10-11 subunits ranging in size from 22 to 150 kD. Transcript variant 1, of this gene, consists of at least 32 exons and encodes a larger isoform than variant 2. This isoform contains three binding domains: microtubule (N-terminus), dynein and Arp-1 (C-terminus). Transcript variant 2 lacks exons 1-5, but contains intron 5 sequence. The intron 5 sequence introduces an alternative translation start site, which is located 12 nucleotides immediately upstream of exon 6.

Two clones out of the 298 positives were identified as dynactin by data base searching (Table 10). Both align with regions of the sequence common to the two splice variants (NM_004082 and NM_023019;), thus it is not possible to know to which one they correspond (Figure 23).

Table 10 – *Independent Dynactin clones isolated in the YTH screen.*

First Nucleotide		Positive clones
Isoform 1 (NM_004082**)**	**Isoform 2** (NM_023019)	
1819 (in frame)	3021 (out of frame)	171T
2350 (out of frame)	3552 (out of frame)	138T

Dynein is the major molecular motor protein responsible for a variety of microtubule-based minus-end–directed movements of vesicles and organelles, as well as several steps in mitosis (Paschal and Vallee 1987; Hirokawa et al. 1990; Karki and Holzbaur 1999; Mallik and Gross 2004; Pilling et al. 2006). The dynein/dynactin complex is essential for a diversity of cellular trafficking events, such as vesicular trafficking from the endoplasmic reticulum to the Golgi and lysosomal motility (Caviston and Holzbaur 2006).

Dynactin (Figure 23) binds to both microtubules and cytoplasmic dynein. It is involved in a diverse array of cellular functions, including ER-to-Golgi transport, the centripetal movement of lysosomes and endosomes, spindle formation, chromosome movement, nuclear positioning, and axonogenesis. Understanding the role of dynactin in dynein function has recently become more important with the realization that these proteins may be targets in human neurodegenerative diseases (Hafezparast et al. 2003; Puls et al. 2003). Yet, in spite of the importance of this issue, definitive evidence on the *in vivo* role of dynactin in dynein attachment to membranes does not exist.

Figure 23 – *Alignment of the amino acid sequence of the two isoforms of Dynactin using a CLUSTAL W multiple sequence alignment. PP1 binding motifs are highlighted in blue colour. The first amino acid of the positive clones is highlighted in red colour. (Isoform 1: NM_004082.2; isoform 2: NM_023019.1).*

A key gap in the understanding of dynein function is how this motor protein interacts with membrane compartments. The multiprotein complex dynactin is a candidate factor proposed to link dynein to membrane compartments (Schroer 2004). Although the original work on dynactin suggested that highly purified dynein could mediate vesicle attachment to microtubules in the absence of dynactin, a more recent and relatively small number of *in vitro* experiments have led to the generally accepted model that the attachment of dynein to membrane vesicles requires dynactin (Waterman-Storer et al. 1997; Karki and Holzbaur 1999; Muresan et al. 2001).

An alternative model suggests that dynein light and intermediate chain subunits may link dynein to other membrane associated proteins independently of dynactin (Tai et al. 1999;

Tynan et al. 2000; Yano et al. 2001). In this competing view, dynactin plays a role in regulating or coordinating dynein functions such as processivity (King and Schroer 2000).
Phosphorylation may directly modulate enzymatic or motor activity. Phosphorylation of dynein or of an accessory factor may also regulate the affinity of the motor with its cargo, the organelle which is being transported. Studies on the microtubule motor kinesin have provided evidence for both types of regulatory mechanisms (Sato-Yoshitake et al. 1992; Hollenbeck 1993; Matthies et al. 1993; McIlvain et al. 1994).
It should be noted that, when examined in whole-cell extracts, a significant fraction of the p150 isoform does not bind to microtubules (Tokito et al. 1996). The differential affinity may reflect differences in the posttranslational modification of the dynactin complex. The binding of the related polypeptide CLIP-170 to microtubules has been shown to be modulated by its phosphorylation state (Rickard and Kreis 1991); p150 may be regulated in a similar manner. It was determined that $p150^{Glued}$ is a phosphoprotein (Farshori and Holzbaur 1997), although the effects of phosphorylation on the affinity of $p150^{Glued}$ for microtubules has yet to be determined. It has been proposed that the phosphorylation site of CLIP-170 may map to a cluster of serine residues near the microtubule-binding motif (Pierre et al. 1992) and $p150^{Glued}$ also has a number of serine residues adjacent to the microtubule-binding motif.
The interaction between dynein and dynactin becomes attenuated with aging, although it remains unclear why several studies have shown that the activity of dynein was affected by phosphorylation of its subunit (Dillman and Pfister 1994; Lin et al. 1994; Allan 1995; Niclas et al. 1996). Other studies have shown that aging affects the activity of protein phosphatases in brain (Norris et al. 1998; Jiang et al. 2001; Jouvenceau and Dutar 2006), and it was also reported that the activity of protein phosphatases decreased in Alzheimer's Disease brains (Gong et al. 1993; Gong et al. 1995; Ladner et al. 1996; Vogelsberg-Ragaglia et al. 2001). Then, age dependent alterations in the activity of protein phosphatases or other unknown modulator might affect the dynein-dynactin interactions. Recent findings suggest that aging attenuates the dynein-dynactin interaction (Kimura et al. 2007), representing one of the risk factors for age-related impaired dynein function and even for accumulation of disease proteins.
Dynactin 1 has two potential PP1 BMs (KIKF / KVTF) as determined by bioinformatic analysis, but the clones isolated only have the one nearest to the C-terminus. The interaction of the two clones with PP1α was supported when tested in SD/QDO/X-α-Gal medium; the same being true for the two other PP1 isoforms tested (Figure 24). These

results suggest that it is precisely the PP1 binding motif KVTF, nearest to the C-terminus, that is functionally active.

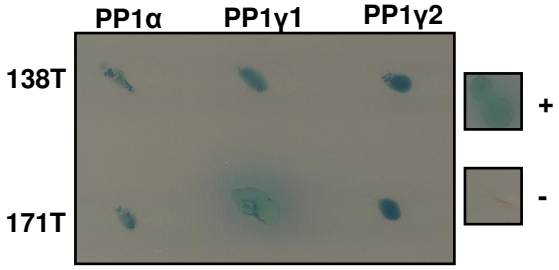

Figure 24 – *Analysis of interaction of the isolated dynactin positives with the various PP1 isoforms: α, γ1 and γ2. The interaction was tested in SD/QDO/x-α-gal medium. Plus and minus represent the positive and negative controls, respectively.*

3.3.5.4 Chr9orf75

Chr9orf75 was the most abundant positive clone in the YTH screen with a total of 45 clones, corresponding to approximately 15% of all positives isolated (Table 11). The mRNA (NM_173691) corresponding to this ORF record is supported by experimental evidence; however, the coding sequence is predicted.

Table 11 – *Independent Chr9orf75 clones isolated in the YTH screen.*

First Nucleotide	Positive clones
- 90 (out of frame)	40T, 41T
-15 (out of frame)	91T, 151T, 170T
102 (in frame)	13T
184 (out of frame)	209T
189 (in frame)	100T, 169T
201 (in frame)	117T, 186T
206 (out of frame)	181T
274 (out of frame)	65T, 223T
325 (out of frame)	104T, 110T, 190T
373 (out of frame)	43T, 74T, 84T, 139T, 154T, 221T, 228T, 239T, 272Q
374 (out of frame)	142T, 172T
375 (in frame)	129T
496 (out of frame)	180T
577 (out of frame)	53T
622 (out of frame)	148T, 149T
670 (out of frame)	105T, 155T, 164T, 199T, 232T, 235T, 237T, 265Q, 267Q, 292Q, 298T
701 (out of frame)	150T

Chr9orf75 was described as a PP1 interactor but there is no knowledge of its physiologic function (Trinkle-Mulcahy et al. 2006). The nucleotide and the corresponding amino acid sequence of Chr9orf75 are presented in Figure 25.

```
                                    cgggaccccgagtgccactccagcctcaccc
cctgccagtgccactcctagccagcgccagtgcgtctccgcagccaccagcaccaacgaa
ctccttcaccgtccacccccggggtctgcaccgcggcgcgggcgcccgcctgctctccaa
cgggcactcggcccctgagccccgggccggccctgccaaccgcctcgcgggctccccgcc
tgggtcgggacagtggaagccaaaggtggagtcgggggatccctccctccacccgccccc
cagccccgggaccccgagtgccactccagcctcacccccgccagtgccactcctagcca
gcgccagtgcgtctccgcagccaccagcaccacgactccttcgagatacggccggccccc
aagccagttatggagaccatccccttgggggacctccaggcccgggcgctggccagcctc
          M  E  T  I  P  L  G  D  L  Q  A  R  A  L  A  S  L
cgcgcaaactctccgaaattctttcatggtcatccccaagagcaatgcctccggggctcct
 R  A  N  S  R  N  S  F  M  V  I  P  K  S  N  A  S  G  A  P
cctcctgaggggaggcagtccgtggagctgccaaagggagacctgggcccggcctccccg
 P  P  E  G  R  Q  S  V  E  L  P  K  G  D  L  G  P  A  S  P
agccaggagctcggatcccagccggtgcctggaggggatggtgcgcctgccctcgggaag
 S  Q  E  L  G  S  Q  P  V  P  G  G  D  G  A  P  A  L  G  K
agccccctggaggtcgaggcacagtgggcagtcgaggaggggcctgtcccaggacagcc
 S  P  L  E  V  E  A  Q  W  A  V  E  E  G  A  C  P  R  T  A
accgccctcgctgaccgggctattaggtggcagaggccgtcctcaccgccccccttcctg
 T  A  L  A  D  R  A  I  R  W  Q  R  P  S  S  P  P  P  F  L
ccggctgcttcggaagaagctgagcctgctgagggcctcagggttcctggcttggccaag
 P  A  A  S  E  E  A  E  P  A  E  G  L  R  V  P  G  L  A  K
aatagccgggaatatgtgaggccggggctgcctgtcaccttcatcgatgaggtagactcg
 N  S  R  E  Y  V  R  P  G  L  P  V  T  F  I  D  E  V  D  S
gaggaggccccccaagcagccaaactaccctacctcccgcaccctgccaggcctctgcac
 E  E  A  P  Q  A  A  K  L  P  Y  L  P  H  P  A  R  P  L  H
cctgccaggcccgggtgcgtggcagagcttcagccccggggcagcaacaccttcacagtg
 P  A  R  P  G  C  V  A  E  L  Q  P  R  G  S  N  T  F  T  V
gtgcccaagaggaagccagggactctgcaggaccagcacttcagtcaggccaacagggag
 V  P  K  R  K  P  G  T  L  Q  D  Q  H  F  S  Q  A  N  R  E
cctcggccacgggaggccgaggaggaggaggctagttgcctcctggggcccacgttgaag
 P  R  P  R  E  A  E  E  E  E  A  S  C  L  L  G  P  T  L  K
aagcgctaccccaccgtgcatgagatcgaggtgattggcggctacctggccctgcagaag
 K  R  Y  P  T  V  H  E  I  E  V  I  G  G  Y  L  A  L  Q  K
tcctgcctcaccaaggctggctcctcaagaaagaagatgaagatctccttcaacgacaaa
 S  C  L  T  K  A  G  S  S  R  K  K  M  K  I  S  F  N  D  K
agcctgcagaccacatttgagtaccttccgagagctccctagagcaggaggaagaggtg
 S  L  Q  T  T  F  E  Y  P  S  E  S  S  L  E  Q  E  E  E  V
gaccagcaggaggaggaggaggaggaggaggaagaggaagaggaggaagagggatcc
 D  Q  Q  E  E  E  E  E  E  E  E  E  E  E  E  E  E  G  S
ggctcagaggagaagccctttgcactcttcctgccccgggccacgtttgtgagcagcgtg
 G  S  E  E  K  P  F  A  L  F  L  P  R  A  T  F  V  S  S  V
agacccgagagctctcggctgccagagggtagctcaggcctgtccagctacaccccgaag
 R  P  E  S  S  R  L  P  E  G  S  S  G  L  S  S  Y  T  P  K
cactctgtggccttcagcaagtggcaggagcaggcgctggagcaggccccgagggaggca
 H  S  V  A  F  S  K  W  Q  E  Q  A  L  E  Q  A  P  R  E  A
gagcccccgcccgtggaggccatggtgagatgcgggggagtggagcgctgggggagtct
 E  P  P  P  V  E  A  M  V  R  C  G  G  V  E  R  W  G  E  S
gacacccgggcgagcccatgtgtccacattctgtcctctcactttcagctcacacccgcc
 D  T  R  A  S  P  C  V  H  I  L  S  S  H  F  Q  L  T  P  A
agtcagaatgacctctcggacttccgcagcgagccagccctgtatttctaagcccagcac
 S  Q  N  D  L  S  D  F  R  S  E  P  A  L  Y  F
tgccaggaccaaggctgagcccagctgtgggagtcccggaagctgggcagtagccaggga
ctactgcacccgcttctgccttgtttggcctcactgtatcccacccaccccctcctggccc
tggaagcagctagggtgcctcctgccatcggggccaggtctgggtctcactccccggccc
tggtttgggagggtccaaggggggaagtggggtggggaactgcctgtgggtgagtgccagg
ggcctgctgggtggtggccatctgcgacccggcaggggggctgtgcagattctgcacctgg
ccattccctgtcctgtctcctcagcctgcctcacagtggccatggggtgtcggggtgaag
ggctgtcccagctacttgtcctctgcaggaccctaagcccctgcccgcagcccacatgcc
ctctgtgatgagtggcgtctttcctgcctctgatgatggactcaataaacagcactggac
aaggct
```

Figure 25 - *Nucleotide and corresponding amino acid sequence of Chr9orf75. PP1 binding motifs are highlighted in blue color (positions 103-107 and 269-275 in a.a. sequence).The first nucleotide of Chr9orf75 transcript variant 1 (NM_173691) is in green and the first nucleotides of the several positive clones are highlighted in red color. Upstream of the first nucleotide of transcript variant 1 (green), are the 90 nt derived from clones 91T, 151T and 170T.*

Of all the 45 positives obtained for this protein five contained 15 (clones 91T, 151T and 170T) and 90 (clones 40T and 41T) nucleotides upstream of the first nucleotide of the sequence present in the Genbank entry. However, a very recent update of the Chr9orf75 Genbank entry describes a new transcript variant, transcript variant 2, starting at an upstream ATG codon (NM_173691.3). Transcript variant 1 (in Figure 25) lacks a segment in the 3' coding region, compared to variant 2, which results in a shorter protein (isoform 1, in Figure 26). The two proteins are encoded in the same reading frame.

```
Chr9orf75_isoform1  ------------------------------------------------------------
Chr9orf75_isoform2  MLLEAERRRGGGAAGARLLERYRRVPGVRALRADSVLIIETVPGFPPAPPAPGAAQIRAA

Chr9orf75_isoform1  ------------------------------------------------------------
Chr9orf75_isoform2  EVLVYGAPPGRVSRLLERFDPPAAPRRRGSPERARPPPPPPPPAPPRPPPAAPSPPAAPG

Chr9orf75_isoform1  ------------------------------------------------------------
Chr9orf75_isoform2  PRGGGASPGARRSDFLQKTGSNSFTVHPRGLHRGAGARLLSNGHSAPEPRAGPANRLAGS

Chr9orf75_isoform1  ------------------------------------------------------------
Chr9orf75_isoform2  PPGSGQWKPKVESGDPSLHPPPSPGTPSATPASPPASATPSQRQCVSAATSTNDSFEIRP

Chr9orf75_isoform1  -----METIPLGDLQARALASLRANSRNSFMVIPKSNASGAPPPEGRQSVELPKGDLGPA
Chr9orf75_isoform2  APKPVMETIPLGDLQARALASLRANSRNSFMVIPKSKASGAPPPEGRQSVELPKGDLGPA
                         *******************************:***********************

Chr9orf75_isoform1  SPSQELGSQPVPGGDGAPALGKSPLEVEAQWAVEEGACPRTATALADRAIRWQRPSSPPP
Chr9orf75_isoform2  SPSQELGSQPVPGGDGAPALGKSPLEVEAQWAVEEGACPRTATALADRAIRWQRPSSPPP
                    ************************************************************

Chr9orf75_isoform1  FLPAASEEAEPAEGLRVPGLAKNSREYVRPGLPVTFIDEVDSEEAPQAAKLPYLPHPARP
Chr9orf75_isoform2  FLPAASEEAEPAEGLRVPGLAKNSREYVRPGLPVTFIDEVDSEEAPQAAKLPYLPHPARP
                    ************************************************************

Chr9orf75_isoform1  LHPARPGCVAELQPRGSNTFTVVPKRKPGTLQDQHFSQANREPRPREAEEEEASCLLGPT
Chr9orf75_isoform2  LHPARPGCVAELQPRGSNTFTVVPKRKPGTLQDQHFSQANREPRPREAEEEEASCLLGPT
                    ************************************************************

Chr9orf75_isoform1  LKKRYPTVHEIEVIGGYLALQKSCLTKAGSSRKKMKISFNDKSLQTTFEYPSESSLEQEE
Chr9orf75_isoform2  LKKRYPTVHEIEVIGGYLALQKSCLTKAGSSRKKMKISFNDKSLQTTFEYPSESSLEQEE
                    ************************************************************

Chr9orf75_isoform1  EVDQQEEEEEEEEEEEEEEGSGSEEKPFALFLPRATFVSSVRPESSRLPEGSSGLSSYT
Chr9orf75_isoform2  EVDQQEEEEEEEEEEEEEEGSGSEEKPFALFLPRATFVSSVRPESSRLPEGSSGLSSYT
                    ************************************************************

Chr9orf75_isoform1  PKHSVAFSKWQEQALEQAPREAEPPPVEAMVRCGGVERWGESDTRASPCVHILSSHFQLT
Chr9orf75_isoform2  PKHSVAFSKWQEQALEQAPREAEPPPVEAMVRCGGVERWGESDTRASPCVHILSSHFQLT
                    ************************************************************

Chr9orf75_isoform1  PASQNDLSDFRSEPALYF
Chr9orf75_isoform2  PASQNDLSDFRSEPALYF
                    ******************
```

Figure 26 – *Alignment of the amino acid sequence of the two isoforms of Chr9orf75 using a CLUSTAL W multiple sequence alignment. PP1 binding motifs are highlighted in blue colour.*

Since Chr9orf75 has two potential PP1 BMs (RAIRW / KISF), several clones were selected for analysis of interaction with PP1. Clones 13 and 100 have the complete coding sequence of the corresponding protein in the correct frame. Clones 40 and 170 are also complete clones, but out of frame, and with 90 and 15 nucleotides more, respectively, than the predicted sequence for Chr9orf75. Clone 150 does not have the RAIRW PP1 BM and is out of frame, and clone 148 misses part of that PP1 BM and is also out of frame. All have the second PP1 BM corresponding to the aminoacids KISF.

All clones tested were found to interact with PP1α, as expected, but also revealed a positive interaction with PP1γ1 and PP1γ2 (Figure 27). Light blue colonies also represent positive interactions that took longer to turn blue in the presence of X-α-GAL. Interestingly, the fact of some clones being incomplete or out of frame was not sufficient to impede interaction with the PP1 isoforms.

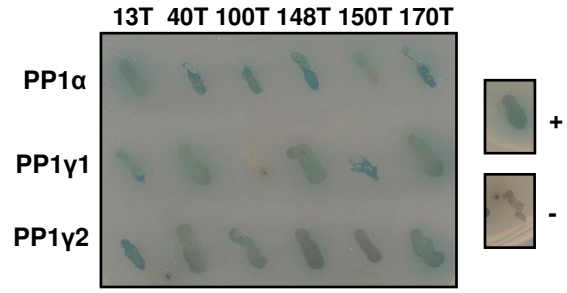

Figure 27 – *Analysis of interaction of the protein Chr9orf75 with the PP1 isoforms: α, γ1 and γ2, by yeast co-transformation. The interaction was tested in SD/QDO/x-α-gal medium. Plus and minus represent the positive and negative controls, respectively.*

Almost all of the PP1 interacting proteins contain a degenerate RVxF-motif. The Chr9orf75 protein has two PP1 BMs predicted by bioinformatic analysis of its sequence. However, while the predicted KISF motif has a sequence very similar to the PP1 BMs that usually are present in the PP1 binding proteins, the other one BM (RAIRW) differs more from the known PP1 BMs and is less likely to be physiologically functional.

3.3.6 Analysis of Chr9orf75 and PP1 interaction

3.3.6.1 pC9orf75-GFP expression in HeLa Cells

The cDNA corresponding to Chr9orf75 was subcloned into the pEGFP vector in frame with the GFP (Green Fluorescent Protein) protein. Thus, the GFP-tag was used as a biological marker, overcoming the need for an antibody against Chr9orf75. It was an important resource, allowing the employment of several techniques described below, by expression of pC9orf75-GFP fusion protein in human HeLa cells, a cervical cancer cell line (Figure 28).

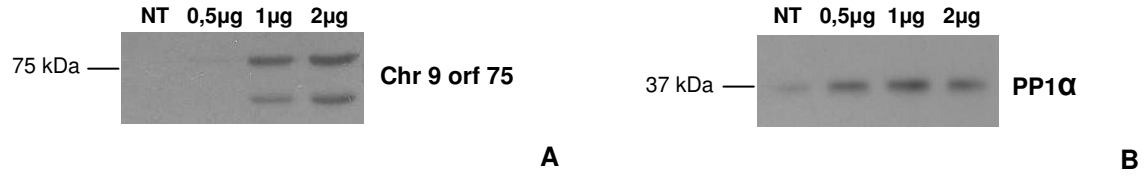

Figure 28 – *pC9orf75-GFP expression in HeLa cells. The lanes correspond to non transfected (NT) cells and cells transfected with 0,5 µg, 1 µg and 2 µg of pC9orf75-GFP DNA.* ***A****. Immunoblot analysis of pC9orf75-GFP in lysates of transfected HeLa cells, using an antibody against the GFP tag.* ***B****. Immunoblot analysis of endogenous PP1α levels with increasing amounts of transfected Chr9orf75. Detection was performed with an anti-PP1α antibody (CBC2C).*

The expression of pC9orf75-GFP in HeLa cells was successful and as can be observed in Figure 28A pC9orf75-GFP fusion protein transfection revealed two bands, when the anti-GFP antibody was used. The immmunoreactive proteins have apparent molecular mass of 86,6 kDa and 66,4 kDa, respectively. As the theoretical molecular mass of the Chr9orf75 protein is 47,3 kDa and the GFP-tag has approximately 30 kDa, the expected molecular mass for the fusion protein would be around 77 kDa. The observed higher molecular mass protein (86,6 kDa) probably represents the full length fusion protein. The abnormal migration observed may be due to post-translational modifications of the protein. The smaller band has a corresponding molecular mass of 66,4 kDa that may result from proteolytic cleavage of the higher molecular mass protein. When the immunoblot was probed with an anti-PP1α antibody, an apparent increase of PP1α cellular protein levels could be observed with increasing amounts of transfected pC9orf75-GFP.

3.3.6.2 Co-immunoprecipitation of Chr9orf75 with PP1

With the purpose of confirming and provide an *ex vivo* evidence for the interaction of Chr9orf75 with PP1, immunoprecipitation of protein extracts obtained from HeLa cells transfected with pC9orf75-GFP was performed, using highly specific anti-PP1α (CBC2C) and anti-PP1γ (CBC3C) antibodies. Proteins from cells lysates and immunoprecipitates (IPs) were separated on a 10% SDS-PAGE gel and transferred to a nitrocellulose membrane, immunobloted with anti-GFP and anti-PP1 antibodies and developed by ECL (Figure 29).

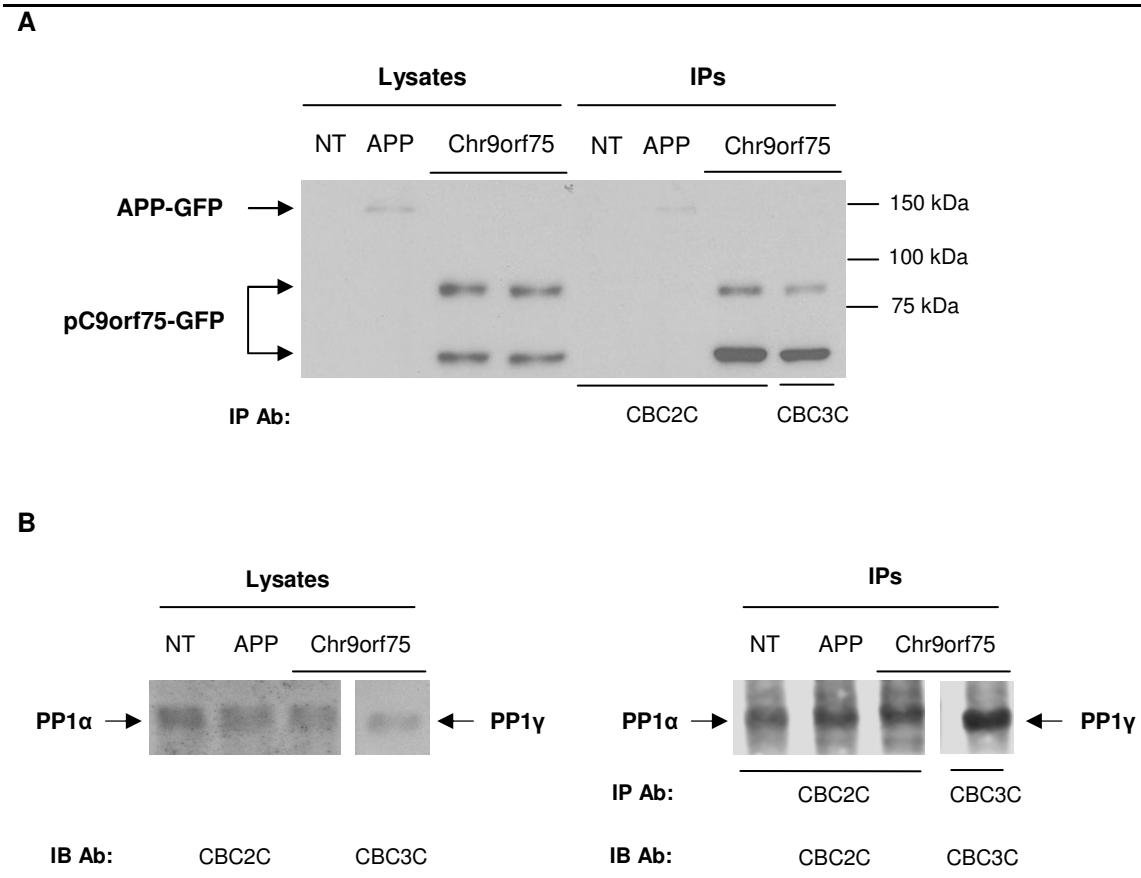

Figure 29 – *Co-immunoprecipitation of Chr9orf75 with PP1. Immunoblot analysis of HeLa cells tranfected with pC9orf75-GFP (or APP-GFP, as a control) and immunoprecipitated with anti-PP1α and anti-PP1γ1antibodies.* ***A****. Membrane immunoblotted with anti-GFP antibody.* ***B****. Membrane immunoblotted with anti-PP1α (CBC2C) and anti-PP1γ (CBC3C) antibodies. NT, non-tranfected cells; APP, cells transfected with APP-GFP; Chr9orf75, cells transfected with pC9orf75-GFP; IP Ab, immunoprecipitation antibody; and IB Ab, immunoblot antibody.*

From the analysis of Figure 29 it is obvious that Chr9orf75 co-immunoprecipitates with PP1α and PP1γ. Appropriate controls were included in parallel: immunoprecipitation from non-transfected cells and from cells transfected with APP (Alzheimer's amyloid precursor protein).

In agreement with the observed in Figure 28, two bands were again observed for pC9orf75-GFP construct, with the previously refered molecular mass. Since protein degradation is an unlikely explanation, given the use of protease inhibitors during the process of immunoprecipitation, this observation leads to believe that the complete protein may have been cleaved *in vivo*. This cleavage must occur on the N-terminus side of the protein, since the GFP tag is on the C-terminus and detection was achieved with an anti-GFP antibody. This experiment clearly shows that Chr9orf75 interacts with PP1 isoforms α and γ, in agreement with the yeast co-transformation assays (Figure 27). This interaction is likely to be direct, given the presence of a canonical PP1 binding motif (KISF) in the Chr9orf75 protein.

3.3.6.3 Overlay assay of Chr9orf75 with PP1

In order to further confirm the interaction of Chr9orf75 with PP1, a blot overlay analysis was performed. For this purpose, protein extracts from pC9orf75-GFP transfected HeLa cells were loaded on a 10% SDS-PAGE gel and transferred to nitrocellulose membrane. Lysate from non-transfected cells was used as negative control. The membrane was incubated with PP1γ1 (1 µg/mL; purified in our laboratory by A. P. Vintém), immunobloted with the anti-PP1γ1 antibody (CBC3C) and developed by ECL (Figure 30).

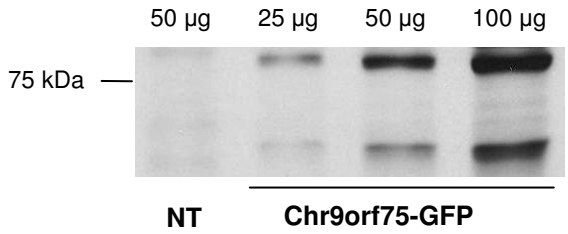

Figure 30 – *Overlay assay of Chr9orf75 with PP1γ1. The total protein amounts of HeLa cell lysate loaded on each well are indicated on top. NT, lysate from non transfected cells; Chr9orf75-GFP , lysate from cells transfected with the pC9orf75-GFP construct.*

The results obtained from this experiment confirm that, as expected, the interaction of the Chr9orf75 protein with PP1γ1, must be direct (i.e. without the need for a bridging protein). Again, these results are in agreement with the presence of a functional PP1 BM in Chr9orf75.

3.3.6.4 Subcellular localization of Chr9orf75 in HeLa cells

With the purpose of studying the subcellular localization of Chr9orf75, HeLa cells were transfected with the pC9orf75-GFP construct. The expression of the fusion protein allowed the analysis of its subcellular localization and its co-localization with PP1α. HeLa cells were transfected with the referred plasmid and subjected to immunocytochemistry with the anti-PP1α antibody, detected with anti-rabbit Texas Red-conjugated antibody. Confocal fluorescence microscopy analysis revealed that pC9orf75-GFP distribution is almost exclusively nuclear and apparently excluded from nucleolar structures (Figure 31). Specific nucleoli markers, or co-localization with PP1γ1 (enriched in nucleoli), should clarify this observation.

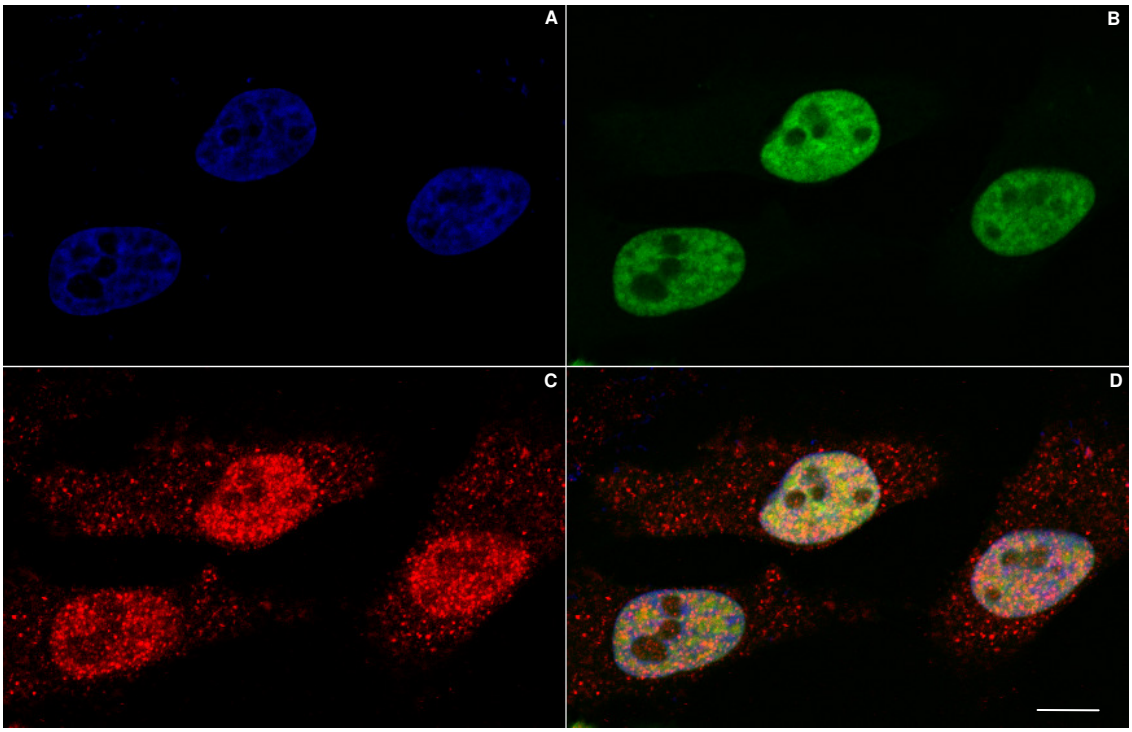

Figure 31 – *Subcellular localization of pC9orf75-GFP and co-localization with PP1α.* ***A****, nucleic acids were stained using DAPI (blue).* ***B****, green fluorescence of the exogenous pC9orf75-GFP protein.* ***C****, endogenous PP1α (red) detected with anti-rabbit Texas Red-conjugated antibody.* ***D****, nuclear co-localization of PP1α and Chr9orf75 can be observed in the merge (yellow/orange). Bar, 10 µm.*

Around 68% of the pC9orf75-GFP population has an exclusively nuclear distribution, while in 32% of the population pC9orf75-GFP was found not only in the nucleus of HeLa cells, but also distributed throughout the cytoplasm (Figure 32). Of note is that neither of these two distribution patterns was apparently dependent on the levels of transfection.

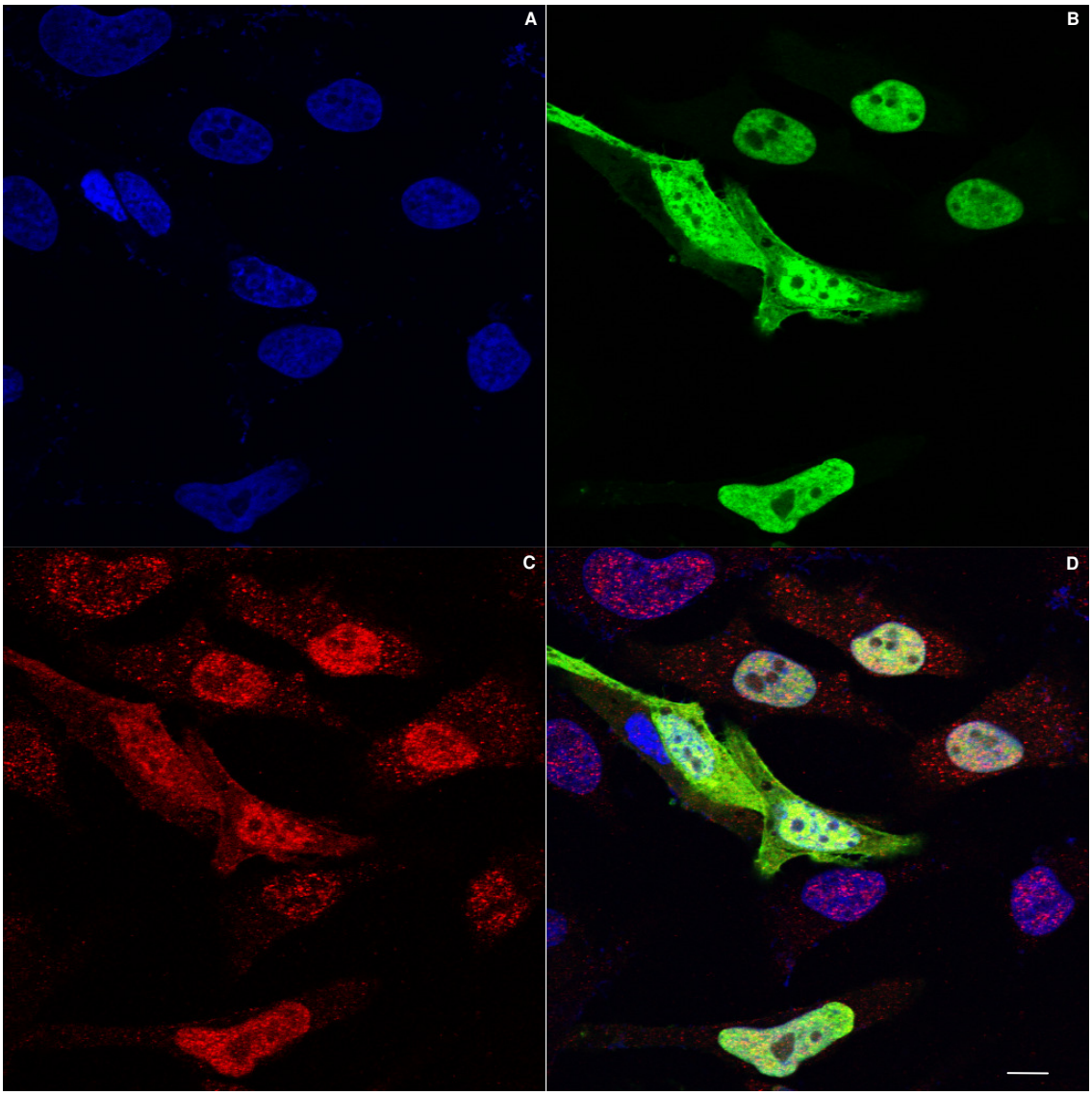

Figure 32 – *Subcellular localization of pC9orf75-GFP and co-localization with PP1α.* ***A****, nucleic acids were stained using DAPI (blue).* ***B****, pC9orf75-GFP green fluorescence.* ***C****, endogenous PP1α (red) detected with Texas Red-conjugated anti-PP1α antibody.* ***D****, co-localization observed in the merged image (yellow/orange). Bar, 10 µm.*

Cells with high pC9orf75-GFP cytoplasmic distribution exhibited a less rounded morphology; around 90% of this population (Figures 32 and 33), and pC9orf75-GFP could also be observed in the plasma membrane and in fillopodia-like structures (ROIs in Figure 33). Very interestingly, while in non-transfected cells cytoplasmic PP1α is not observed in the plasma membrane (under the conditions used), Chr9orf75 cytoplasmic presence relocates PP1α to the referred structures (Figure 32 and 33), where they co-localize.

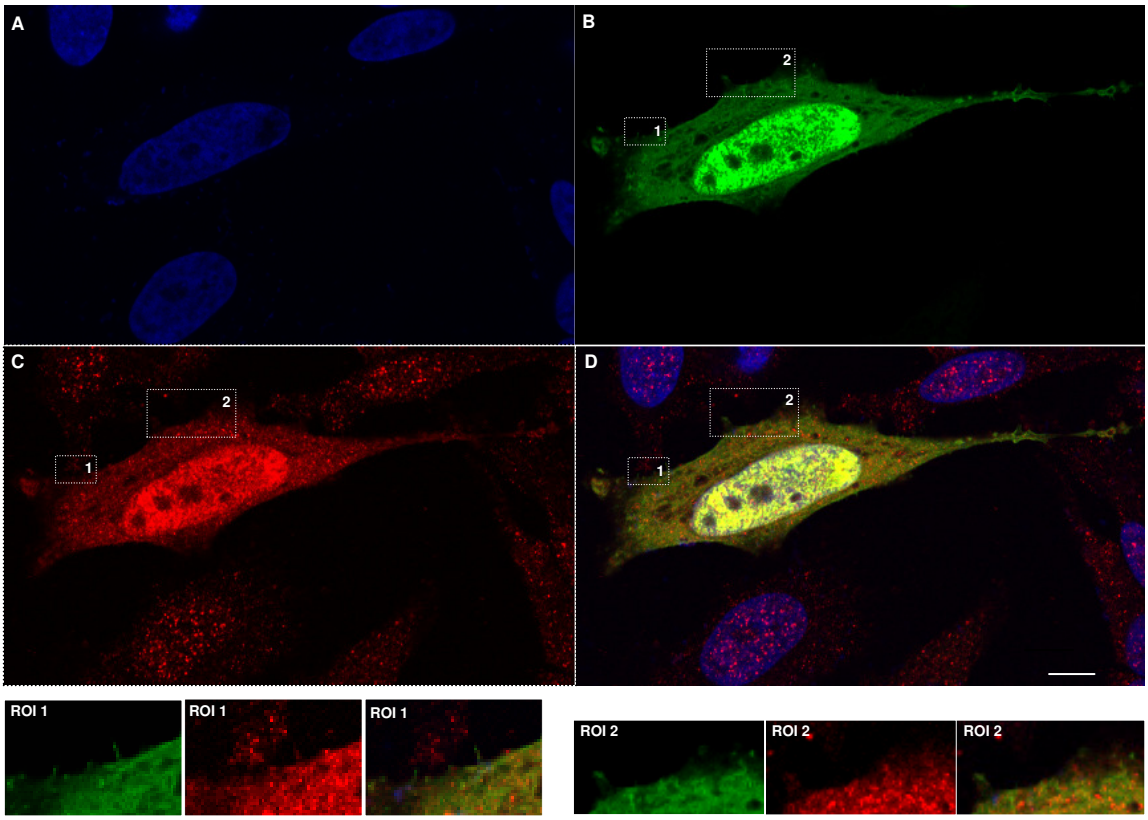

Figure 33 – *Subcellular localization of pC9orf75-GFP and co-localization with PP1α.* ***A****, nucleic acids were stained using DAPI (blue).* ***B****, pC9orf75-GFP green fluorescence.* ***C****, endogenous PP1α (red) detected with Texas Red-conjugated anti PP1α antibody.* ***D****, co-localization observed in the merged image (yellow/orange). ROI, Region of interest. Bar, 10 µm.*

Co-localization analysis using an anti-PP1α antibody revealed a high degree of nuclear pC9orf75-GFP/PP1α co-localization. Interestingly, PP1α nuclear staining apparently increased in pC9orf75-GFP transfected cells, in comparison to non-transfected cells, in a pC9orf75-GFP dose-dependent manner (Figure 34). Nonetheless, in the more highly transfected cells not only the nuclear abundance of PP1α increases but its cytoplasmic amounts also appear to increase slightly, suggesting that PP1α protein levels may be up-regulated by Chr9orf75.

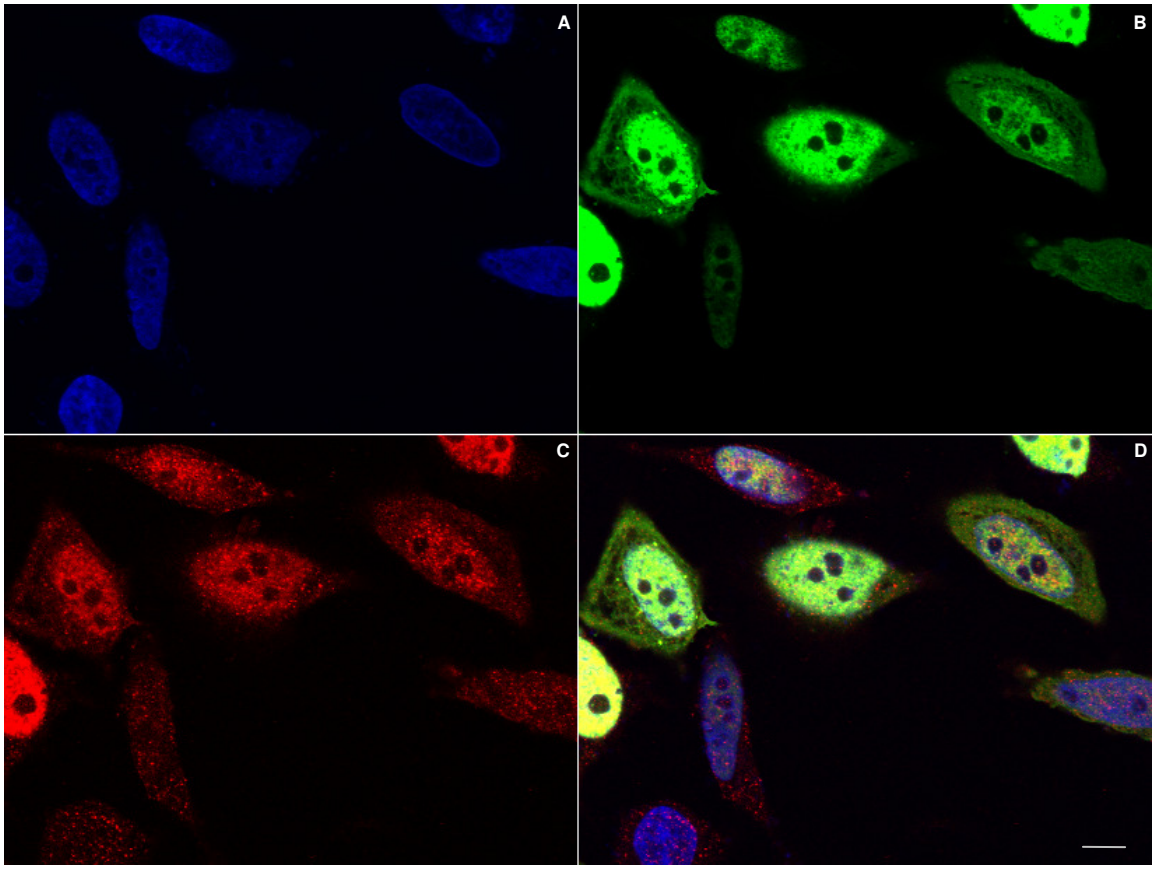

Figure 34 – *Subcellular localization of pC9orf75-GFP and co-localization with PP1α.* ***A,*** *nucleic acids were stained using DAPI (blue).* ***B****, pC9orf75-GFP green fluorescence.* ***C,*** *endogenous PP1α (red) detected with Texas Red-conjugated anti PPα antibody.* ***D****, co-localization observed in the merged image (yellow/orange). Bar, 10 µm.*

3.4 DISCUSSION

The involvement of PP1α in diverse cellular processes is correlated with its binding to a diverse set of regulatory subunits. Using the YTH system, new PP1α interactors from human brain were identified in order to gain insight into the various roles of PP1α in several cellular processes, brain function and neurodegeneration.

The 1.72×10^7 human brain cDNA clones screened originated 298 positive clones, two of which were assigned as false positives, while the others correspond to 74 different proteins. Of those 20 are known PP1 interactors and 41 are putative proteins so far never associated with PP1. The results obtained validated the method as a promising approach to understand the multiple functions of the PP1α catalytic subunit, being a method of choice to screen a large number of proteins for putative interactions. The identification of all the positive clones obtained in the screen was an established objective of the analysis since the beginning of this study. This strategy turned out to be very successful because several novel and interesting PPα interacting proteins could be identified, which would never be found if only the more abundant positives were studied. Some “bonafide”, previously characterized, PP1 binding proteins were identified in this screen, like Nek2A and spinophilin. These findings validated the YTH technique, by confirming that expression of the reporter genes was due to a specific interaction between the bait protein (PP1α) and the identified library protein.

Some of the positive clones isolated encoded proteins found to be fused out of frame to the GAL4-BD. It would therefore be expected that the wrong reading frame might code for an artificial protein that would not bind PP1α. This was the case even for some of the well known PP1 binding proteins identified. Thus, the fact that several “bonafide” PP1 regulators were fused to the GAL4-BD in a wrong reading frame strongly suggests that the correct protein might still be produced by a well known mechanism in yeast, called programmed translational frame shift or translational recoding (Shah et al. 2002). Some specific sequences, 7 nucleotides long, are known to induce ribosomal frame shifting. This is a directional and reading frame specific event. Several programmed frame shift heptanucleotides have been identified: CUU-AGG-C, CUU-AGU-U and GGU-CAG-A (Shah et al. 2002). So it is concluded that translational recoding may be a feasible explanation for these observations. Moreover, this mechanism could be enhanced because of the use of selective media without some amino acids. Thus, the yeast translation machinery might be using alternative codons favouring the activation of the nutritional reporter genes, allowing growth in the selective media.

In what concerns PP1α and brain associated cellular events, this screen provided a large amount of data that will be useful in the search for brain-specific PP1α binding proteins that may be used in therapeutic and diagnostic approaches regarding neurodegenerative disorders and aging.

For example two novel interactors for PP1α were described, dynactin-1 and synphilin-1A, which assign new roles to PP1α in physiological processes such as cellular processes involving the motor protein dynein and might suggest its involvement in neurodegenerative disorders. Interactions with two previously known PP1 interactors were also described: SARA and Chr9orf75. The first associates PP1α with the TGF-β receptor signalling pathway while for the second no function is yet assigned. The interaction between PP1α and these four proteins was confirmed by co-transformation in yeast strain AH109, were interactions with other PP1 isoforms were also analysed. In all cases quantitative analysis would be the logical next step, in order to better understand the strength of the interactions among these proteins and the different PP1 isoforms.

The interactions should also be confirmed by other biochemical approaches such as immunoprecipitation, overlay or pull-down assays. A more detailed analysis of binding to PP1 was performed for Chr9orf75, the most abundant interaction identified on the screen and also the least characterised. Very recently, a new transcript variant was described for this protein but at the time of this study, the only isoform known was the shorter one. Positive clones 40T and 41T contain 90 nucleotides upstream of the first nucleotide presented in the Chr9orf75 Genbank entry and considered at the time of analysis, and clones 91T, 151T and 170T contain 15 nucleotides upstream. These results are now corroborated by the update of the Genbank information, since the new isoform (isoform 2) described has a longer 5` sequence.

The various techniques used revealed that the corresponding Chr9orf75 protein may occur as a precursor protein, given that it suffers a proteolytic cleavage near its N-terminus. This apparent cleavage originates a fragment reduced in ≈ 20 kDa, which corresponds to approximately 178 aminoacids (Figure 35). This being the case, the smaller protein fragment lacks the most N-terminal PP1 BM, but conserves the canonical motif, thus being still able to bind PP1. This was confirmed by all the binding assays used: yeast co-transformation, immunoprecipitation and overlay. As a result, the simplest interpretation of this results indicates that the binding likely occurs directly and not through binding to a third bridging protein.

A

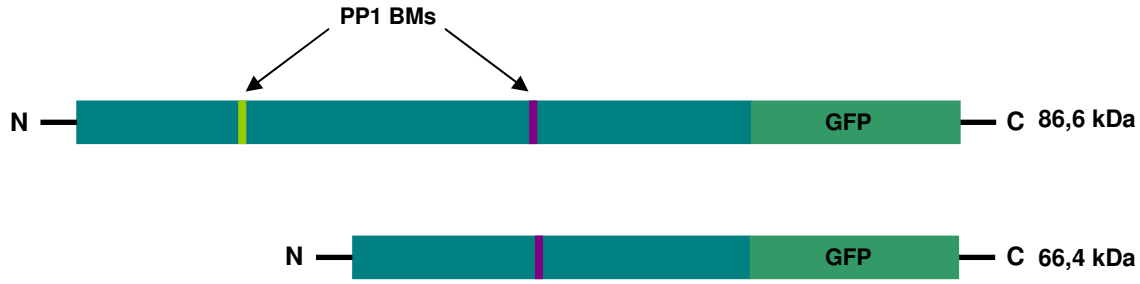

B

METIPLGDLQARALASLRANSRNSFMVIPKSNASGAPPPEGRQSVELPKGDLGPASPSQELGSQPVPGGD
GAPALGKSPLEVEAQWAVEEGACPRTATALAD**RAIRW**QRPSSPPPFLPAASEEAEPAEGLRVPGLAKNSR
EYVRPGLPVTFIDEVDSEEAPQAAKLP**YLPHPARPLHPARPGCVAELQ**PRGSNTFTVVPKRKPGTLQDQH
FSQANREPRPREAEEEEASCLLGPTLKKRYPTVHEIEVIGGYLALQKSCLTKAGSSRKKM**KISF**NDKSLQ
TTFEYPSESSLEQEEEVDQQEEEEEEEEEEEEEEGSGSEEKPFALFLPRATFVSSVRPESSRLPEGSSG
LSSYTPKHSVAFSKWQEQALEQAPREAEPPPVEAMVRCGGVERWGESDTRASPCVHILSSHFQLTPASQN
DLSDFRSEPALYF

Figure 35 – *Analysis of the observed Chr9orf75 protein forms.* ***A*** *The two detected forms of the Chr9orf75 protein: the full-length 86,6 kDa protein on the top and the cleaved one below, originating a shorter fragment of about 66,4 kDa. Cleavage occurs N-terminally and leads to the loss of approximately 178 aminoacids and one of the PP1 BMs (indicated in light green and purple). GFP, C-terminal tag.* ***B*** *The estimated position of cleavage in the aminoacid sequence of Chr9orf75 protein is underlined and the PP1 BMs highlighted in green and purple*

Although both this fragments can bind PP1 the higher abundance of the full-length protein in transfected cells (Figures 27 and 30), contrast the smaller fragment enriched in the co-immunoprecipitates (Figure 28A). This suggests that either the Chr9orf75 N-terminally truncated form is the favoured PP1 binding partner, or that proteolitic cleavage occurred during the immunoprecipitation. As previously mentioned, Chr9orf75 exists as full-length and an N-terminal truncated protein. In all of the analyses performed the C-terminus was detected using the GFP antibody, and it would be very interesting to be able to analyse if the two protein forms are targeted to different subcellular compartments.

Another important validation of the putative interactions discovered with the YTH system is the confirmation of co-expression of the two binding partners either in the same cell-type or in the same subcellular compartment. A condition for *in vivo* interaction of two proteins is their simultaneous presence in the same subcellular compartment. It is, therefore, important to determine the subcellular localization of these proteins, the

particular structures to which they associate and the processes where they are involved. With this intent, the subcellular distribution and co-localization with PP1α was evaluated for Chr9orf75. The expression of the protein Chr9orf75 fused to GFP in HeLa cells revealed that Chr9orf75 is mainly nuclear, and co-localizes with PP1α in this subcellular compartment. Increasing expression of Chr9orf75 enhances the amount of PP1α in the cell, although it remains to verify if this is due to a gene transactivation effect or to an alteration on mRNA/protein half-life. Furthermore, cytoplasmic/plasma membrane localization of Chr9orf75 recruits PP1α to the same subcellular compartments (Figures 32 and 33).

It will be of crucial interest to perform functional assays for both the nuclear and the cytoplasmic Chr9orf75 pools.

4 FINAL CONCLUSIONS

The regulation of the subcellular localization of signalling pathway components is a key determinant in the effective initiation and maintenance of signalling cascades. Regulation of signal transduction pathways through protein/protein interactions can thus make possible the activation of a particular pathway by co-localizing protein kinases and phosphatases with their downstream substrates. Therefore, the identification and characterization of the proteins implicated in neuronal pathways are imperative as a mean to understand these cellular events and associated pathologies.

PP1 is involved in several important physiological processes, such as cell cycle control, apoptosis, transcription, motility, metabolism and memory, regulating them through the dephosphorylation of multiple key substrates. This plasticity of PP1 is due to interaction with diverse regulators and targeting subunits that function as inhibitors, substrate specifiers and substrate targeting proteins.

Several previously known PP1 regulator proteins were identified in the screen here described, among them are Nek2, spinophilin and ASPP1, thus validating the method used. Also, other less characterised PP1 interactors were also found, like SARA and Chr9orf75. Additionally, proteins known in other contexts were here identified as putative PP1 regulators and some had the interaction reconfirmed. That was the case for dynactin-1 and synphilin-1A. Even more interesting was the fact that a great number of the proteins identified were completely new proteins. These results provide new perspectives of PP1α function in the human brain and several neuronal processes and validate the Yeast Two-Hybrid System as a tool to understand the roles played by PP1 in several cellular regulatory events.

The majority of the recovered clones encoded partial cDNA sequences but each showed specific interaction with PP1α in the YTH system. The large number of totally new putative PP1α binding proteins opens new fields of study. The uncharacterized proteins need to be further analysed in order to identify their functions, allowing new roles to be attributed to PP1α, not only in human brain processes but also in other cellular functions. For the known proteins it is also needed a more comprehensive study in order to establish their binding and regulation by PP1α. That is already ongoing in our laboratory with synphilin-1A, dynactin-1 and SARA.

Chr9orf75, a totally uncharacterized protein and the most abundant positive in this screen, was further studied and some further insights were obtained: protein physiological form, binding to PP1 and subcellular localization. Chr9orf75 was detected in two protein forms, a full-length protein and a smaller form, apparently resulting from N-terminal cleavage. Both proteins forms bind strongly to PP1, through a canonical PP1 BM. In HeLa cells

Chr9orf75 was most often found enriched in the nucleus, but also distributed throughout the cytoplasm, and could also be observed in the plasma membrane and in fillopodia-like structures. Cellular co-localization of Chr9orf75 with PP1α was observed and, apparently, increasing amounts of Chr9orf75 concomitantly increase nuclear and cytoplasmic abundance of PP1α.

For therapeutic approaches a complete understanding of PP1 regulation is essential for the development of drugs that interfere with PP1 function. Of all mammalian tissues, the brain expresses the highest levels of protein kinases and phosphatases. Phosphatases play important roles in numerous physiological and cellular events and exist in macromolecular signalling complexes in association with specific regulatory subunits. PP1c subunits are thought to always occur associated with regulatory and scaffold subunits that change PP1c conformation, targeting it to distinct subcellular locations and regulate its activity and substrate specificity. So, since such PP1 regulatory proteins are often tissue or cell type specific (unlike PP1c itself), they should provide much better and specific targets for therapeutic and diagnostic approaches. For this reason PP1 holoenzymes are potential drug targets to be investigated for pharmacological intervention and diagnosis in disease.

The PP1α interactome thus defined constitutes an important extension of the knowledge of PP1α physiological involvement in various brain processes. The number of proteins known to bind and regulate PP1α has been significantly extended and this may hopefully lead to significant insights into PP1α regulation. Given the number of protein phosphatases and phosphoprotein substrates encoded in the human genome, a large number of PP1 interacting proteins certainly remain to be discovered. In conclusion, the results obtained opened new and interesting insights that will need to be explored in detail in the future.

5 REFERENCES

Allan V. (1995) Protein phosphatase 1 regulates the cytoplasmic dynein-driven formation of endoplasmic reticulum networks in vitro. *J Cell Biol* **128,** 879-891.

Altschul S. F., Gish W., Miller W., Myers E. W. and Lipman D. J. (1990) Basic local alignment search tool. *J Mol Biol* **215,** 403-410.

Andreassen P. R., Lacroix F. B., Villa-Moruzzi E. and Margolis R. L. (1998) Differential subcellular localization of protein phosphatase-1 alpha, gamma1, and delta isoforms during both interphase and mitosis in mammalian cells. *J Cell Biol* **141,** 1207-1215.

Attisano L. and Wrana J. L. (2000) Smads as transcriptional co-modulators. *Curr Opin Cell Biol* **12,** 235-243.

Attisano L. and Wrana J. L. (2002) Signal transduction by the TGF-beta superfamily. *Science* **296,** 1646-1647.

Avraham E., Szargel R., Eyal A., Rott R. and Engelender S. (2005) Glycogen synthase kinase 3beta modulates synphilin-1 ubiquitylation and cellular inclusion formation by SIAH: implications for proteasomal function and Lewy body formation. *J Biol Chem* **280,** 42877-42886.

Ayllon V., Martinez A. C., Garcia A., Cayla X. and Rebollo A. (2000) Protein phosphatase 1alpha is a Ras-activated Bad phosphatase that regulates interleukin-2 deprivation-induced apoptosis. *Embo J* **19,** 2237-2246.

Ayllon V., Cayla X., Garcia A., Fleischer A. and Rebollo A. (2002) The anti-apoptotic molecules Bcl-xL and Bcl-w target protein phosphatase 1alpha to Bad. *Eur J Immunol* **32,** 1847-1855.

Barford D. and Neel B. G. (1998) Revealing mechanisms for SH2 domain mediated regulation of the protein tyrosine phosphatase SHP-2. *Structure* **6,** 249-254.

Barford D., Das A. K. and Egloff M. P. (1998a) The structure and mechanism of protein phosphatases: insights into catalysis and regulation. *Annu. Rev. Biophys. Biomol. Struct.* **27,** 133-164.

Barford D., Das A. K. and Egloff M. P. (1998b) The structure and mechanism of protein phosphatases: insights into catalysis and regulation. *Annu Rev Biophys Biomol Struct* **27,** 133-164.

Barker H. M., Brewis N. D., Street A. J., Spurr N. K. and Cohen P. T. (1994) Three genes for protein phosphatase 1 map to different human chromosomes: sequence, expression and gene localisation of protein serine/threonine phosphatase 1 beta (PPP1CB). *Biochim Biophys Acta* **1220,** 212-218.

Bennett D. and Alphey L. (2002) PP1 binds Sara and negatively regulates Dpp signaling in Drosophila melanogaster. *Nat Genet* **31,** 419-423.

Berndt N. (2003) *Roles and regulation of serine/threonine- specific protein phosphatases in the cell cycle.* , Vol. 5. Life in Progress, Roscoff, France.

Berndt N., Dohadwala M. and Liu C. W. (1997) Constitutively active protein phosphatase 1alpha causes Rb-dependent G1 arrest in human cancer cells. *Curr Biol* **7,** 375-386.

Berndt N., Campbell D. G., Caudwell F. B., Cohen P., da Cruz e Silva E. F., da Cruz e Silva O. B. and Cohen P. T. (1987) Isolation and sequence analysis of a cDNA clone encoding a type-1 protein phosphatase catalytic subunit: homology with protein phosphatase 2A. *FEBS Lett* **223,** 340-346.

Bollen M. (2001) Combinatorial control of protein phosphatase-1. *Trends Biochem Sci* **26,** 426-431.

Burd C. G. and Emr S. D. (1998) Phosphatidylinositol(3)-phosphate signaling mediated by specific binding to RING FYVE domains. *Mol Cell* **2,** 157-162.

Caviston J. P. and Holzbaur E. L. (2006) Microtubule motors at the intersection of trafficking and transport. *Trends Cell Biol* **16,** 530-537.

Ceulemans H. and Bollen M. (2004) Functional diversity of protein phosphatase-1, a cellular economizer and reset button. *Physiol Rev* **84,** 1-39.

Chen J., Martin B. L. and Brautigan D. L. (1992) Regulation of protein serine-threonine phosphatase type-2A by tyrosine phosphorylation. *Science* **257,** 1261-1264.

Chen R. H., Moses H. L., Maruoka E. M., Derynck R. and Kawabata M. (1995) Phosphorylation-dependent interaction of the cytoplasmic domains of the type I and type II transforming growth factor-beta receptors. *J Biol Chem* **270,** 12235-12241.

Chen X., Rubock M. J. and Whitman M. (1996) A transcriptional partner for MAD proteins in TGF-beta signalling. *Nature* **383,** 691-696.

Chien C. T., Bartel P. L., Sternglanz R. and Fields S. (1991) The two-hybrid system: a method to identify and clone genes for proteins that interact with a protein of interest. *Proc Natl Acad Sci U S A* **88,** 9578-9582.

Cho U. S. and Xu W. (2007) Crystal structure of a protein phosphatase 2A heterotrimeric holoenzyme. *Nature* **445,** 53-57.

Chung K. K., Zhang Y., Lim K. L., Tanaka Y., Huang H., Gao J., Ross C. A., Dawson V. L. and Dawson T. M. (2001) Parkin ubiquitinates the alpha-synuclein-interacting protein, synphilin-1: implications for Lewy-body formation in Parkinson disease. *Nat Med* **7,** 1144-1150.

Cohen P. T. (1997) Novel protein serine/threonine phosphatases: variety is the spice of life. *Trends Biochem Sci* **22,** 245-251.

Cohen P. T. (2002) Protein phosphatase 1--targeted in many directions. *J Cell Sci* **115,** 241-256.

Cohen P. T., Collins J. F., Coulson A. F., Berndt N. and da Cruz e Silva O. B. (1988) Segments of bacteriophage lambda (orf 221) and phi 80 are homologous to genes coding for mammalian protein phosphatases. *Gene* **69,** 131-134.

Cohen P. T. W. (2004) *Overview of protein serine/threonine phosphatases.*, Vol. 5, pp 1-20. Springer-Vertlag, Berlin, Germany.

Colland F., Jacq X., Trouplin V., Mougin C., Groizeleau C., Hamburger A., Meil A., Wojcik J., Legrain P. and Gauthier J. M. (2004) Functional proteomics mapping of a human signaling pathway. *Genome Res* **14,** 1324-1332.

da Cruz e Silva E. F. and Cohen P. T. (1987a) Isolation and sequence analysis of a cDNA clone encoding the entire catalytic subunit of phosphorylase kinase. *FEBS Lett* **220,** 36-42.

da Cruz e Silva E. F., da Cruz e Silva O. A., Zaia C. T. and Greengard P. (1995a) Inhibition of protein phosphatase 1 stimulates secretion of Alzheimer amyloid precursor protein. *Mol Med* **1,** 535-541.

da Cruz e Silva E. F., Fox C. A., Ouimet C. C., Gustafson E., Watson S. J. and Greengard P. (1995b) Differential expression of protein phosphatase 1 isoforms in mammalian brain. *J Neurosci* **15,** 3375-3389.

da Cruz e Silva E. F. a. O. C., J. P. (1997) Protein phosphatases as potential mediators of neurotoxicity, in *Comprehensive Toxicology*, Vol. XI (I. G. M., C. A., and Gandolphi, A. J., ed.), pp 181-199. Elsevier, Amsterdam.

da Cruz e Silva O. B. and Cohen P. T. (1987b) A second catalytic subunit of type-2A protein phosphatase from rabbit skeletal muscle. *FEBS Lett* **226,** 176-178.

da Cruz e Silva O. B., da Cruz e Silva E. F. and Cohen P. T. (1988) Identification of a novel protein phosphatase catalytic subunit by cDNA cloning. *FEBS Lett* **242,** 106-110.

da Cruz e Silva O. B., Alemany S., Campbell D. G. and Cohen P. T. (1987) Isolation and sequence analysis of a cDNA clone encoding the entire catalytic subunit of a type-2A protein phosphatase. *FEBS Lett* **221,** 415-422.

Dalby B., Cates S., Harris A., Ohki E. C., Tilkins M. L., Price P. J. and Ciccarone V. C. (2004) Advanced transfection with Lipofectamine 2000 reagent: primary neurons, siRNA, and high-throughput applications. *Methods* **33,** 95-103.

Das A. K., Helps N. R., Cohen P. T. and Barford D. (1996) Crystal structure of the protein serine/threonine phosphatase 2C at 2.0 A resolution. *Embo J* **15,** 6798-6809.

Delobel P., Flament S., Hamdane M., Mailliot C., Sambo A. V., Begard S., Sergeant N., Delacourte A., Vilain J. P. and Buee L. (2002) Abnormal Tau phosphorylation of the Alzheimer-type also occurs during mitosis. *J Neurochem* **83,** 412-420.

den Elzen N. R. and O'Connell M. J. (2004) Recovery from DNA damage checkpoint arrest by PP1-mediated inhibition of Chk1. *Embo J* **23,** 908-918.

Di Guglielmo G. M., Le Roy C., Goodfellow A. F. and Wrana J. L. (2003) Distinct endocytic pathways regulate TGF-beta receptor signalling and turnover. *Nat Cell Biol* **5,** 410-421.

Dillman J. F., 3rd and Pfister K. K. (1994) Differential phosphorylation in vivo of cytoplasmic dynein associated with anterogradely moving organelles. *J Cell Biol* **127,** 1671-1681.

Dohadwala M., da Cruz e Silva E. F., Hall F. L., Williams R. T., Carbonaro-Hall D. A., Nairn A. C., Greengard P. and Berndt N. (1994) Phosphorylation and inactivation of protein phosphatase 1 by cyclin-dependent kinases. *Proc Natl Acad Sci U S A* **91,** 6408-6412.

Egloff M. P., Cohen P. T., Reinemer P. and Barford D. (1995) Crystal structure of the catalytic subunit of human protein phosphatase 1 and its complex with tungstate. *J Mol Biol* **254,** 942-959.

Egloff M. P., Johnson D. F., Moorhead G., Cohen P. T., Cohen P. and Barford D. (1997) Structural basis for the recognition of regulatory subunits by the catalytic subunit of protein phosphatase 1. *Embo J* **16,** 1876-1887.

Engelender S., Kaminsky Z., Guo X., Sharp A. H., Amaravi R. K., Kleiderlein J. J., Margolis R. L., Troncoso J. C., Lanahan A. A., Worley P. F., Dawson V. L., Dawson T. M. and Ross C. A. (1999) Synphilin-1 associates with alpha-synuclein and promotes the formation of cytosolic inclusions. *Nat Genet* **22,** 110-114.

Estojak J., Brent R. and Golemis E. A. (1995) Correlation of two-hybrid affinity data with in vitro measurements. *Mol Cell Biol* **15,** 5820-5829.

Eyal A. and Engelender S. (2006) Synphilin isoforms and the search for a cellular model of lewy body formation in Parkinson's disease. *Cell Cycle* **5,** 2082-2086.

Eyal A., Szargel R., Avraham E., Liani E., Haskin J., Rott R. and Engelender S. (2006) Synphilin-1A: an aggregation-prone isoform of synphilin-1 that causes neuronal death and is present in aggregates from alpha-synucleinopathy patients. *Proc Natl Acad Sci U S A* **103,** 5917-5922.

Fardilha M., Wu W., Sa R., Fidalgo S., Sousa C., Mota C., da Cruz e Silva O. A. and da Cruz e Silva E. F. (2004) Alternatively spliced protein variants as potential therapeutic targets for male infertility and contraception. *Ann N Y Acad Sci* **1030,** 468-478.

Farshori P. and Holzbaur E. L. (1997) Dynactin phosphorylation is modulated in response to cellular effectors. *Biochem Biophys Res Commun* **232,** 810-816.

Fields S. and Song O. (1989) A novel genetic system to detect protein-protein interactions. *Nature* **340,** 245-246.

Fields S. and Sternglanz R. (1994) The two-hybrid system: an assay for protein-protein interactions. *Trends Genet* **10,** 286-292.

Finley R. L., Jr. and Brent R. (1994) Interaction mating reveals binary and ternary connections between Drosophila cell cycle regulators. *Proc Natl Acad Sci U S A* **91,** 12980-12984.

Flores-Delgado G., Liu C. W., Sposto R. and Berndt N. (2007) A limited screen for protein interactions reveals new roles for protein phosphatase 1 in cell cycle control and apoptosis. *J Proteome Res* **6,** 1165-1175.

Fresu M., Bianchi M., Parsons J. T. and Villa-Moruzzi E. (2001) Cell-cycle-dependent association of protein phosphatase 1 and focal adhesion kinase. *Biochem J* **358,** 407-414.

Gandy S. (1994) Targets for Alzheimer's disease research: from basic mechanisms to rational therapies. *Neurobiol Aging* **15 Suppl 2,** S157-160.

Gandy S. and Greengard P. (1994) Regulated cleavage of the Alzheimer amyloid precursor protein: molecular and cellular basis. *Biochimie* **76,** 300-303.

Gandy S., Caporaso G., Buxbaum J., Frangione B. and Greengard P. (1994) APP processing, A beta-amyloidogenesis, and the pathogenesis of Alzheimer's disease. *Neurobiol Aging* **15,** 253-256.

Gillooly D. J., Simonsen A. and Stenmark H. (2001) Cellular functions of phosphatidylinositol 3-phosphate and FYVE domain proteins. *Biochem J* **355,** 249-258.

Gong C. X., Singh T. J., Grundke-Iqbal I. and Iqbal K. (1993) Phosphoprotein phosphatase activities in Alzheimer disease brain. *J Neurochem* **61,** 921-927.

Gong C. X., Shaikh S., Wang J. Z., Zaidi T., Grundke-Iqbal I. and Iqbal K. (1995) Phosphatase activity toward abnormally phosphorylated tau: decrease in Alzheimer disease brain. *J Neurochem* **65,** 732-738.

Griffith J. P., Kim J. L., Kim E. E., Sintchak M. D., Thomson J. A., Fitzgibbon M. J., Fleming M. A., Caron P. R., Hsiao K. and Navia M. A. (1995) X-ray structure of calcineurin inhibited by the immunophilin-immunosuppressant FKBP12-FK506 complex. *Cell* **82,** 507-522.

Guarente L. (1993) Strategies for the identification of interacting proteins. *Proc Natl Acad Sci U S A* **90,** 1639-1641.

Guo C. Y., Brautigan D. L. and Larner J. M. (2002) Ionizing radiation activates nuclear protein phosphatase-1 by ATM-dependent dephosphorylation. *J Biol Chem* **277,** 41756-41761.

Hafezparast M., Klocke R., Ruhrberg C., Marquardt A., Ahmad-Annuar A., Bowen S., Lalli G., Witherden A. S., Hummerich H., Nicholson S., Morgan P. J., Oozageer R., Priestley J. V., Averill S., King V. R., Ball S., Peters J., Toda T., Yamamoto A., Hiraoka Y., Augustin M., Korthaus D., Wattler S., Wabnitz P., Dickneite C., Lampel S., Boehme F., Peraus G., Popp A., Rudelius M., Schlegel J., Fuchs H., Hrabe de Angelis M., Schiavo G., Shima D. T., Russ A. P., Stumm G., Martin J. E. and Fisher E. M. (2003) Mutations in dynein link motor neuron degeneration to defects in retrograde transport. *Science* **300,** 808-812.

Hayes S., Chawla A. and Corvera S. (2002) TGF beta receptor internalization into EEA1-enriched early endosomes: role in signaling to Smad2. *J Cell Biol* **158,** 1239-1249.

Helps N. R., Luo X., Barker H. M. and Cohen P. T. (2000) NIMA-related kinase 2 (Nek2), a cell-cycle-regulated protein kinase localized to centrosomes, is complexed to protein phosphatase 1. *Biochem J* **349,** 509-518.

Herzig S. and Neumann J. (2000) Effects of serine/threonine protein phosphatases on ion channels in excitable membranes. *Physiol Rev* **80,** 173-210.

Hirokawa N., Sato-Yoshitake R., Yoshida T. and Kawashima T. (1990) Brain dynein (MAP1C) localizes on both anterogradely and retrogradely transported membranous organelles in vivo. *J Cell Biol* **111,** 1027-1037.

Hollander M. C., Zhan Q., Bae I. and Fornace A. J., Jr. (1997) Mammalian GADD34, an apoptosis- and DNA damage-inducible gene. *J Biol Chem* **272,** 13731-13737.

Hollenbeck P. J. (1993) Phosphorylation of neuronal kinesin heavy and light chains in vivo. *J Neurochem* **60,** 2265-2275.

Honkanen R. E. and Golden T. (2002) Regulators of serine/threonine protein phosphatases at the dawn of a clinical era? *Curr Med Chem* **9,** 2055-2075.

Hormi-Carver K. K., Shi W., Liu C. W. and Berndt N. (2004) Protein phosphatase 1alpha is required for murine lung growth and morphogenesis. *Dev Dyn* **229,** 791-801.

Hsu J. Y., Sun Z. W., Li X., Reuben M., Tatchell K., Bishop D. K., Grushcow J. M., Brame C. J., Caldwell J. A., Hunt D. F., Lin R., Smith M. M. and Allis C. D. (2000) Mitotic phosphorylation of histone H3 is governed by Ipl1/aurora kinase and Glc7/PP1 phosphatase in budding yeast and nematodes. *Cell* **102,** 279-291.

Huang X. and Honkanen R. E. (1998) Molecular cloning, expression, and characterization of a novel human serine/threonine protein phosphatase, PP7, that is homologous to Drosophila retinal degeneration C gene product (rdgC). *J Biol Chem* **273,** 1462-1468.

Hubbard M. J. and Cohen P. (1993) On target with a new mechanism for the regulation of protein phosphorylation. *Trends Biochem Sci* **18,** 172-177.

Hurley T. D., Yang J., Zhang L., Goodwin K. D., Zou Q., Cortese M., Dunker A. K. and Depaoli-Roach A. A. (2007) Structural basis for regulation of protein phosphatase 1 by inhibitor-2. *J Biol Chem*.

Ingebritsen T. S. and Cohen P. (1983) The protein phosphatases involved in cellular regulation. 1. Classification and substrate specificities. *Eur J Biochem* **132,** 255-261.

Ishii K., Kumada K., Toda T. and Yanagida M. (1996) Requirement for PP1 phosphatase and 20S cyclosome/APC for the onset of anaphase is lessened by the dosage increase of a novel gene sds23+. *Embo J* **15,** 6629-6640.

Ito T., Niwa J., Hishikawa N., Ishigaki S., Doyu M. and Sobue G. (2003) Dorfin localizes to Lewy bodies and ubiquitylates synphilin-1. *J Biol Chem* **278,** 29106-29114.

Iwatsubo T., Yamaguchi H., Fujimuro M., Yokosawa H., Ihara Y., Trojanowski J. Q. and Lee V. M. (1996) Purification and characterization of Lewy bodies from the brains of patients with diffuse Lewy body disease. *Am J Pathol* **148,** 1517-1529.

Jiang C. H., Tsien J. Z., Schultz P. G. and Hu Y. (2001) The effects of aging on gene expression in the hypothalamus and cortex of mice. *Proc Natl Acad Sci U S A* **98,** 1930-1934.

Johansen J. W. and Ingebritsen T. S. (1986) Phosphorylation and inactivation of protein phosphatase 1 by pp60v-src. *Proc Natl Acad Sci U S A* **83,** 207-211.

Johnson S. A. and Hunter T. (2005) Kinomics: methods for deciphering the kinome. *Nat Methods* **2,** 17-25.

Jouvenceau A. and Dutar P. (2006) A role for the protein phosphatase 2B in altered hippocampal synaptic plasticity in the aged rat. *J Physiol Paris* **99,** 154-161.

Karki S. and Holzbaur E. L. (1999) Cytoplasmic dynein and dynactin in cell division and intracellular transport. *Curr Opin Cell Biol* **11,** 45-53.

Katayama H., Zhou H., Li Q., Tatsuka M. and Sen S. (2001) Interaction and feedback regulation between STK15/BTAK/Aurora-A kinase and protein phosphatase 1 through mitotic cell division cycle. *J Biol Chem* **276,** 46219-46224.

Kimura N., Imamura O., Ono F. and Terao K. (2007) Aging attenuates dynactin-dynein interaction: down-regulation of dynein causes accumulation of endogenous tau and amyloid precursor protein in human neuroblastoma cells. *J Neurosci Res* **85,** 2909-2916.

King S. J. and Schroer T. A. (2000) Dynactin increases the processivity of the cytoplasmic dynein motor. *Nat Cell Biol* **2,** 20-24.

Kolonin M. G., Zhong, J. and Finley, R.L. (2000) Interaction mating methods in two-hybrid systems. *Methods Enzymol* **328,** 26-46.

Kruger R., Kuhn W., Muller T., Woitalla D., Graeber M., Kosel S., Przuntek H., Epplen J. T., Schols L. and Riess O. (1998) Ala30Pro mutation in the gene encoding alpha-synuclein in Parkinson's disease. *Nat Genet* **18,** 106-108.

Kwon Y. G., Lee S. Y., Choi Y., Greengard P. and Nairn A. C. (1997) Cell cycle-dependent phosphorylation of mammalian protein phosphatase 1 by cdc2 kinase. *Proc Natl Acad Sci U S A* **94,** 2168-2173.

Labbe E., Silvestri C., Hoodless P. A., Wrana J. L. and Attisano L. (1998) Smad2 and Smad3 positively and negatively regulate TGF beta-dependent transcription through the forkhead DNA-binding protein FAST2. *Mol Cell* **2,** 109-120.

Ladner C. J., Czech J., Maurice J., Lorens S. A. and Lee J. M. (1996) Reduction of calcineurin enzymatic activity in Alzheimer's disease: correlation with neuropathologic changes. *J Neuropathol Exp Neurol* **55,** 924-931.

Lagna G., Hata A., Hemmati-Brivanlou A. and Massague J. (1996) Partnership between DPC4 and SMAD proteins in TGF-beta signalling pathways. *Nature* **383,** 832-836.

Lawe D. C., Patki V., Heller-Harrison R., Lambright D. and Corvera S. (2000) The FYVE domain of early endosome antigen 1 is required for both phosphatidylinositol 3-phosphate and Rab5 binding. Critical role of this dual interaction for endosomal localization. *J Biol Chem* **275,** 3699-3705.

Lee G., Tanaka M., Park K., Lee S. S., Kim Y. M., Junn E., Lee S. H. and Mouradian M. M. (2004) Casein kinase II-mediated phosphorylation regulates alpha-synuclein/synphilin-1 interaction and inclusion body formation. *J Biol Chem* **279,** 6834-6839.

Lee H. G., Ueda M., Zhu X., Perry G. and Smith M. A. (2006) Ectopic expression of phospho-Smad2 in Alzheimer's disease: uncoupling of the transforming growth factor-beta pathway? *J Neurosci Res* **84,** 1856-1861.

Lesage B., Beullens M., Ceulemans H., Himpens B. and Bollen M. (2005) Determinants of the nucleolar targeting of protein phosphatase-1. *FEBS Lett* **579,** 5626-5630.

Liani E., Eyal A., Avraham E., Shemer R., Szargel R., Berg D., Bornemann A., Riess O., Ross C. A., Rott R. and Engelender S. (2004) Ubiquitylation of synphilin-1 and alpha-synuclein by SIAH and its presence in cellular inclusions and Lewy bodies imply a role in Parkinson's disease. *Proc Natl Acad Sci U S A* **101,** 5500-5505.

Lievens J. C., Woodman B., Mahal A. and Bates G. P. (2002) Abnormal phosphorylation of synapsin I predicts a neuronal transmission impairment in the R6/2 Huntington's disease transgenic mice. *Mol Cell Neurosci* **20,** 638-648.

Lim K. L., Chew K. C., Tan J. M., Wang C., Chung K. K., Zhang Y., Tanaka Y., Smith W., Engelender S., Ross C. A., Dawson V. L. and Dawson T. M. (2005) Parkin mediates nonclassical, proteasomal-independent ubiquitination of synphilin-1: implications for Lewy body formation. *J Neurosci* **25,** 2002-2009.

Lin H. Y., Wang X. F., Ng-Eaton E., Weinberg R. A. and Lodish H. F. (1992) Expression cloning of the TGF-beta type II receptor, a functional transmembrane serine/threonine kinase. *Cell* **68,** 775-785.

Lin Q., Buckler E. S. t., Muse S. V. and Walker J. C. (1999) Molecular evolution of type 1 serine/threonine protein phosphatases. *Mol Phylogenet Evol* **12,** 57-66.

Lin S. X., Ferro K. L. and Collins C. A. (1994) Cytoplasmic dynein undergoes intracellular redistribution concomitant with phosphorylation of the heavy chain in response to serum starvation and okadaic acid. *J Cell Biol* **127,** 1009-1019.

Lin T. H., Tsai P. C., Liu H. T., Chen Y. C., Wang L. H., Hsieh F. K. and Huang H. B. (2005) Characterization of the Protein Phosphatase 1-Binding Motifs of Inhibitor-2 and DARPP-32 by Surface Plasmon Resonance. *J Biochem (Tokyo)* **138,** 697-700.

Liu C. W., Wang R. H., Dohadwala M., Schonthal A. H., Villa-Moruzzi E. and Berndt N. (1999) Inhibitory phosphorylation of PP1alpha catalytic subunit during the G(1)/S transition. *J Biol Chem* **274,** 29470-29475.

Liu F., Pouponnot C. and Massague J. (1997) Dual role of the Smad4/DPC4 tumor suppressor in TGFbeta-inducible transcriptional complexes. *Genes Dev* **11,** 3157-3167.

Luss H., Klein-Wiele O., Boknik P., Herzig S., Knapp J., Linck B., Muller F. U., Scheld H. H., Schmid C., Schmitz W. and Neumann J. (2000) Regional expression of protein phosphatase type 1 and 2A catalytic subunit isoforms in the human heart. *J Mol Cell Cardiol* **32,** 2349-2359.

MacMillan L. B., Bass M. A., Cheng N., Howard E. F., Tamura M., Strack S., Wadzinski B. E. and Colbran R. J. (1999) Brain actin-associated protein phosphatase 1 holoenzymes containing spinophilin, neurabin, and selected catalytic subunit isoforms. *J Biol Chem* **274,** 35845-35854.

Mallik R. and Gross S. P. (2004) Molecular motors: strategies to get along. *Curr Biol* **14,** R971-982.

Mallozzi C., De Franceschi L., Brugnara C. and Di Stasi A. M. (2005) Protein phosphatase 1alpha is tyrosine-phosphorylated and inactivated by peroxynitrite in erythrocytes through the src family kinase fgr. *Free Radic Biol Med* **38,** 1625-1636.

Margolis S. S., Walsh S., Weiser D. C., Yoshida M., Shenolikar S. and Kornbluth S. (2003) PP1 control of M phase entry exerted through 14-3-3-regulated Cdc25 dephosphorylation. *Embo J* **22,** 5734-5745.

Maroteaux L., Campanelli J. T. and Scheller R. H. (1988) Synuclein: a neuron-specific protein localized to the nucleus and presynaptic nerve terminal. *J Neurosci* **8,** 2804-2815.

Marx F. P., Holzmann C., Strauss K. M., Li L., Eberhardt O., Gerhardt E., Cookson M. R., Hernandez D., Farrer M. J., Kachergus J., Engelender S., Ross C. A., Berger K., Schols L., Schulz J. B., Riess O. and Kruger R. (2003) Identification and functional characterization of a novel R621C mutation in the synphilin-1 gene in Parkinson's disease. *Hum Mol Genet* **12,** 1223-1231.

Massague J. (1998) TGF-beta signal transduction. *Annu Rev Biochem* **67,** 753-791.

Massague J. and Chen Y. G. (2000) Controlling TGF-beta signaling. *Genes Dev* **14,** 627-644.

Massague J. and Wotton D. (2000) Transcriptional control by the TGF-beta/Smad signaling system. *Embo J* **19,** 1745-1754.

Matthies H. J., Miller R. J. and Palfrey H. C. (1993) Calmodulin binding to and cAMP-dependent phosphorylation of kinesin light chains modulate kinesin ATPase activity. *J Biol Chem* **268,** 11176-11187.

McIlvain J. M., Jr., Burkhardt J. K., Hamm-Alvarez S., Argon Y. and Sheetz M. P. (1994) Regulation of kinesin activity by phosphorylation of kinesin-associated proteins. *J Biol Chem* **269,** 19176-19182.

Meraldi P. and Nigg E. A. (2001) Centrosome cohesion is regulated by a balance of kinase and phosphatase activities. *J Cell Sci* **114,** 3749-3757.

Muresan V., Stankewich M. C., Steffen W., Morrow J. S., Holzbaur E. L. and Schnapp B. J. (2001) Dynactin-dependent, dynein-driven vesicle transport in the absence of membrane proteins: a role for spectrin and acidic phospholipids. *Mol Cell* **7,** 173-183.

Neumann J. (2002) Altered phosphatase activity in heart failure, influence on Ca2+ movement. *Basic Res Cardiol* **97 Suppl 1,** I91-95.

Niclas J., Allan V. J. and Vale R. D. (1996) Cell cycle regulation of dynein association with membranes modulates microtubule-based organelle transport. *J Cell Biol* **133,** 585-593.

Norris C. M., Halpain S. and Foster T. C. (1998) Alterations in the balance of protein kinase/phosphatase activities parallel reduced synaptic strength during aging. *J Neurophysiol* **80,** 1567-1570.

Okochi M., Walter J., Koyama A., Nakajo S., Baba M., Iwatsubo T., Meijer L., Kahle P. J. and Haass C. (2000) Constitutive phosphorylation of the Parkinson's disease associated alpha-synuclein. *J Biol Chem* **275,** 390-397.

Ouimet C. C., da Cruz e Silva E. F. and Greengard P. (1995) The alpha and gamma 1 isoforms of protein phosphatase 1 are highly and specifically concentrated in dendritic spines. *Proc Natl Acad Sci U S A* **92,** 3396-3400.

Panopoulou E., Gillooly D. J., Wrana J. L., Zerial M., Stenmark H., Murphy C. and Fotsis T. (2002) Early endosomal regulation of Smad-dependent signaling in endothelial cells. *J Biol Chem* **277,** 18046-18052.

Paschal B. M. and Vallee R. B. (1987) Retrograde transport by the microtubule-associated protein MAP 1C. *Nature* **330,** 181-183.

Patki V., Lawe D. C., Corvera S., Virbasius J. V. and Chawla A. (1998) A functional PtdIns(3)P-binding motif. *Nature* **394,** 433-434.

Pei J. J., Sersen E., Iqbal K. and Grundke-Iqbal I. (1994) Expression of protein phosphatases (PP-1, PP-2A, PP-2B and PTP-1B) and protein kinases (MAP kinase and P34cdc2) in the hippocampus of patients with Alzheimer disease and normal aged individuals. *Brain Res* **655,** 70-76.

Piek E., Heldin C. H. and Ten Dijke P. (1999) Specificity, diversity, and regulation in TGF-beta superfamily signaling. *Faseb J* **13,** 2105-2124.

Pierre P., Scheel J., Rickard J. E. and Kreis T. E. (1992) CLIP-170 links endocytic vesicles to microtubules. *Cell* **70,** 887-900.

Pilling A. D., Horiuchi D., Lively C. M. and Saxton W. M. (2006) Kinesin-1 and Dynein are the primary motors for fast transport of mitochondria in Drosophila motor axons. *Mol Biol Cell* **17,** 2057-2068.

Planel E., Yasutake K., Fujita S. C. and Ishiguro K. (2001) Inhibition of protein phosphatase 2A overrides tau protein kinase I/glycogen synthase kinase 3 beta and cyclin-dependent kinase 5 inhibition and results in tau hyperphosphorylation in the hippocampus of starved mouse. *J Biol Chem* **276,** 34298-34306.

Polymeropoulos M. H., Lavedan C., Leroy E., Ide S. E., Dehejia A., Dutra A., Pike B., Root H., Rubenstein J., Boyer R., Stenroos E. S., Chandrasekharappa S., Athanassiadou A., Papapetropoulos T., Johnson W. G., Lazzarini A. M., Duvoisin R. C., Di Iorio G., Golbe L. I. and Nussbaum R. L. (1997) Mutation in the alpha-synuclein gene identified in families with Parkinson's disease. *Science* **276,** 2045-2047.

Printen J. A., Brady M. J. and Saltiel A. R. (1997) PTG, a protein phosphatase 1-binding protein with a role in glycogen metabolism. *Science* **275,** 1475-1478.

Puls I., Jonnakuty C., LaMonte B. H., Holzbaur E. L., Tokito M., Mann E., Floeter M. K., Bidus K., Drayna D., Oh S. J., Brown R. H., Jr., Ludlow C. L. and Fischbeck K. H. (2003) Mutant dynactin in motor neuron disease. *Nat Genet* **33,** 455-456.

Puntoni F. and Villa-Moruzzi E. (1997) Protein phosphatase-1 alpha, gamma 1, and delta: changes in phosphorylation and activity in mitotic HeLa cells and in cells released from the mitotic block. *Arch Biochem Biophys* **340,** 177-184.

Ribeiro C. S., Carneiro K., Ross C. A., Menezes J. R. and Engelender S. (2002) Synphilin-1 is developmentally localized to synaptic terminals, and its association with synaptic vesicles is modulated by alpha-synuclein. *J Biol Chem* **277,** 23927-23933.

Rickard J. E. and Kreis T. E. (1991) Binding of pp170 to microtubules is regulated by phosphorylation. *J Biol Chem* **266,** 17597-17605.

Roberts A. B., and Sporn, M. B. (1990) *Peptide Growth Factors and Their Receptors*, Vol. 95, pp 419–472. Springer-Verlag, Heidelberg, Germany.

Rudenko A., Bennett D. and Alphey L. (2004) PP1beta9C interacts with Trithorax in Drosophila wing development. *Dev Dyn* **231,** 336-341.

Sasaki K., Shima H., Kitagawa Y., Irino S., Sugimura T. and Nagao M. (1990) Identification of members of the protein phosphatase 1 gene family in the rat and enhanced expression of protein phosphatase 1 alpha gene in rat hepatocellular carcinomas. *Jpn J Cancer Res* **81,** 1272-1280.

Sato-Yoshitake R., Yorifuji H., Inagaki M. and Hirokawa N. (1992) The phosphorylation of kinesin regulates its binding to synaptic vesicles. *J Biol Chem* **267,** 23930-23936.

Schroer T. A. (2004) Dynactin. *Annu Rev Cell Dev Biol* **20,** 759-779.

Serebriiskii I. G., Khazak V. and Golemis E. A. (2001a) Redefinition of the yeast two-hybrid system in dialogue with changing priorities in biological research. *Biotechniques* **30,** 634-636, 638, 640 passim.

Serebriiskii I. G., Toby G. G., Finley R. L., Jr. and Golemis E. A. (2001b) Genomic analysis utilizing the yeast two-hybrid system. *Methods Mol Biol* **175,** 415-454.

Shah A. A., Giddings M. C., Parvaz J. B., Gesteland R. F., Atkins J. F. and Ivanov I. P. (2002) Computational identification of putative programmed translational frameshift sites. *Bioinformatics* **18,** 1046-1053.

Shi W., Sun C., He B., Xiong W., Shi X., Yao D. and Cao X. (2004) GADD34-PP1c recruited by Smad7 dephosphorylates TGFbeta type I receptor. *J Cell Biol* **164,** 291-300.

Shi Y. and Massague J. (2003) Mechanisms of TGF-beta signaling from cell membrane to the nucleus. *Cell* **113,** 685-700.

Singleton A. B., Farrer M., Johnson J., Singleton A., Hague S., Kachergus J., Hulihan M., Peuralinna T., Dutra A., Nussbaum R., Lincoln S., Crawley A., Hanson M., Maraganore D., Adler C., Cookson M. R., Muenter M., Baptista M., Miller D., Blancato J., Hardy J. and Gwinn-Hardy K. (2003) alpha-Synuclein locus triplication causes Parkinson's disease. *Science* **302,** 841.

Spillantini M. G., Schmidt M. L., Lee V. M., Trojanowski J. Q., Jakes R. and Goedert M. (1997) Alpha-synuclein in Lewy bodies. *Nature* **388,** 839-840.

Sridhar R., Hanson-Painton O. and Cooper D. R. (2000) Protein kinases as therapeutic targets. *Pharm Res* **17,** 1345-1353.

Stenmark H. and Aasland R. (1999) FYVE-finger proteins--effectors of an inositol lipid. *J Cell Sci* **112 (Pt 23),** 4175-4183.

Stenmark H., Aasland R. and Driscoll P. C. (2002) The phosphatidylinositol 3-phosphate-binding FYVE finger. *FEBS Lett* **513,** 77-84.

Stenmark H., Aasland R., Toh B. H. and D'Arrigo A. (1996) Endosomal localization of the autoantigen EEA1 is mediated by a zinc-binding FYVE finger. *J Biol Chem* **271,** 24048-24054.

Tai A. W., Chuang J. Z., Bode C., Wolfrum U. and Sung C. H. (1999) Rhodopsin's carboxy-terminal cytoplasmic tail acts as a membrane receptor for cytoplasmic dynein by binding to the dynein light chain Tctex-1. *Cell* **97,** 877-887.

Takahashi H. and Wakabayashi K. (2001) The cellular pathology of Parkinson's disease. *Neuropathology* **21,** 315-322.

Takeda A., Mallory M., Sundsmo M., Honer W., Hansen L. and Masliah E. (1998) Abnormal accumulation of NACP/alpha-synuclein in neurodegenerative disorders. *Am J Pathol* **152,** 367-372.

Terrak M., Kerff F., Langsetmo K., Tao T. and Dominguez R. (2004) Structural basis of protein phosphatase 1 regulation. *Nature* **429,** 780-784.

Terry-Lorenzo R. T., Carmody L. C., Voltz J. W., Connor J. H., Li S., Smith F. D., Milgram S. L., Colbran R. J. and Shenolikar S. (2002) The neuronal actin-binding proteins, neurabin I and neurabin II, recruit specific isoforms of protein phosphatase-1 catalytic subunits. *J Biol Chem* **277,** 27716-27724.

Thompson L. J., Bollen M. and Fields A. P. (1997) Identification of protein phosphatase 1 as a mitotic lamin phosphatase. *J Biol Chem* **272,** 29693-29697.

Tian Q. and Wang J. (2002) Role of serine/threonine protein phosphatase in Alzheimer's disease. *Neurosignals* **11,** 262-269.

Tokito M. K., Howland D. S., Lee V. M. and Holzbaur E. L. (1996) Functionally distinct isoforms of dynactin are expressed in human neurons. *Mol Biol Cell* **7,** 1167-1180.

Trinkle-Mulcahy L., Sleeman J. E. and Lamond A. I. (2001) Dynamic targeting of protein phosphatase 1 within the nuclei of living mammalian cells. *J Cell Sci* **114,** 4219-4228.

Trinkle-Mulcahy L., Andersen J., Lam Y. W., Moorhead G., Mann M. and Lamond A. I. (2006) Repo-Man recruits PP1 gamma to chromatin and is essential for cell viability. *J Cell Biol* **172,** 679-692.

Tsukazaki T., Chiang T. A., Davison A. F., Attisano L. and Wrana J. L. (1998) SARA, a FYVE domain protein that recruits Smad2 to the TGFbeta receptor. *Cell* **95,** 779-791.

Tynan S. H., Purohit A., Doxsey S. J. and Vallee R. B. (2000) Light intermediate chain 1 defines a functional subfraction of cytoplasmic dynein which binds to pericentrin. *J Biol Chem* **275,** 32763-32768.

Ueberham U., Ueberham E., Gruschka H. and Arendt T. (2006) Altered subcellular location of phosphorylated Smads in Alzheimer's disease. *Eur J Neurosci* **24,** 2327-2334.

Valdimarsdottir G., Goumans M. J., Itoh F., Itoh S., Heldin C. H. and ten Dijke P. (2006) Smad7 and protein phosphatase 1alpha are critical determinants in the duration of TGF-beta/ALK1 signaling in endothelial cells. *BMC Cell Biol* **7,** 16.

Varmuza S., Jurisicova A., Okano K., Hudson J., Boekelheide K. and Shipp E. B. (1999) Spermiogenesis is impaired in mice bearing a targeted mutation in the protein phosphatase 1cgamma gene. *Dev Biol* **205,** 98-110.

Ventura F., Doody J., Liu F., Wrana J. L. and Massague J. (1994) Reconstitution and transphosphorylation of TGF-beta receptor complexes. *Embo J* **13,** 5581-5589.

Vidal M. and Legrain P. (1999) Yeast forward and reverse 'n'-hybrid systems. *Nucleic Acids Res* **27,** 919-929.

Villa-Moruzzi E. and Puntoni F. (1996) Phosphorylation of phosphatase-1alpha in cells expressing v-src. *Biochem Biophys Res Commun* **219,** 863-867.

Vogelsberg-Ragaglia V., Schuck T., Trojanowski J. Q. and Lee V. M. (2001) PP2A mRNA expression is quantitatively decreased in Alzheimer's disease hippocampus. *Exp Neurol* **168,** 402-412.

Wagey R. T. and Krieger C. (1998) Abnormalities of protein kinases in neurodegenerative diseases. *Prog Drug Res* **51,** 133-183.

Wakabayashi K., Matsumoto K., Takayama K., Yoshimoto M. and Takahashi H. (1997) NACP, a presynaptic protein, immunoreactivity in Lewy bodies in Parkinson's disease. *Neurosci Lett* **239,** 45-48.

Wakabayashi K., Engelender S., Yoshimoto M., Tsuji S., Ross C. A. and Takahashi H. (2000) Synphilin-1 is present in Lewy bodies in Parkinson's disease. *Ann Neurol* **47,** 521-523.

Wakabayashi K., Mori F., Oyama Y., Kurihara A., Kamada M., Yoshimoto M. and Takahashi H. (2003) Lewy bodies in Betz cells of the motor cortex in a patient with Parkinson's disease. *Acta Neuropathol* **105,** 189-192.

Wakabayashi K., Engelender S., Tanaka Y., Yoshimoto M., Mori F., Tsuji S., Ross C. A. and Takahashi H. (2002) Immunocytochemical localization of synphilin-1, an alpha-synuclein-associated protein, in neurodegenerative disorders. *Acta Neuropathol* **103,** 209-214.

Wakula P., Beullens M., Ceulemans H., Stalmans W. and Bollen M. (2003) Degeneracy and function of the ubiquitous RVXF motif that mediates binding to protein phosphatase-1. *J Biol Chem* **278,** 18817-18823.

Wang H. and Brautigan D. L. (2002) A novel transmembrane Ser/Thr kinase complexes with protein phosphatase-1 and inhibitor-2. *J Biol Chem* **277,** 49605-49612.

Watanabe T., da Cruz e Silva E. F., Huang H. B., Starkova N., Kwon Y. G., Horiuchi A., Greengard P. and Nairn A. C. (2003) Preparation and characterization of recombinant protein phosphatase 1. *Methods Enzymol* **366,** 321-338.

Waterman-Storer C. M., Karki S. B., Kuznetsov S. A., Tabb J. S., Weiss D. G., Langford G. M. and Holzbaur E. L. (1997) The interaction between cytoplasmic dynein and dynactin is required for fast axonal transport. *Proc Natl Acad Sci U S A* **94,** 12180-12185.

Westphal R. S., Tavalin S. J., Lin J. W., Alto N. M., Fraser I. D., Langeberg L. K., Sheng M. and Scott J. D. (1999) Regulation of NMDA receptors by an associated phosphatase-kinase signaling complex. *Science* **285,** 93-96.

Wrana J. L. (2000) Regulation of Smad activity. *Cell* **100,** 189-192.

Wrana J. L., Attisano L., Wieser R., Ventura F. and Massague J. (1994) Mechanism of activation of the TGF-beta receptor. *Nature* **370,** 341-347.

Wrana J. L., Attisano L., Carcamo J., Zentella A., Doody J., Laiho M., Wang X. F. and Massague J. (1992) TGF beta signals through a heteromeric protein kinase receptor complex. *Cell* **71,** 1003-1014.

Wu G., Chen Y. G., Ozdamar B., Gyuricza C. A., Chong P. A., Wrana J. L., Massague J. and Shi Y. (2000) Structural basis of Smad2 recognition by the Smad anchor for receptor activation. *Science* **287,** 92-97.

Xu Y., Xing Y., Chen Y., Chao Y., Lin Z., Fan E., Yu J. W., Strack S., Jeffrey P. D. and Shi Y. (2006) Structure of the protein phosphatase 2A holoenzyme. *Cell* **127,** 1239-1251.

Yamano H., Ishii K. and Yanagida M. (1994) Phosphorylation of dis2 protein phosphatase at the C-terminal cdc2 consensus and its potential role in cell cycle regulation. *Embo J* **13,** 5310-5318.

Yang J., Roe S. M., Cliff M. J., Williams M. A., Ladbury J. E., Cohen P. T. and Barford D. (2005) Molecular basis for TPR domain-mediated regulation of protein phosphatase 5. *Embo J* **24,** 1-10.

Yang M., Wu Z. and Fields S. (1995) Protein-peptide interactions analyzed with the yeast two-hybrid system. *Nucleic Acids Res* **23,** 1152-1156.

Yano H., Lee F. S., Kong H., Chuang J., Arevalo J., Perez P., Sung C. and Chao M. V. (2001) Association of Trk neurotrophin receptors with components of the cytoplasmic dynein motor. *J Neurosci* **21,** RC125.

Zarranz J. J., Alegre J., Gomez-Esteban J. C., Lezcano E., Ros R., Ampuero I., Vidal L., Hoenicka J., Rodriguez O., Atares B., Llorens V., Gomez Tortosa E., del Ser T., Munoz D. G. and de Yebenes J. G. (2004) The new mutation, E46K, of alpha-synuclein causes Parkinson and Lewy body dementia. *Ann Neurol* **55,** 164-173.

Zhang Y., Musci T. and Derynck R. (1997) The tumor suppressor Smad4/DPC 4 as a central mediator of Smad function. *Curr Biol* **7,** 270-276.

Zhang Y., Feng X. H. and Derynck R. (1998) Smad3 and Smad4 cooperate with c-Jun/c-Fos to mediate TGF-beta-induced transcription. *Nature* **394,** 909-913.

Zhou S., Zawel L., Lengauer C., Kinzler K. W. and Vogelstein B. (1998) Characterization of human FAST-1, a TGF beta and activin signal transducer. *Mol Cell* **2,** 121-127.

APPENDIX

I. CULTURE MEDIA AND SOLUTIONS

LB (Luria-Bertani) Medium

To 950 mL of deionised H_2O add:
LB 25 g
Agar 20 g (for plates only)
Shake until the solutes have dissolved. Adjust the volume of the solution to 1 liter with deionised H_2O. Sterilize by autoclaving.

SOB Medium

To 950 mL of deionised H_2O add:
25,5 g SOB Broth
Shake until the solutes have dissolved. Add 10mL of a 250mM KCl (prepared by dissolving 1.86g of KCl in 100 mL of deionised H_2O). Adjust the pH to 7.0 with 5N NaOH. Adjust the volume of the solution to 1 liter with deionised H_2O. Sterilize by autoclaving. Just prior to use add 5 mL of a sterile solution of 2M $MgCl_2$ (prepared by dissolving 19 g of $MgCl_2$ in 90 mL of deionised H_2O; adjust the volume of the solution to 1000 mL with deionised H_2O and sterilize by autoclaving).

SOC Medium

SOC is identical to SOB except that it contains 20 mM glucose. After the SOB medium has been autoclaved, allow it to cool to 60ºC and add 20mL of a sterile 1M glucose (this solution is made by dissolving 18 g of glucose in 90 mL of deionised H_2O; after the sugar has dissolved, adjust the volume of the solution to 1 L with deionised H_2O and sterilize by filtration through a 0.22-micron filter).

Yeast Media

10X dropout solution (DO10X)

This solution contains all but one or more of the following components:

	10X concentration (mg/L)	SIGMA #
L-Isoleucine	300	I-7383
L-Valine	1500	V-0500
L-Adenine hemisulfate salt	200	A-9126
L-Arginine HCl	200	A-5131
L-Histidine HCl monohydrate	200	H-9511
L-Leucine	1000	L-1512
L-Lysine HCl	300	L-1262
L-Methionine	200	M-9625
L-Phenylalanine	500	P-5030
L-Threonine	2000	T-8625
L-Tryptophan	200	T-0254
L-Tyrosine	300	T-3754
L-Uracil	200	U-0750

10X dropout supplements may be autoclaved and stored for up to 1 year.

YPD medium

To 950mL of deionised H_2O add:
50 g YPD
20 g Agar (for plates only)
Shake until the solutes have dissolved. Adjust the volume to 1 L with deionised H_2O and sterilize by autoclaving. Allow medium to cool to 60ºC and add glucose to 2% (50mL of a sterile 40% stock solution).

SD synthetic medium

To 800mL of deionised H_2O add:
6.7g Yeast nitrogen base without amino acids (DIFCO)
20g Agar (for plates only)
Shake until the solutes have dissolved. Adjust the volume to 850mL with deionised H_2O and sterilize by autoclaving. Allow medium to cool to 60ºC and add glucose to 2% (50mL of a sterile 40% stock solution) and 100mL of the appropriate 10X dropout solution.

2X YPDA

Prepare YPD as above. After the autoclaved medium has cooled to 55ºC add 15mL of a 0.2% adenine hemisulfate solution per liter of medium (final concentration is 0.003%).

Solutions

50X TAE Buffer

242 g Tris base
57.1 mL glacial acetic acid
100 mL 0.5M EDTA (pH 8.0)

TE Buffer (pH 7.5)

10 mM Tris-HCl (pH 7.5)
1 mM EDTA, pH 8.0

Loading Buffer (LB)

0.25% bromophenol blue
30% glycerol

STET

8% Sucrose
5% Triton X-100
50 mM Tris-HCl (pH 8,5)
50 mM EDTA

Competent Cell Solutions:

Solution I (1L)

9.9 g $MnCl_2.4H_2O$
1.5 g $CaCl_2.2H_2O$
150 g glycerol
30 mL KHAc 1M;
adjust pH to 5.8 with HAc, filter through a 0.2µm filter and store at 4ºC

Solution II (1L)

20 mL 0.5M MOPS (pH 6.8)
1.2 g RbCl
11g $CaCl_2.2H_2O$
150 g glycerol;
filter through a 0.2µm filter and store at 4ºC

Miniprep Solutions:

Solution I

50 mM glucose
25 mM Tris.HCl (pH 8.0)
10 mM EDTA

Solution II

0.2 N NaOH
1% SDS

Solution III

3 M potassium acetate
2 M glacial acetic acid

Midiprep Solutions

Cell Resuspension Solution

50 mM Tris-HCl (pH 7.5)
10 mM EDTA
100 µg/mL RNAase A

Cell Lysis Solution

0.2 M NaOH
1% SDS

Neutralization Solution

4.09 M Guanidine hydrochloride (pH 4.8)
759 mM potassium acetate
2.12 M Glacial acetic acid

Column Wash Solution

60 mM potassium acetate
8.3 mM Tris-HCl (pH 7.5)
0.04 mM EDTA
60 % ethanol

SDS-PAGE and Immunobloting Solutions

LGB (Lower Gel Buffer)

To 900 mL of deionised H_2O add:
181.65 g Tris
4 g SDS
Mix until the solutes have dissolved. Adjust the pH to 8.9 and adjust the volume to 1L with deionised H_2O.

UGB (Upper Gel Buffer)

To 900 mL of deionised H_2O add:
75.69 g Tris
Mix until the solute has dissolved. Adjust the pH to 6.8 and adjust the volume to 1L with deionised H_2O.

30%Acrylamide/0.8% Bisacrylamide

To 70 mL of deionised H_2O add:
29.2 g Acrylamide
0.8 g Bisacrylamide
Mix until the solutes have dissolved. Adjust the volume to 100mL with deionised H_2O. Store at 4ºC.

Loading Gel Buffer

250 mM Tris-HCl (pH 6.8)
8% SDS
40% Glycerol
2% 2-mercaptoethanol
0.01% Bromophenol blue

1X Running Buffer

25 mM Tris-HCl (pH8.3)
250 mM Glycine
0.1% SDS

1X Transfer buffer

25 mM Tris-HCl (pH8.3)
192 mM Glycine
20% Methanol

1X TBS

10 mM Tris-HCl (pH 8.0)
150 mM NaCl

1X TBST

10 mM Tris-HCl (pH 8.0)
150 mM NaCl
0.05% Tween

Membrane Stripping Solution

2% SDS
62.5 mM Tris-Hcl (pH= 6.7)
100 mM β-Mercaptoethanol

Yeast Two-Hybrid Solutions

Yeast plasmid rescue – Breaking buffer

2 % Triton X-100
1 % SDS
100 mM NaCl
10 mM Tris-HCl (pH 8.0)

Solutions for preparation of yeast protein extracts

- Protease inhibitor solution

Always prepare solution fresh just before using. Place on ice to prechill. To prepare 688µl add in a microfuge tube:
66µl Pepstatin A (1 mg/mL stock solution in DMSO)
2µl Leupeptin (10.5 mM stock solution)
500µl Benzamidine (200 mM stock solution)
120µl Aprotinin (2.1 mg/mL stock solution)

- PMSF (phenylmethyl-sulfonyl fluoride) stock solution (100X)

Dissolve 0.1742g of PMSF in 10mL isopropanol. Wrap tube in foil and store at RT.

- Cracking buffer stock solution

To 80mL of deionised H_2O add:
48g Urea
5g SDS
4mL 1M Tris-HCl (pH6.8)
20µl 0.5M EDTA
40mg Bromophenol blue
Mix until the solutes have dissolved. Adjust the volume to 100mL with deionised H_2O.

- Cracking buffer

To prepare 1.13mL add in a microfuge tube:
1 mL Cracking buffer stock solution (recipe above)
10 µl β-mercaptoethanol
70 µl Protease inhibitor solution (recipe above)
50µl 100X PMSF stock solution

Immunoprecipitation solutions

Lysis Buffer

50 mM Tris-HCl (pH 8)
120 mM NaCl
4% CHAPS

Lysis Buffer + Protease inhibitors

Add to 4 mL of Lysis buffer the following quantities for a final volume of 5 mL:
23,8 µl Pepstatin A (1 mg/mL stock solution in DMSO)
0,72 µl Leupeptin (5 mg/mL stock solution)
180 µl Benzamidine (200 mM stock solution)
43,2 µl Aprotinin (2.1 mg/mL stock solution)
176 µl PMSF 100X

Washing solution

50 mM Tris-HCl
120 mM NaCl

Cell Culture Solutions and Immunocytochemistry

PBS (1x)

For a final volume of 500 mL, dissolve one pack of BupH Modified Dulbecco's Phosphate Buffered Saline Pack (Pierce) in deionised H_2O. Final composition:

8 mM Sodium Phosphate
2 mM Potassium Phosphate
40 mM NaCl
10 mM KCl

Sterilize by filtering through a 0.2 μm filter and store at 4 ºC

1 mg/mL Poly-L-ornithine solution (10x)

To a final volume of 100 mL, dissolve in deionised H_2O 100 mg of poly-L-ornithine (Sigma-Aldrich, Portugal).

4% Paraformaldehyde Fixative solution

For a final volume of 100 mL, add 4 g of paraformaldehyde to 25 mL deionised H_2O. Dissolve by heating the mixture at 58 ºC while stirring. Add 1-2 drops of 1 M NaOH to clarify the solution and filter (0.2 μm).
Add 50 mL of 2X PBS and adjust the volume to 100 mL with deionised H_2O.

Complete MEM + GLUTAMAX

For a final volume of 500 mL, add:

50 mL (10% v/v) Fetal Bovine Serum (FBS) (Gibco BRL, Invitrogen)

5 mL Non-Essential aminoacids (100x)

100 U/mL penicillin

100 mg/mL streptomycin 5 mL

FBS is heat-inactivated for 30 min at 56 ºC. For cells maintenance, prior to pH adjustment add 100 U/mL penicillin and 100 mg/mL streptomycin [10 mL Streptomycin/ Penicilin/Amphotericin solution (Gibco BRL, Invitrogen)

MEM + GLUTAMAX Components

Amino Acids:	Concentration (mg/L)
L-Alanyl-Glutamine	406
L-Arginine hydrochloride	126
L-Cystine	24
L-Histidine hydrochloride	42
L-Isoleucine	52
L-Leucine	52
L-Lysine hydrochloride	73
L-Methionine	15
L-Phenylalanine	32
L-Threonine	48
L-Tyrosine	10
L-Valine	46
Vitamins:	
Choline chloride	1
D-Calcium pantothenate	1
Folic Acid	1
Niacinamide	1
Riboflavin	0.1
Thiamine hydrochloride	1
i-Inositol	2
Inorganic Salts:	
Calcium Chloride ($CaCl_2.2H_2O$)	264
Magnesium Sulfate ($MgSO_4.7H_2O$)	200
Potassium Chloride	400
Sodium Bicarbonate	2200
Sodium Chloride	6800
Sodium Phosphate monobasic ($NaH_2PO_4.2H_2O$)	158
Other components:	
D-Glucose	1000
Phenol Red	10

II. BACTERIA AND YEAST STRAINS

· **E. coli XL1- blue**: *recA endA1 gyrA96 thi-1 hsdR17 supE44 relA1 lac[F' proAB lacZ⊿M15 Tn10(Tet^r)]*

· **S. cerevisiae AH109**: MATa, trp1-901, leu2-3, 112, ura3-52, his3-200, gal4Δ, gal 80Δ, LYS2:: $GAL1_{UAS}$-$GAL1_{TATA}$-HIS3, $GAL2_{UAS}$-$GAL2_{TATA}$-ADE2, URA3::$MEL1_{UAS}$-$MEL1_{TATA}$-lacZ, MEL1

· **S. cerevisiae Y187**: MATα, ura3-52, his3-200, ade2-101, trp1-901, leu2-3, 112, gal4Δ, met-, gal 80Δ, URA3:: $GAL1_{UAS}$-$GAL1_{TATA}$-lacZ, MEL1

III. PLASMIDS

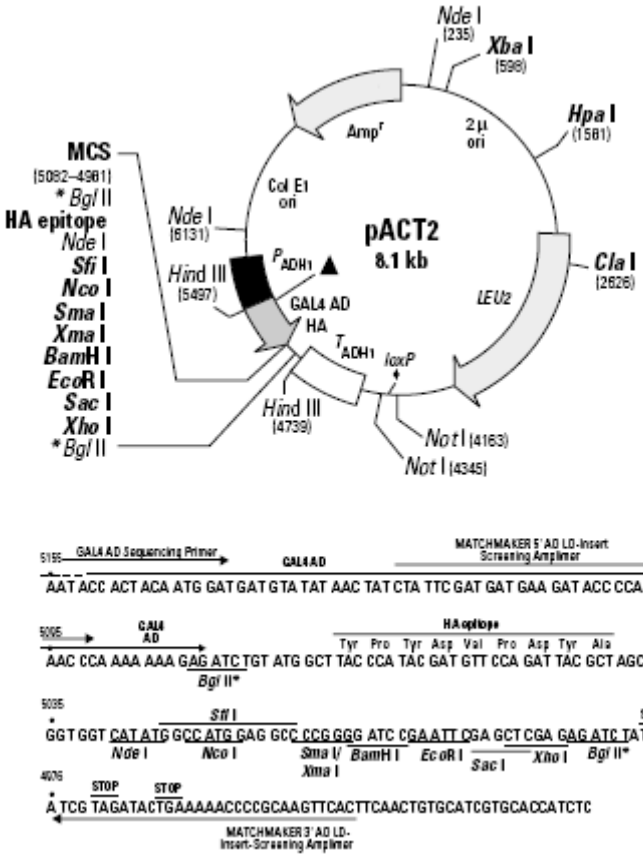

pACT2 *(Clontech) map and MCS. Unique sites are coloured blue. pACT2 is used to generate a hybrid containing the GAL4 AD, an epitope tag and a protein encoded by a cDNA in a fusion library. The hybrid protein is expressed at medium levels in yeast host cells from an enhanced, truncated ADH1 promoter and is target to the nucleus by the SV40 T-antigen nuclear localization sequence. pACT2 contains the LEU2 gene for selection in Leu⁻ auxotrophic yeast strains.*

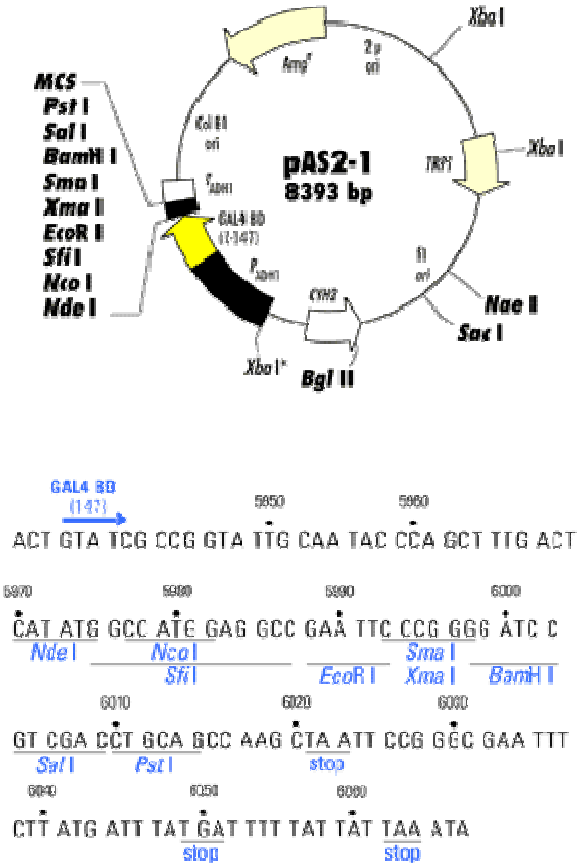

pAS2-1 (*Clontech*) *map and MCS. Unique sites are coloured blue. pAS2-1 is a cloning vector used to generate fusions of a bait protein with the GAL4 DNA-BD. The hybrid protein is expressed at high levels in yeast host cells from the full-length ADH1 promoter. The hybrid protein is target to the yeast nucleus by nuclear localization sequences. pAS2-1 contains the TRP1 gene for selection in Trp⁻ auxotrophic yeast strains.*

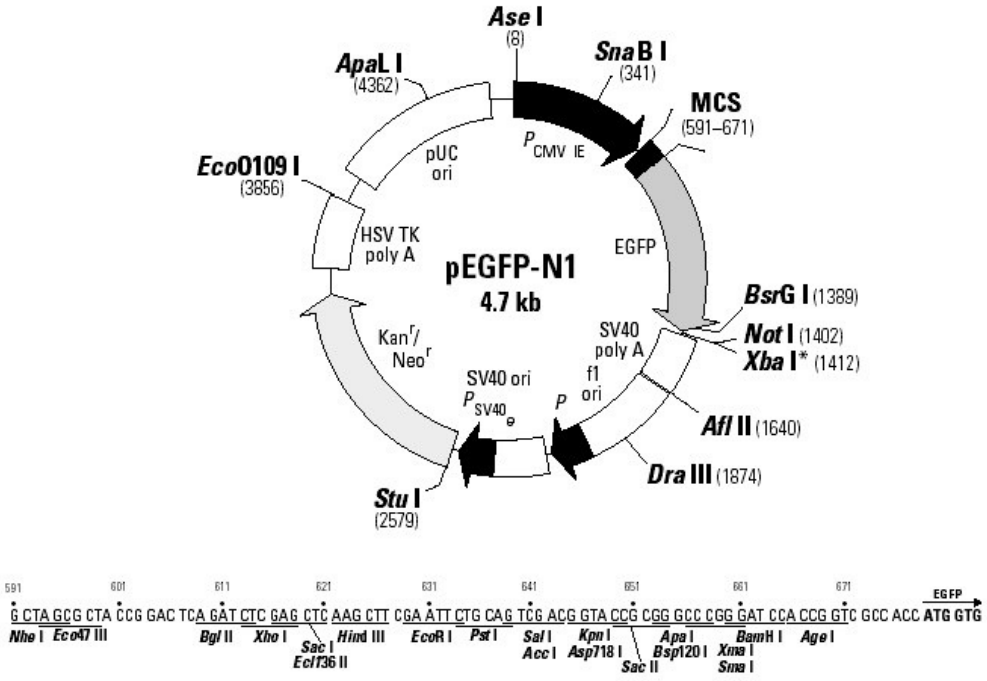

pEGFP-N1 *vector map and MCS (Clontech). This eukaryotic exppression vector was used to express pC9orf75-GFP fusion protein in HeLa cells.*

IV. PRIMERS

Primer	Sequence (5'::::: 3')	Nt No.	MT (ºC)
GAL4 AD	TACCACTACAATGGATG	17	48
GAL4 BD	TCATCGGAAGAGAGTAG	17	50
Amplimer 3' (reverse)	ATCGTAGATACTGAAAAACCCCGCAAGTTCAC	32	84
C9orf75-F4	CCCGGAATTCCGATGGAGACCATCCCCTTG	30	96
C9orf75-R5	ACGCGTCGACGTGAAATACAGGGCTGGCTC	30	96
pEGFP-N1-FW	GTAGGCGTGTACGGTGGGAG	20	54
pEGFP-N1-RV	GCCGTCCAGCTCGACCAGG	19	60